THE ROLE OF METABOLIC HORMONE FIBROBLAST GROWTH FACTOR 21 (FGF21) IN MAMMALIAN HIBERNATION USING TRANSGENIC GROUND SQUIRRELS

A DISSERTATION SUBMITTED TO THE FACULTY OF THE GRADUATE
SCHOOL OF THE UNIVERSITY OF MINNESOTA BY

BETHANY THERESA NELSON

IN PARTIAL FULFILLMENT OF THE REQUIREMENTS FOR THE
DEGREE OF DOCTOR OF PHILOSOPHY

MATTHEW T. ANDREWS

OCTOBER 2012

Acknowledgements

This project was completed with the help and support of many people. To start I would like to thank my advisor, Dr. Matthew T. Andrews, for his encouragement and positive attitude. He always made time to answer my questions and this work could not have been done without his guidance. I would also like to acknowledge the former members of the Andrews' lab for their support, training, assistance and friendship. These individuals include, but are not limited to, Sarah Ristvedt, Amanda Klein, Marshall Hampton, Vicki Zbikowski, Heather Moline, Anne Kendall, Sarah Timm, Scott Wendroth, Richard Melvin, and Kevin Russeth.

In addition I would like to thank our collaborators at University of Texas Southwestern Medical Center. Dr. Steven Kliewer provided invaluable guidance and ideas throughout the project. Dr. Robert Gerard produced the adenoviral construct for expressing thirteen-lined ground squirrel FGF21 and insight into our results. Dr. Xushan Ding performed RACE PCR to identify the thirteen-lined ground squirrel FGF21 sequence, Q-RT-PCR of many genes, ELISA analysis of FGF21 concentrations. Dr. Jamie Boney-Montoya assayed ERK1/2 phosphorylation by thirteen-lined ground squirrel FGF21 in adipocytes. The assistance and advice from our collaborators at UTSW made this project possible.

Finally, I would like to thank all members of my committee, my advisor, Matthew Andrews, Lester Drewes, Grant Anderson, Jean Regal, and Deborah Ferrington, for their support and encouragement throughout this process.

Dedication

I would like to dedicate this dissertation to my parents, Kenneth and Christine Stern, for their encouragement, advice, and insight through my education. Also my siblings, Joshua, Sarah, Benjamin, and Laura for their support.

And to my loving husband Jason, for his understanding, support, and continued encouragement, without which I would not be where I am today.

And to my daughter, Magdalena, with all my love.

ABSTRACT

Hibernation is a natural adaptation that allows certain mammals to survive physiological extremes that are lethal to humans. Near freezing body temperatures, heart rates of 4 to 6 beats per minute and depressed metabolism are characteristic of hibernation torpor bouts that are periodically interrupted by brief interbout arousals (IBAs). The molecular basis of torpor induction is unknown, however studies of fibroblast growth factor 21 (FGF21) in starved mice have shown the involvement of this hormone in promoting fat utilization and reducing body temperature and physical activity—all hallmarks of mammalian hibernation. We hypothesized that increased FGF21 sensitizes the natural hibernating thirteen-lined ground squirrel (*Ictidomys tridecemlineatus*) to enter torpor and changes the metabolic profile to indicate increased lipolysis. In this study we isolated the FGF21 cDNA from the ground squirrel and found that levels of FGF21 mRNA in liver and FGF21 protein in serum are elevated during IBAs compared to summer active animals. The effects of elevating circulating FGF21 concentrations 50 to 100-fold via adenoviral-mediated overexpression were examined at key times in the annual hibernation cycle. FGF21 overexpression decreased blood insulin and free fatty acid concentrations sampled 7 days after injection in fed squirrels kept at 23 °C with a 12:12 l:d cycle in April, effects similar to those observed in obese mice. However, elevated FGF21 concentrations did not cause torpor in thirteen-lined ground squirrels. We conclude that FGF21 is strongly regulated during torpor and IBA in hibernating thirteen-lined ground squirrels but that its overexpression is not sufficient to cause torpor.

TABLE OF CONTENTS

LIST OF TABLES

LIST OF FIGURES

LIST OF ABBREVIATIONS

IBA	Interbout arousal	iii
FGF21	Fibroblast growth factor 21	iii
T_b	Body temperature	3
MR	Metabolic rate	3
HR	Heart rate	3
TLG	Thirteen-lined ground squirrel	4
FA	Fatty acids	6
TG	Triglycerides	6
WAT	White adipose tissue	6
PPARγ	Peroxisome proliferator activated receptor gamma	7
BAT	Brown adipose tissue	7
TRP	Transient receptor potential	8
RQ	Respiratory quotient	11
PDK4	Pyruvate dehydrogenase kinase 4	12
BHB	Beta hydroxy butyrate	13
HSL	Hormone sensitive lipase	13
PTL	Pancreatic triglyceride lipase	13
PPARα	Peroxisome proliferator activated receptor alpha	14
CPT1	Carnitine palmitoyl transferase	14
HMGCS	Hydroxymethylglutaryl CoA synthase	14
PGC1α	Peroxisome proliferator activated receptor gamma coactivator 1 alpha	14
NST	Nonshivering thermogenesis	15
UCP1	Uncoupling protein 1	16
HIT	Hibernation induction trigger	19
DADLE	Delta opioid D-Ala^2-D-Leu^2 enkephalin	19
AMPK	AMP-activated protein kinase	20

FGFR	Fibroblast growth factor receptor	21
HS	Heparin sulfate proteoglycans	23
ChREBP	Carbohydrate response-element binding protein	29
KO	Knock out	32
PNLIPRP2	Pancreatic triglyceride lipase related protein 2	32
CEL	Carboxy ester lipase	32
CLPS	Pancreatic colipase	32
CPT1a	Carnitine palmitoyltransferase 1a	32
G6Pase	Glucose-6-phosphatase	33
PEPCK	Phosphoenolpyruvate carboxykinase	33
ATGL	Adipose triglyceride lipase	33
UCP1	Uncoupling protein 1	39
ECG	Electrocardiogram	48
AdRR5	RR5 control adenoviral construct	54
AdFGF21	Squirrel FGF21 expressing adenoviral construct	54
NEFA	Non-esterified fatty acids	57
ELISA	Enzyme linked immunosorbent assay	68
AUG	August active state	68
TOR	Winter torpid state	68
MAR	March active state	68
Q-RT-PCR	Quantitative reverse transcriptase polymerase chain reaction	68
IBI COV	Interbeat interval coefficient of variation	79
CycA	Cyclophilin A	119
GAPDH	Glyceraldehyde-3-phosphate dehydrogenase	119
RPL13a	60s ribosomal protein 13A	119
SDHA	Succinate dehydrogenase complex subunit A	119

CHAPTER 1

INTRODUCTION

Torpor and Hibernation

A heterotherm reduces metabolic heat production and allows their body temperature to decrease, entering a state called torpor. Heterotherms can survive physiological extremes of body temperature, heart rate and respiration that result in tissue damage and death in homeotherms. The natural adaptations that allow heterotherms to withstand physiological extremes can be employed to develop novel therapeutic strategies to advance health care. For example, an understanding of the adaptations for survival of body temperatures near 5 °C can improve the ability to reduce human body temperatures during surgery and improve surgical outcomes. The mechanisms employed by heterotherms for resistance to ischemia and reperfusion injury can be used to improve the outcomes for stroke victims. People that are confined to a bed for long periods of time can be helped by applying mechanisms that prevent muscle and bone disuse atrophy in hibernators. Also, the success of organ transplants could be increased by using heterothermic strategies to increase the preservation and storage of organs. The extreme weight changes and changes in insulin sensitivity that occur in hibernators can be used to produce novel strategies to treat obesity and metabolic disorders. By understanding these natural adaptation used by heterotherms, human health care can be improved in several ways (For review see Andrews 2007).

Metabolic Challenges. Endotherms are animals capable of maintaining a body temperature near 37 °C despite the ambient temperature they are exposed to. Cellular temperatures between 36 and 39 °C are required in the central nervous system for alert consciousness and normal motor activity (Morrison, Nakamura et al.

2008). Cellular temperatures below this range reduce enzyme efficiency and diffusion capacity leading to reduced cellular energy availability and ion flow. An ambient temperature slightly below the optimal body temperature range allows heat produced by metabolism to be released and requires the lowest energy expenditure. The range of optimal ambient temperatures for an animal to maintain body temperature without increasing metabolic rate is called the thermoneutral zone. Environmental temperatures vary greatly from the thermoneutral zone and temperatures significantly below the thermoneutral zone cause a thermal gradiant and significant heat loss. To combat heat loss endotherms increase metabolic rate and produce more heat to maintain body temperature despite the thermal gradient. The increase of metabolic rate consumes more energy and in many environments when ambient temperatures significantly decline, there is a simultaneous scarcity of food. The reduced availability of food and necessity to increase metabolic rate to maintain body temperature poses a significant challenge. Some animals cope with this challenge by increasing body mass through increased fat storage in anticipation of reduced food availability and later use the stored fat for insulation and as a fuel source. Certain animals have adapted the strategy of reducing energy use during times of food scarcity and differentially regulating body temperature to passively cool through the thermal gradient. This state of hypometabolism employed by heterotherms is called torpor.

Hibernation and Daily Torpor. Torpor is a state of lowered physiological activity characterized by the regulated reduction in body temperature (T_b), metabolic rate (MR), and other physiological functions including heart rate (HR) and respiration. Torpor is a strategy employed by several mammals and birds, including several species of hummingbirds, in order to reduce energy expenditure, especially in environments where food availability is decreased. Seasonal hibernation and daily torpor are two common patterns of torpor used by mammals and birds, and some species exhibit an intermediate torpor pattern (Geiser and Ruf 1995).

Seasonal hibernation is a natural adaptation found in several mammals to combat the challenges of reduced food availability and ambient temperatures that commonly occur during winter. Torpor that occurs in some species during draughts and at high temperatures is called estivation. Before hibernation animals acquire excess adipose tissue and as ambient temperatures and food availability decrease, hibernators enter torpor bouts with reduced MR and T_b. Most hibernating species stop eating during the hibernation season, but some species store food for consumption during arousal periods. An example seasonal hibernator is the thirteen-lined ground squirrel (*Ictidomys tridecemlineatus*). During torpor thirteen-lined ground (TLG) squirrels reduce oxygen consumption to 2% of the active rate, reduce T_b to 4 to 7 °C, and reduce HR from 300-400 beats per minute to 3-10 beats per minute (Hampton, Nelson et al. 2010). Bouts of torpor last from days to several weeks during hibernation and are interrupted by inter-bout arousals (IBA). During IBA the animal returns to active levels of MR, T_b, and HR for a short period of time, approximately 24 hours. Spontaneous hibernators, like TLG squirrels, enter torpor seasonally regardless of food availability, and facultative hibernators only employ torpor when food and/or water availability is scarce. Facultative hibernators remain active through most of the year if food and water are widely available (Frank, Brooks et al. 1998).

The shorter length of torpor bouts observed in daily heterotherms distinguishes daily torpor from hibernation. The length of torpor bouts observed in daily heterotherms is only hours and torpor bouts in hibernators last days to weeks (Geiser and Ruf 1995). Daily torpor is employed by many mammals, and in contrast to hibernation, also many birds. Decreases in T_b and MR observed in daily torpor are less than that observed in seasonal hibernators. Daily torpor is not seasonal like hibernation and occurs throughout the year, although it is more frequently observed in winter. Daily torpor is usually employed in response to an acute shortage of energy supply, but can be observed regularly in some species even when food is available. Another difference between daily heterotherms and hibernators is that hibernators fatten before entering torpor and daily torpor is entered when body mass is low. Daily torpor is inhibited by leptin, a hormone released from adipose tissue that inhibits appetite, and leptin prevents daily torpor from occurring in fattened animals (Geiser, Kortner et al. 1998; Geiser 2004). Rather than stored body fat the main energy source used by daily heterotherms is ingested food (Geiser 2004). The house mouse (*Mus musculus*) is a species that uses daily torpor in response to food scarcity. Torpor is more frequently observed in mice kept at the standard laboratory temperature of 23 °C, a temperature below the thermoneutral zone, than mice kept at higher ambient temperatures (Overton and Williams 2004). A mouse is considered torpid at a T_b below 31 °C and during torpor a mouse reaches a lower T_b limit between 16 and 19 °C (Hudson and Scott 1979). The T_b range observed during torpor in mice is warmer than that observed in most seasonal hibernators.

Seasonal Hibernators Store Excess Fat. Seasonal hibernators increase lipid reserves prior to hibernation and use the lipid reserves for fuel during hibernation. The use of lipid reserves during hibernation results in a body mass minimum at spring arousal from hibernation and the increased food consumption during summer results in a body mass maximum that can be double the body mass just before hibernation. Serum lipid increases with increased body mass and concentrations of proteins important for fatty acid (FA) and triglyceride (TG) synthesis are the highest in white adipose tissue (WAT) and liver tissue during weight gain (Reviewed in Dark 2005). Insulin concentrations and responsiveness increase as lipogenesis occurs and body mass increases (Buck, Squire et al. 2002). The maximum serum concentration of insulin and insulin resistance occur when the volume of WAT is at the annual maximum (Florant, Lawrence et al. 1985; Martin 2008). In conditions that are not ideal for lipogenesis, for example when food is restricted, MR is reduced and lipid mass still increases despite the lack of available energy (Forger, Dark et al. 1986). The mechanism for signaling a larger volume of adipose tissue is necessary for hibernation and reducing MR prior to hibernation is unknown, but leptin is a signaling molecule that corresponds to adipose tissue volume and may be involved. In TLG squirrels and bats leptin is at the highest level prior to hibernation at the annual lipid mass maximum (Dark 2005; Hampton, Melvin et al. 2011). But, high leptin levels increase energy expenditure and inhibit daily torpor in several species. High leptin at body mass peak could increase energy expenditure when MR is decreased and could inhibit torpor. These are undesirable effect of leptin for a hibernator, and leptin may not be the signal for adequate WAT mass prior to hibernation (Reviewed in Dark 2005).

Peroxisome proliferator activated receptor γ (PPARγ) is a nuclear receptor involved in transcriptional regulation during the metabolic response, especially to high fat intake. PPARγ regulates transcription of genes involved in the uptake of glucose and FA and the conversion to TGs for storage. Increased free FA after feeding increases PPARγ (Kersten, Desvergne et al. 2000; Lefebvre, Chinetti et al. 2006). Hibernators increase feeding in preparation for hibernation and increased PPARγ activity is expected during the fattening phase in late summer and early fall. The changes in PPARγ associated with torpor vary with species but there is a trend for seasonal hibernators to have increased PPARγ either before or during torpor relative to activity. In TLG squirrels protein levels of PPARγ in brown adipose tissue (BAT) and WAT are increased during torpor relative to activity (Eddy, Morin et al. 2005). In the jerboa, a small desert rodent that hibernates seasonally after fattening, PPARγ mRNA levels are increased in WAT before hibernation but are not increased during torpor in WAT and in BAT PPARγ mRNA levels are lower before and during torpor relative to activity (Kabine, El Kebbaj et al. 2004). In the little brown bat, PPARγ protein levels are increased during torpor relative to activity in liver, BAT, and WAT (Eddy and Storey 2003).

Body Temperature is Alternatively Regulated Before Torpor.

Homeothermic mammals regulate T_b to remain at a constant high temperature in a wide range of environmental temperatures. Heat produced by metabolism is dissipated through the thermal gradient between T_b and environmental temperature. An environmental temperature slightly below T_b allows metabolic functions to occur with the lowest energy expenditure. A homeothermic mammal exposed to low environmental temperatures can lose excessive body heat and have reduced T_b due to failure of physiological defenses against the cold environment. This pathological decrease of T_b called hypothermia is physiologically different from the decreased T_b observed during torpor. During torpor the physiological defenses that maintain T_b are alternatively regulated and T_b is allowed to passively reduce through the thermal gradient.

The physiological system that maintains T_b has three main sections, including sensory of temperature, neurological response to temperature, and a physiological response controlled by the neurological system. Thermosensitive neurons detect environmental and internal temperatures. Skin thermosensitive neurons are affected by ambient temperatures and most are activated in response to cold and initiate cold-defensive responses before core T_b changes. Core body thermosensitive neurons are found in the brain, spinal cord, and abdomen. There are transient receptor potential (TRP) channels in thermosensitive neurons that are activated within specific temperature ranges, and cumulatively thermosensitive TRP channels cover a large temperature range. The afferent pathway of thermosensitive neurons leads to the hypothalamus. The regulation of core T_b is mediated within the hypothalamus and the preoptic anterior hypothalamus is the main regulator of T_b. T_b is regulated by multiple responses and each is regulated independently. Behavioral responses, including moving to a region of preferred environmental temperature, are the initial response to maintain T_b. The common autonomic thermoregulatory responses for reducing T_b in mammals are sweating, panting, and vasodilation. Several autonomic responses increase and maintain high T_b including mitochondrial oxidation in BAT, increased HR, shivering thermogenesis in skeletal tissue, and cutaneous vasoconstriction to conserve heat (reviewed in Heller, Crawshaw et al. 1978; Romanovsky 2007; Morrison, Nakamura et al. 2008).

Homeotherms defend a small T_b range through thermoregulatory responses. In heterotherms the regulation of T_b is adjusted before T_b drops below the range defended during activity and torpor occurs. During entrance into torpor the lower limit of range of temperatures defended by thermoregulatory responses is progressively lowered and MR decreases (Heller, Colliver et al. 1977). The decreased MR produces less heat and the decreased lower limit of the defended T_b allows the animal to passively cool through the thermal gradient. Decreased T_b reduces biochemical reaction rates, and the slower reaction rates further reduce the MR (Geiser 2004). If T_b falls below the range defended by the thermoregulatory response, metabolic heat production increases and slows the entrance into torpor (Lyman 1958; Strumwasser 1959). During the maintenance of torpor, T_b is maintained by metabolic heat production when the environmental temperature drops below the defended T_b (Heller and Colliver 1974). So, in contrast to the pathological failure of the thermoregulatory responses that result in decreased T_b during hypothermia, the thermoregulatory system is functional during torpor and allows decreased T_b.

Metabolic Rate is Reduced during Torpor Induction. There are several descriptions of the physiological changes that occur during torpor induction, but the torpor induction mechanism is unknown. During torpor induction MR and fuel use are reduced. HR and respiration reduce concurrently with MR, and then T_b passively decreases. MR reduction during hibernation reduces energy consumption and creates significant energy savings over the hibernation season. Even considering the energetically costly periodic IBAs of a hibernator, a euthermic animal expends more than 5 times as much energy over the hibernation season (Armitage, Blumstein et al. 2003).

The rate of oxygen consumption is commonly used to measure the reduction of MR observed during torpor. Oxygen is consumed by the process of making ATP in the mitochondria, and when decreased oxygen consumption rate indicates decreased ATP production. ATP concentrations are maintained within a small range, even during the extreme metabolic changes that occur during torpor (Burlington, Meininger et al. 1976; Lyman, Willis et al. 1982; Lust, Wheaton et al. 1989). Together maintenance of ATP concentrations and decreased oxygen consumption indicate the production and consumption of ATP are decreased during torpor. The decreased use of ATP through decreased MR is a broad reduction of biological reactions. The thousands of reactions involved in metabolism are regulated through transcription, translation, enzymatic function, and phosphorylation. The broad reduction of the reactions involved in metabolism requires the coordination of signaling mechanisms and responses. A few single biomolecules have been indicated to induce torpor, like hibernation induction trigger, but it is not likely that only one signaling molecule induces torpor. In addition to the metabolic rate reduction during torpor induction requiring the coordination of multiple responses, if only one biomolecule was necessary to induce torpor this process could be more easily compromised. Compromising torpor induction may cause torpor to occur in animals during times when food is widely available and the animal needs to fatten or during reproduction and be a disadvantage to heterotherms. Thus, it is more likely that there are multiple biomolecules that signal season and light cycles, food availability, and ambient temperature and these signals coordinately result in reduced metabolic rate and torpor induction.

Glycolysis is Inhibited During Torpor. In addition to an overall reduction of MR, torpid animals reduce dependence on glucose for fuel. During hibernation some species, like TLG squirrels, do not eat for several months and this lack of food consumption necessitates a reduced reliance on glucose for fuel. There are multiple lines of evidence that indicate reduced glycolysis during torpor. Respiratory quotient (RQ) is a measurement of the amount of CO_2 expired divided by the amount of O_2 consumed and is a dimensionless number. A RQ of 1.0 represents almost pure carbohydrate being used, whereas a RQ of 0.7 represents a reliance on lipids for fuel. A RQ of 0.7 during torpor indicates the use of lipids rather than carbohydrates (Lyman and Chatfield 1955). Glucose catabolism is reduced during torpor (Tashima, Adelstein et al. 1970; Andrews, Russeth et al. 2009). Overall levels of mRNAs and proteins involved in glucose metabolism are lower in multiple tissues during hibernation (Brauch, Dhruv et al. 2005; Yan, Barnes et al. 2008; Epperson, Rose et al. 2010; Shao, Liu et al. 2010; Hampton, Melvin et al. 2011; Hindle, Karimpour-Fard et al. 2011). The concentration and activity of multiple enzymes involved in glycolysis are reduced during torpor, including decreased concentrations of fructose-2,6-bisphosphate, increased inhibition of fructose-1,6-bisphosphate aldolase, and decreased activity of phosphofructokinase and pyruvate dehydrogenase (Storey 1987; Brooks and Storey 1992; MacDonald and Storey 2002). Glycogen phosphorylase activity is also decreased during torpor, indicating less breakdown of glycogen to glucose (Storey 1987; Brooks and Storey 1992). One important modulator of reduced glycolysis is pyruvate dehydrogenase kinase 4 (PDK4), an enzyme that inhibits pyruvate dehydrogenase and blocks pyruvate from being converted to acetyl-CoA. PDK4 mRNA and protein levels are increased during hibernation and fewer glycolytic intermediates enter the citric acid cycle (Andrews, Squire et al. 1998; Buck, Squire et al. 2002). Although there is significant reduction is the use of glucose, glucose and glycogen levels gradually decline over torpor bouts and the hibernation season (Burlington and Klain 1967; Galster and Morrison 1970; Galster and Morrison 1975; Andrews, Russeth et al. 2009). This indicates that glucose is still being catabolized, but at a significantly reduced rate.

Lipids are the Main Fuel Source During Hibernation. A reliance on the use of lipids for fuel coincides with the reduction of glucose use during torpor. There are several lines of evidence that exhibit the use of lipids during hibernation and torpor. Seasonal hibernators increase the amount of stored adipose tissue prior to hibernation and these lipid reserves are used for fuel during hibernation, when adiposity is decreased (For review see Dark 2005). A RQ of 0.7 during torpor indicates the use of lipids for fuel (Lyman and Chatfield 1955; Tahti 1978; Lyman, Willis et al. 1982). WAT stores lipids as TGs composed of glycerol and three FAs and the amount of lipid stored in WAT decreases during hibernation (Moreau-Hamsany, Castex et al. 1988). As lipid stores are broken down glycerol and FAs are released into the blood and carried by albumin. Albumin transcript levels are increased in October prior to hibernation in TLG squirrel WAT (Hampton, Melvin et al. 2011). Free FA and glycerol serum concentrations are increased during hibernation (Nelson, Otis et al. 2010; Epperson, Karimpour-Fard et al. 2011). Ketones are a lipid-derived metabolite used for fuel during starvation and serum ketone levels increase during torpor (Baumber, South et al. 1971; Rauch and Behrisch 1981; Krilowicz 1985; Andrews, Russeth et al. 2009). Heart and brain preferentially metabolize the ketone β-hydroxybutyrate (BHB) at the low temperatures experienced during torpor (Andrews, Russeth et al. 2009).

The level of specific mRNAs and proteins involved in lipid oxidation are increased during hibernation (Yan, Barnes et al. 2008; Shao, Liu et al. 2010; Hindle, Karimpour-Fard et al. 2011). Hormone sensitive lipase (HSL) is a typical lipase that breaks down TGs in WAT (Steinberg and Khoo 1977). In addition to HSL, pancreatic triglyceride lipase (PTL) levels increase in squirrels prior to and during hibernation (Wilson, Deeb et al. 1992; Andrews, Squire et al. 1998; Bauer, Squire et al. 2001; Squire and Andrews 2003; Squire, Lowe et al. 2003). HSL is not responsive to norepinephrine activation at cold temperatures, and the increased expression of PTL is important for continued lipolysis at the low T_b of hibernation (Dark, Miller et al. 2003; Squire, Lowe et al. 2003).

Nuclear Signaling in Hibernation. Peroxisome proliferator activated receptor α (PPARα) is a nuclear receptor that affects transcription of genes important for the use of FAs for fuel during fasting (Mandard, Muller et al. 2004). PPARα activity is induced by FAs or pharmacologically by the fibrate class of hypolipedemic drugs. PPARα liver mRNA is increased during torpor in the jerboa. In the jerboa two splice variants of PPARα have been found including the active PPARα1wt form and the inactive truncated form. During torpor the inactive truncated PPARα form is reduced, and the availability of the active form is increased (El Kebbaj, Andreoletti et al. 2009). In jerboa WAT PPARα mRNA levels are increased before torpor (Kabine, El Kebbaj et al. 2004). PPARα regulates several genes in the liver that are upregulated during hibernation including acyl CoA oxidase, apolipoprotein A1, carnitine palmitoyl transferase 1 (CPT1), fatty acid binding protein, hydroxy methylglutaryl synthase (HMGCS), and long chain acyl CoA dehydrogenase (Epperson and Martin 2002; Epperson, Dahl et al. 2004; El Kebbaj, Andreoletti et al. 2009; Shao, Liu et al. 2010).

Fasting induces expression of peroxisome proliferator activated receptor (PPAR) gamma coactivator 1 α (PGC1α). PGC1α is a coactivator of transcription factors important for increasing expression of genes involved in gluconeogenesis and fatty acid oxidation (Lin, Handschin et al. 2005; Finck and Kelly 2006). PCG1α liver mRNA level is increased during torpor compared the activity state in jerboa (El Kebbaj, Andreoletti et al. 2009). In TLG squirrels PGC1α protein levels are increased during torpor relative to active levels in heart, skeletal muscle, BAT, and WAT (Eddy, Morin et al. 2005). In the little brown bat, PGC1α protein levels are increased during torpor relative to activity in liver, BAT, and WAT (Eddy and Storey 2003).

Hibernation is Interrupted by Energetically Costly Arousals. Hibernators need to arouse from torpor in order to survive. Not only do hibernators arouse at the end of the hibernation season, but hibernation is also regularly interrupted by IBAs. IBAs occur between several days and several weeks apart and last approximately 24 hours (Lyman, Willis et al. 1982; Carey, Andrews et al. 2003; Geiser 2004; Dark 2005). IBAs involve a spontaneous and rapid increase in T_b while ambient temperatures are still low and the thermal gradient poses an energetically expensive challenge (Dark 2005; Karpovich, Toien et al. 2009). Due to energetic cost, IBAs are contradictory to the energy savings torpor provides. Although the purpose of IBAs is not understood, one hypothesis is that IBAs are necessary for transcription and translation to replace necessary biomolecules. Transcription and translation do not occur at the low T_b experienced by hibernators (van Breukelen and Martin 2001; Van Breukelen and Martin 2002; van Breukelen and Martin 2002).

BAT Thermogenesis is Critical for Arousal from Torpor. For arousal from torpor to occur T_b must increase against a large thermal gradient from the low T_b of torpor to that of the active state. There are several autonomic responses that increase and maintain high T_b in mammals including non-shivering thermogenesis (NST) in BAT, increased HR, shivering thermogenesis in skeletal tissue, and cutaneous vasoconstriction to conserve heat. Shivering thermogenesis is not efficient and does not occur at the near freezing body temperatures observed in hibernators (Smith and Horwitz 1969; McArthur, Hanstock et al. 1990; Hashimoto, Gao et al.

2002). Prior to shivering thermogenesis, the heat produced in BAT by NST is critical for the initial warming during arousal from torpor. BAT expresses uncoupling protein 1 (UCP1), which uncouples the mitochondrial oxidation from the synthesis of ATP and thereby produces heat. There are clusters of neurons in the hypothalamus and brainstem that control NST. BAT is innervated by sympathetic nervous system efferents, and the release of norepinephrine enhances NST activity and capacity (Richard, Carpentier et al. 2010; Cannon and Nedergaard 2011). There are several lines of evidence that indicate increased BAT NST capacity during hibernation and activity during arousal from torpor. Increased sympathetic nervous system tone initiates arousal from torpor (Milsom, Zimmer et al. 1999; Drew, Buck et al. 2007). During torpor and arousal BAT temperature is warmer than peripheral tissue temperatures (Horwitz, Smith et al. 1968; Smith and Horwitz 1969; Barger, Barnes et al. 2006). The volume of BAT and amount of UCP1 are increased in cold adaptation during hibernation (Boyer, Barnes et al. 1998; Liu, Lin et al. 1998; Barger, Barnes et al. 2006; Kitao and Hashimoto 2012). The expression of genes involved in NST are increased during hibernation in the Arctic ground squirrel (Yan, Burman et al. 2006). The BAT of hamsters, a food storing hibernator with short bouts of torpor, has increased thermogenic capacity during hibernation (Kitao and Hashimoto 2012). These changes in BAT activity emphasize its importance during hibernation.

Metabolic Shift to Glucose Production during Arousal. Low serum glucose levels observed during torpor are restored to active levels during arousal from torpor (Galster and Morrison 1975; Andrews, Russeth et al. 2009). During arousal the RQ returns to near 1.0, indicating glucose metabolism (Lyman, Willis et al. 1982).

Glycerol and lactate are used in gluconeogenesis during hibernation and the rate of gluconeogenesis increases upon arousal (Burlington and Klain 1967; Galster and Morrison 1975; Green, Brosnan et al. 1984; Yeh, Tam et al. 1995; Staples and Hochachka 1998). Glycogen levels are also increased in liver and muscle tissues during arousal (Galster and Morrison 1975). Thus during arousal there is an increase in gluconeogenesis and glucose is used in glycolysis for energy production and to restore glycogen reserves.

Insulin and Glucagon during Hibernation. Insulin and glucagon are hormones released by the pancreas with opposing roles in glucose homeostasis. After feeding, blood glucose levels increase resulting in increased release of insulin and decreased release of glucagon from the pancreas. The release of insulin stimulates glucose uptake in muscle, liver, and adipose tissues. Insulin also increases glycogenesis and decreases glycogenolysis in liver and muscle tissues, increases glycolysis in liver and muscle tissue, increases FA synthesis in liver, and increases TG synthesis in WAT. The effect of insulin is to use and store glucose and maintain the glucose concentration in the bloodstream.

In agreement with the role of insulin in glucose storage, the serum concentration of insulin is increased during the body mass gain phase and peaks with body mass in hibernators. During hibernation, when fasting occurs and body mass decreases, serum insulin levels decrease (Lyman, Willis et al. 1982; Florant, Lawrence et al. 1985; Tokuyama, Galantino et al. 1991; Boswell, Woods et al. 1994; Buck, Squire et al. 2002). At peak serum concentrations of insulin when body mass is at its peak, insulin sensitivity is decreased in the European hedgehog, a facultative seasonal hibernator that consumes food during arousals, and the yellow-bellied marmot, a seasonal hibernator that relies on stored fat (Lyman, Willis et al. 1982; Florant, Lawrence et al. 1985; Tokuyama, Galantino et al. 1991). Pancreatic insulin mRNA content remains high during hibernation in the ground squirrel, and insulin in the pancreas increases over hibernation in the little brown bat (Bauman 1990; Buck, Squire et al. 2002). The pancreatic storage of insulin during hibernation may be in preparation for a metabolic switch to glucose use upon arousal.

Low blood glucose levels caused by fasting trigger an increased pancreatic release of glucagon and decreased of the release of insulin. Glucagon action in the liver stimulates glycogenolysis and gluconeogenesis, and inhibits glycogenesis and glycolysis resulting in the use of stored carbohydrates to maintain sufficient fasting blood glucose levels. Glucagon also stimulates the adipose tissue breakdown of TGs to glycerol and FAs that can be transferred to the liver where glycerol can be used for gluconeogenesis. As fasting progresses further and stored carbohydrates are depleted, FAs are relied on to produce ketone bodies and there is an increased reliance on proteins and glycerol to produce glucose.

During hibernation glucagon concentrations in the pancreas do not change relative to the summer active levels in multiple species (Lyman, Willis et al. 1982; Bauman, Meryn et al. 1987; Tokuyama, Galantino et al. 1991), and in the little brown bat pancreatic glucagon levels are increased during hibernation (Bauman 1990). Glucagon sensitivity is similar in torpid and active marmots (Cochet, Meister et al. 1999). Thus despite the extreme fasting state of hibernation, glucagon does not cause increased glycogenolysis or gluconeogenesis.

Torpor Induction. There is little known of the mechanisms that induce torpor and hibernation. Observations of the entrance into torpor have noted that HR decreases concomitantly with oxygen consumption, an indicator of overall MR reduction. Increased parasympathetic activation decreases HR during entrance into torpor (Milsom, Zimmer et al. 1999). Parasympathetic activity is critical to initiate successful entrance into torpor, although increased parasympathetic activity alone does not force an animal into torpor (Lyman, Willis et al. 1982).

Torpor induction by an exogenous compound was initially demonstrated by infusing blood or serum from hibernating ground squirrels or woodchucks into summer active animals (Dawe and Spurrier 1969; Dawe, Spurrier et al. 1970). A molecule called hibernation induction trigger (HIT) was later identified as the possible blood-borne trigger that induced torpor in these experiments (Horton, Kaftani et al. 1998). HIT was shown to have similar activity to the delta opioid D-Ala^2-D-Leu^5 enkephalin (DADLE), a synthetic delta opioid receptor agonist (Oeltgen, Nilekani et al. 1988). However, a study in Richardson's ground squirrels was not able to confirm the presence of HIT capable of inducing torpor in summer squirrels, and created doubt whether there is a torpor inducing protein present in the blood of hibernators (Abbotts, Wang et al. 1979). Even though there may not be a torpor inducing protein in hibernator blood, the relationship between HIT and DADLE and the possible role of opioids during torpor is of interest. There are increased opioid receptors in the brain of ground squirrels during torpor and activation of opioid receptors is important for maintenance of torpor in hamsters (Tamura, Shintani et al. 2005; Otis, Ackermann et al. 2010). This suggests that opioid activity contributes to the maintenance of torpor during hibernation and the HIT protein may be involved in the opioid activity.

Hydrogen sulfide gas is a compound that has been shown to reduce T_b and MR in mice (Blackstone, Morrison et al. 2005; Volpato, Searles et al. 2008). Hydrogen sulfide is an endogenously produced signaling molecule and when administered at high concentrations can compete with oxygen binding in mitochondria resulting in reduced oxygen consumption, metabolism, and T_b (Reviewed in Aslami, Schultz et al. 2009). Although hydrogen sulfide induced reductions in T_b and MR are of interest in the medical community, its potential role in the natural process of torpor induction is not clear at this time.

Torpor induced by metabolic stress in constant darkness is associated with increases in 5’-AMP and administration of exogenous 5’-AMP causes reductions in T_b in mice (Zhang, Kaasik et al. 2006). It has been argued that the reductions in T_b caused by administration of 5’-AMP are more like hypothermia than natural torpor induction (Swoap, Rathvon et al. 2007). AMP is a metabolite produced as a result of hydrolysis of ATP and is important for signaling energy status. AMP-activated protein kinase (AMPK) is sensitive to the [AMP]/[ATP] ratio and is involved in regulating many metabolic reactions and a role for AMP in torpor induction may be related to AMPK signaling. Another possible role for AMP in torpor induction is the activation of adenosine receptors by AMP metabolism. Adenosine receptor activation has been suggested to be important for induction of torpor in hamsters and arctic ground squirrels (Jinka, Toien et al. 2011; Tamura, Shintani et al. 2012).

Recently, fibroblast growth factor 21 (FGF21) has been demonstrated to sensitize fasted mice to enter torpor (Inagaki, Dutchak et al. 2007). FGF21 acts as a metabolic hormone and is involved in fasting signaling and signaling resulting from feeding a high fat diet. Mice are a species that employ daily torpor in response to decreased fuel access. Sensitization of fasted mice to enter torpor with increased FGF21 has prompted us to investigate whether FGF21 signaling is involved in torpor induction in a model seasonal hibernator, the thirteen-lined ground squirrel.

Fibroblast Growth Factor 21

Fibroblast Growth Factors. The fibroblast growth factor (FGF) family consists of 22 members, numbered FGF1 to FGF23. This family of proteins has many roles in embryonic and adult development, tissue repair, and metabolism. FGFs were initially identified as mitogens for fibroblasts in the brain and pituitary while subsequent members of this family have been isolated as growth factors for cultured cells or identified by homology-based PCR or by homology-based database searches. Of the 22 FGFs, FGF15 has not been detected in humans and appears to be the mouse ortholog of human FGF19. The FGF family can be divided into three groups with FGFs 1-9, 10, 16-18, 20 and 22 in the canonical group, FGF11-14 in the intracellular group, and FGF 15/19, 21, and 23 in the hormone-like group (Itoh 2010). The human FGFs range from ~150 to 300 amino acids in length, contain a conserved 120 residue core region, and have ~30% to 60% identity. The conserved internal core region has 28 highly conserved and 6 identical amino acids. Highly conserved FGF domain 2 and FGF linker regions are involved in FGF receptor (FGFR) binding. FGFs 1 and 2 have a 12-β-strand trefoil structure with 3 4-stranded β-sheets in a triangular array. In canonical FGFs, β-strands 10 and 11 are involved in binding heparin. FGF interaction with cell surface heparan sulfate proteoglycans stabilize the FGF and limit diffusion and release into interstitial space and this interaction is necessary for efficient FGFR activation (Ornitz and Itoh 2001). Specificity for receptor binding is defined by N-terminal and central region of FGFs (Plotnikov, Hubbard et al. 2000).

FGF Receptors. FGFs bind to 4 receptor tyrosine kinases (FGFR 1-4). FGFRs have an extracellular ligand binding domain, single transmembrane domain, and cytoplasmic domain with catalytic protein tyrosine kinase core and regulatory sequences. The extracelluar ligand binding domains contain 2 or 3 immunoglobulin-like domains and a heparin-binding sequence. FGFR 1, 2, and 3 can be alternatively spliced at the carboxy-terminal half of immunoglobulin domain III resulting in b or c isoforms. FGFR4 is not alternatively spliced. The alternative splicing determines ligand specificity of the receptor and the FGFR isoforms have tissue specific expression. Efficient FGFR activity requires dimerization of the tyrosine kinase receptors with 2 FGFs and 2 heparins. FGFR signaling occurs through tyrosine autophosphorylated sites that bind signaling proteins and docking proteins that become tyrosine phosphorylated and form a complex with additional signaling proteins. The major known pathway downstream of FGFR stimulation involves docking proteins FRS2α and FRS2β, recruitment of Grb2/Sos and activation of Ras/MAPK pathway, including ERK1 and ERK2. PCLγ is another docking protein commonly associated with FGFRs (Eswarakumar, Lax et al. 2005).

Hormone-like FGFs. The hormone-like FGFs belonging to the FGF19 subfamily include FGF19/15, FGF21, and FGF23. Mouse FGF15 is the ortholog to human FGF19 with 50% similarity. FGF15/19 is involved in bile acid synthesis and gallbladder filling and carbohydrate and lipid metabolism. FGF21 is involved in carbohydrate and lipid metabolism. FGF23 is involved in phosphate metabolism (Potthoff, Kliewer et al. 2012).

The FGF19 subfamily of proteins has endocrine activity unlike canonical FGFs that have only autocrine or paracrine activity. Canonical FGFs require binding to heparan sulfate proteoglycans (HS) in the extracellular matrix to induce FGFR activity. Endocrine FGFs have a shorter heparin binding site than paracrine acting FGFs and have poor heparin binding affinities. The solved structure of FGF19 shows the region between β-strands 10 and 12 is completely different from the canonical paracrine acting FGFs, where those FGFs bind to heparin, giving FGF19 an atypical trefoil structure. The β1-β2 loop is another region of heparin binding of canonical FGFs and it substantially differs in FGF19. The solved structure for FGF23 lacks the β11 strand associated with heparin binding in canonical FGFs and also has an atypical β-trefoil structure. The structure of FGF21 has not been solved, but there is sequence divergence at the β11 strand site and FGF21 is expected to have yet another conformation at this site. The poor heparin binding affinity of the FGF19 subfamily along with reduced affinity for FGFRs allows diffusion away from cells and entrance into the bloodstream for the endocrine activity observed with this subfamily of FGFs (Goetz, Beenken et al. 2007).

With low HS binding, endocrine FGFs require binding with a single pass transmembrane protein from the Klotho family for high-affinity receptor binding. FGF23 interacts with Klotho, FGF19/15 and FGF21 interact with βKlotho, and FGF19/15 also interacts with lactose-like Klotho. The amino acid identity of βKlotho is 41% similar to Klotho. Tissue specific expression of Klotho and βKlotho determine the tissue specific activities of the FGF19 subfamily members. Klotho is expressed in the kidney and the brain and βKlotho is expressed in adipose tissue, liver, and pancreas (Kurosu and Kuro-o 2008).

FGF21. Since the discovery of FGF21 insulin sensitizing activity in mice, the interest in FGF21 has intensified producing an exponentially growing body of literature (Kharitonenkov, Shiyanova et al. 2005). The FGF21 gene was discovered by homology based PCR and codes for 210 amino acids. FGF21 mRNA was initially found in liver and at low levels in thymus in mice. Human FGF21 is 75% identical to mouse FGF21 (Nishimura, Nakatake et al. 2000). FGF21 is 35% similar to FGF19 and is 22% similar to FGF23 (Yamashita, Yoshioka et al. 2000).

Intact FGF21 can cross the blood-brain barrier by simple diffusion and FGF21 signaling in the brain may be physiologically relevant (Hsuchou, Pan et al. 2007). FGF21 is not mitogenic as indicated by FGF21 not inducing cell proliferation in multiple cell lines and the transgenic overexpression of FGF21 not increasing tumor growth in mice (Kharitonenkov, Shiyanova et al. 2005; Huang, Yu et al. 2006).

FGF21 Receptors and βKlotho. FGF21 has reduced affinity for FGFRs compared to canonical FGFs that contributes to the ability of FGF21 to escape the interstitial space when released from a cell and enter the bloodstream. For FGF21 to activate an FGFR, the single-pass transmembrane protein βKlotho is required (Kurosu, Choi et al. 2007; Ogawa, Kurosu et al. 2007; Kharitonenkov, Dunbar et al. 2008; Suzuki, Uehara et al. 2008). βKlotho has the strongest interaction with FGFR4, interacts with FGFR -1c and -2c, and has little interaction with FGFR3 (Ogawa, Kurosu et al. 2007; Kharitonenkov, Dunbar et al. 2008; Kurosu and Kuro 2009). FGFR1c is the preferred receptor for FGF21 signaling activity, although FGF21 is capable of causing signaling activity in cells expressing βKlotho and FGFR -2c or -3c. Although βKlotho binds FGFR4, FGF21 does not signal through FGFR4 (Kurosu, Choi et al. 2007; Kharitonenkov, Dunbar et al. 2008; Suzuki, Uehara et al. 2008). This lack of interaction can be alleviated by replacing a sequence in domain 3 of FGFR4 with the corresponding sequence from FGFR1c domain 3, indicating this region of domain 3 is important in the FGF21/FGFR interaction (Gupte, Yang et al. 2011). The domain 1-linker region of FGFR1c reduces the interaction between FGFR1c and either FGF21 or βKlotho. The domain 2/domain 3 region of FGFR1c may directly interact with FGF21 for activity (Yie, Wang et al. 2012). The N-terminus of FGF21 is important for interaction with FGFR1c and the FGF21 C-terminal binds βKlotho. The full activity of FGF21 requires both termini (Wu, Lemon et al. 2008; Micanovic, Raches et al. 2009; Yie, Hecht et al. 2009).

A major site of the FGF21 response is adipose tissue, where FGFR1 is the predominant FGFR. Differentiated adipocytes express βKlotho, but undifferentiated adipocytes do not express βKlotho and FGF21 does not have signaling activity in undifferentiated adipocytes (Ogawa, Kurosu et al. 2007; Kharitonenkov, Dunbar et al. 2008). FGF21 also has activity in liver tissue. The liver expresses βKlotho and predominantly expresses FGFR4 of which FGF21 does not signal through, but liver tissue also expresses FGFR-2, some -3 and very little -1 (Fisher, Estall et al. 2011). Thus, the combination of tissue-specific βKlotho and FGFR expression regulates tissue specificity of FGF21 action (Kurosu and Kuro 2009).

In one study FGF21 was shown to be capable of inducing immediate early transcription factor in adipose tissue in the absence of βKlotho in mice. Although, no other parameters were measured in this study and it remains to be determined if FGF21 has βKlotho independent actions (Tomiyama, Maeda et al. 2010).

Activation of FGF21 Activity through PPARα. PPARα is a nuclear receptor that affects transcription of genes important for the use of FAs for fuel during fasting. Ketogenic diets cause a metabolic response similar to fasting with an increase in circulating FAs and ketogenesis and an increase in PPARα activity in the liver. FGF21 mRNA expression in the liver is increased during fasting and by feeding a ketogenic diet through activation of PPARα (Badman, Pissios et al. 2007; Inagaki, Dutchak et al. 2007; Lundasen, Hunt et al. 2007). Putative PPARα binding sites in the FGF21 promoter have been identified and FGF21 promoter activity is directly induced by PPARα (Inagaki, Dutchak et al. 2007; Lundasen, Hunt et al. 2007). Although during fasting PPARα directly induces FGF21 expression in liver tissue, PPARα agonists do not increase FGF21 expression in WAT (Muise, Azzolina et al. 2008; Zhang, Yeung et al. 2008; Dutchak, Katafuchi et al. 2012).

Subsequent to the initial discovery of FGF21 being regulated by fasting and ketogenic diet through PPARα, there have been multiple examples of FGF21 increases in the liver in similar metabolic situations. These examples include increases in FGF21 induced by PPARα agonists in mice (Muise, Azzolina et al. 2008), in human hepatocytes induced by the FAs linoleate and oleate (Mai, Andres et al. 2009), in suckling mice that are reliant on the use of FAs for fuel (Hondares, Rosell et al. 2010), in dairy cows during early lactation, a time of energy intake deficiency (Schoenberg, Giesy et al. 2011), and increases in mice when given conjugated linoleic acids (Yu, Yu et al. 2012).

Glucagon stimulation during fasting increases liver cell FGF21 mRNA and fasting induced increases in liver FGF21 are attenuated in mice lacking the glucagon receptor, indicating that the FGF21 response is downstream of glucagon activity during fasting (Uebanso, Taketani et al. 2009; Berglund, Kang et al. 2010). Glucagon levels have been shown to be lower after increasing levels of FGF21, indicating there may be a feedback mechanism to suppress glucagon circulation (Kharitonenkov, Shiyanova et al. 2005; Kharitonenkov, Wroblewski et al. 2007; Berglund, Li et al. 2009).

Fasting also induces expression of PGC1α, a coactivator of transcription factors important for increasing expression of genes involved in gluconeogenesis and fatty acid oxidation (Lin, Handschin et al. 2005; Finck and Kelly 2006). Increases in PGC1α indirectly lead to reduced FGF21 expression (Estall, Ruas et al. 2009). FGF21 transgenic mice have increased liver PGC1α mRNA and target genes of PGC1α involved in mitochondrial oxidative phosphorylation and tricarboxylic acid cycle flux are upregulated in FGF21 transgenic mice (Potthoff, Inagaki et al. 2009). Also FGF21 knockout mice have decreased PGC1α mRNA levels in the liver and WAT (Badman, Koester et al. 2009; Potthoff, Inagaki et al. 2009). In whole body PGC1α knockout mice, the downstream effects of FGF21 on gluconeogenesis are reduced, but in liver specific PGC1α knockout mice FGF21 still increases gene transcripts involved in gluconeogenesis (Potthoff, Inagaki et al. 2009; Fisher, Estall et al. 2011). PGC1α also has dynamic interplay with circadian rhythm pathways that are regulated both by light-entraining and in response to metabolic changes (Liu, Li et al. 2007). FGF21 has a circadian rhythm of expression in mouse liver tissue, with increased activation of FGF21 promoter activity by circadian regulators (Tong, Muchnik et al. 2010).

FGF21 expression in the liver is regulated dynamically by both circadian rhythms and by fasting, but the details of this complex interaction have not been elucidated. Possibly FGF21 is regulated in a circadian manner when no major metabolic stressors are present. When fasting occurs, the increase in PPARα and PGC1α activity leads to increases in glycogenolysis and gluconeogenesis. The suppression of FGF21 expression downstream of PGC1α prevents inducing FGF21 expression in early fasting. As fasting progresses, PGC1α levels decrease, alleviating suppression of FGF21 and PPARα activity leads to increases in FGF21 levels in the liver and the release of FGF21 into the bloodstream.

Activation of FGF21 Activity through Feeding Signals. After feeding, blood glucose levels increase and this leads to an increased release of insulin and decreased release of glucagon from the pancreas. The overall effect of insulin is to use and store glucose and maintain its concentration in the bloodstream. Increased insulin levels lead to decreased FGF21 mRNA in liver cells and increased FGF21 increases pancreatic insulin mRNA and storage (Wente, Efanov et al. 2006; Uebanso, Taketani et al. 2009; Tong, Muchnik et al. 2010). A hallmark of FGF21 activity is the lowering of insulin in the bloodstream in multiple models of obesity, diabetes, and in lean animals (Kharitonenkov, Shiyanova et al. 2005; Kharitonenkov, Wroblewski et al. 2007; Coskun, Bina et al. 2008; Berglund, Li et al. 2009; Xu, Lloyd et al. 2009; Xu, Stanislaus et al. 2009; Fisher, Estall et al. 2011).

Increases in cellular glucose concentrations also lead to activation of carbohydrate response element binding protein (ChREBP). ChREBP partners with max-like factor X to activate the synthesis of several enzymes involved in lipogenesis (Uyeda, Yamashita et al. 2002). Glucose increases FGF21 mRNA and protein in liver cells through ChREBP and a putative glucose response element has been identified in the FGF21 promoter region (Iizuka, Takeda et al. 2009; Uebanso, Taketani et al. 2011).

PPARγ increases in response to FAs after feeding and pharmacologically to thiozolidinediones. PPARγ activation leads to transcription of genes important for the uptake of glucose and FAs and the conversion to TGs for storage and differentiation of adipocytes (Kersten, Desvergne et al. 2000; Lefebvre, Chinetti et al. 2006). PPARγ agonists increase FGF21 mRNA in adipocytes but not in liver tissue (Muise, Azzolina et al. 2008; Zhang, Yeung et al. 2008; Dutchak, Katafuchi et al. 2012). Sirtuin 1 (SIRT1) represses PPARγ activity and knockdown of SIRT1 leads to increased FGF21 expression in adipocytes (Picard, Kurtev et al. 2004; Wang, Qiang et al. 2008). FGF21 levels are higher in WAT subsequent to feeding and increased FGF21 leads to adipocyte differentiation. Increased FGF21 also enhances PPARγ activity and increased PPARγ protein concentration (Moyers, Shiyanova et al. 2007; Dutchak, Katafuchi et al. 2012).

Signaling Response Downstream of FGF21. FGF21 is capable of endocrine activity and signals through the FGFR/βKlotho complex. Signaling through the FGFR complex involves docking proteins FRS2α and FRS2β, recruitment of Grb2/Sos and activation of Ras/MAPK pathway, including ERK1 and ERK2 (Eswarakumar, Lax et al. 2005). FGF21 activation of the FGFR complex results in phosphorylation of FRS2α and ERK1/2 and stimulation of pAkt, pGSK-3, pSHP-2, and phosphorylation of MEK1/2, $p70^{S6K}$, Stat3, Raf-1 (Kharitonenkov, Shiyanova et al. 2005; Wente, Efanov et al. 2006; Moyers, Shiyanova et al. 2007). FGF21 signaling has been observed in WAT, liver, and pancreatic cells (Johnson, Weston et al. 2009; Xu, Stanislaus et al. 2009). Egr1 and cFOS, classical downstream targets of ERK1/2, expression are increased in liver and WAT with FGF21 administration (Fisher, Chui et al. 2010; Fisher, Estall et al. 2011). ERK1/2 activation recruits serum response factor and Ets-like protein-1 to the promoter of the FGF21 downstream target gene GLUT1 in adipocytes (Ge, Chen et al. 2011).

FGF21 Response in Adipose Tissue Related to Feeding Signals. The current interest in FGF21 began after it was discovered to lower blood glucose, plasma TGs, fasting insulin, and improve glucose clearance in models of obesity and diabetes by Kharitonenkov and others in 2005. In this study FGF21 was shown to increase GLUT1 glucose transporter mRNA and increase glucose uptake in adipocytes (Kharitonenkov, Shiyanova et al. 2005). Subsequently FGF21 was shown to lower glucose and insulin after glucose stimulation in lean mice, and lower serum glucose, fructosamine, TGs, insulin, glucagon, and improve the lipoprotein profile in diabetic monkeys without inducing hypoglycemia (Wente, Efanov et al. 2006; Kharitonenkov, Wroblewski et al. 2007). Knockdown of FGF21 leads to decreases in GLUT1 and basal and insulin stimulated glucose uptake in adipocytes (Li, Li et al. 2012).

PPARγ activation induces adipocyte differentiation and increases storage of TGs. FGF21 mRNA and protein are increased in WAT in response to PPARγ agonists (Muise, Azzolina et al. 2008; Zhang, Yeung et al. 2008; Dutchak, Katafuchi et al. 2012). FGF21 enhances adipocyte differentiation as indicated by the increased expression of differentiation-related mRNAs and increases in TG content of PPARγ agonist treated cells (Moyers, Shiyanova et al. 2007; Dutchak, Katafuchi et al. 2012). FGF21 enhances PPARγ transcriptional activity and some of the effects of PPARγ agonists require FGF21 activity (Dutchak, Katafuchi et al. 2012). PPARγ agonists increase the amount of GLUT1 expression and glucose uptake induced by FGF21 treatment (Moyers, Shiyanova et al. 2007). This evidence indicates that PPARγ and FGF21 act in concert.

Other effects of FGF21 associated with a feeding response include increasing adipocyte TG content and attenuating lipolysis, and reducing serum FAs (Arner, Pettersson et al. 2008; Berglund, Li et al. 2009; Li, Ge et al. 2009). FGF21 treatment can also increase oxygen consumption, energy expenditure, and physical activity in mice (Coskun, Bina et al. 2008; Xu, Lloyd et al. 2009).

FGF21 Response in Liver Tissue Related to Fasting Signals. The liver has a critical role in the metabolic response to fasting. During fasting liver TG stores are converted to FAs, and along with FAs transported to the liver from adipose tissue, these can be converted to ketone bodies. Ketone bodies are a critical source of fuel as glycogen stores are depleted during long term fasting. The initial effect of FGF21 in liver tissue was observed in FGF21 transgenic mice. FGF21 transgenic mice have less liver fat and when fed a high fat, high carbohydrate diet and they gain less weight than wildtype mice (Kharitonenkov, Shiyanova et al. 2005). FGF21 administration to diet induced obese mice also caused reduction in body weight, body fat mass, liver weight, and liver fat content (Coskun, Bina et al. 2008). FGF21 knockout (KO) mice have increased liver weight and when fed a ketogenic diet FGF21 KO mice accumulate excess lipids in the liver and gain weight when control mice lose weight (Badman, Koester et al. 2009; Hotta, Nakamura et al. 2009). FGF21 expression in the liver leads to lipolysis as indicated by the reduction of liver TGs and increases in serum β-hydroxybutyrate (BHB) with increased FGF21 expression and the opposite effect with knockdown of FGF21 (Inagaki, Dutchak et al. 2007; Badman, Koester et al. 2009). Liver FGF21 expression increases catabolism of liver fat, most notably during the metabolic challenges of long term fasting or a ketogenic diet.

FGF21 mediates the effect of increased liver lipolysis and ketogenesis through transcriptional activation of multiple genes. Increases in FGF21 lead to increases in transcripts of lipases important for the catabolism of TGs, including pancreatic lipase (PTL), pancreatic lipase-related protein 2 (PNLIPRP2), carboxyl ester lipase (CEL), and pancreatic colipase (CLPS). The liver levels of carnitine palmitoyltransferase 1a (CPT1a) and 3-hydroxy-3-methylglutaryl-CoA synthase (HMGCS) proteins, both important for the catabolism of FAs to ketones, are increased in FGF21 transgenic mice (Inagaki, Dutchak et al. 2007). Reduced liver FGF21 results in lower expression of genes involved in lipolysis and ketogenesis, including very long-, long-, and medium- chain Acetyl-CoA dehydrogenase, the β subunit of hydroxyacyl-CoA dehydrogenase, CPT1a, acyl-CoA oxidase, HMGCS, and 3-beta hydroxybutyrate dehydrogenase (Badman, Pissios et al. 2007). In mice fed a high fat diet, administration of FGF21 reduces genes involved in lipogenesis (Xu, Lloyd et al. 2009). FGF21 administration also induces the gluconeogenic genes glucose-6-phosphatase (G6Pase) and phosphoenolpyruvate carboxykinase (PEPCK) and PGC1α (Berglund, Li et al. 2009; Fisher, Estall et al. 2011). In FGF21 KO mice, fasting induced increases in CEL, PTL, PNLIPRP2, PGC1α, and G6Pase are attenuated and the induction of gluconeogenesis is alleviated (Potthoff, Inagaki et al. 2009).

FGF21 Response in Adipose Tissue with Fasting Signals. Although FGF21 increases glucose uptake and TG storage in adipose tissue during feeding with PPARγ signaling, FGF21 can also have the opposite effect. In 2005, Kharitonenkov and others noted smaller subcutaneous adipocytes in mice treated with FGF21 indicating increased lipolysis (Kharitonenkov, Shiyanova et al. 2005). Increased PPARα activity increases FGF21 in liver and serum and results in increases of HSL and adipose triglyceride lipase (ATGL) in WAT in mice. Adipocytes treated with FGF21 have increased glycerol release indicating the breakdown of lipids (Inagaki, Dutchak et al. 2007). Overexpression of FGF21 in adipocytes increases ATGL and HSL and decreases TGs, while knockdown of FGF21 has the opposite effect (Li, Li et al. 2012). Treatment of diet induced obese mice with FGF21 causes reduced fat mass, increases in PPARα, ATGL, HSL, PGC1α expression, and reduced leptin (Coskun, Bina et al. 2008). FGF21 KO mice have increased TG accumulation in adipose tissue and larger adipocytes (Hotta, Nakamura et al. 2009; Johnson, Weston et al. 2009). In fasted FGF21 KO mice leptin levels are increased and when FGF21 KO mice are fed a ketogenic diet there are lower levels of HSL, ATGL, PPARs, and PGC1α (Badman, Koester et al. 2009; Hotta, Nakamura et al. 2009). This evidence indicates FGF21 increases lipolysis in adipocytes, although FGF21 can also increase lipogenesis and reduce lipolysis in this tissue.

Interaction of Fasting and Feeding in FGF21 Activity. The opposing roles of FGF21 in adipose tissue indicate that it may stimulate lipolysis during starvation with corresponding PPARα activity and attenuate lipolysis with feeding and PPARγ activity. This opposing regulation may be mediated through corresponding metabolic signals that indicate a fasting or excessive feeding metabolic challenge. Although this initially appears to be contradictory and has caused several disagreements between experts in the field, it is conceivable that this dynamic interplay is precisely the role of FGF21. My proposal for the role of the FGF21 metabolic response includes both feeding and fasting as important for FGF21 regulation. When there are no metabolic stressors present and a consistent and regular consumption of food is available, FGF21 has low levels of expression that vary with a circadian rhythm (Tong, Muchnik et al. 2010). The circadian changes in PGC1α and the suppression of FGF21 downstream of increased PGC1α regulate circadian rhythm of FGF21 expression (Estall, Ruas et al. 2009). When food availability is reduced and fasting is initiated, PPARα activity increases and leads to increased expression of FGF21 in the liver and release of FGF21 protein into the bloodstream (Inagaki, Dutchak et al.

2007). If the fasting state is extended and PGC1α levels begin to decrease, the PPARα induced expression of FGF21 is more prominent. The role of FGF21 during fasting is to increase expression of genes involved in lipolysis in WAT and increase gluconeogenesis, increase lipolysis, reduce lipogenesis, and increase ketogenesis in the liver (Badman, Pissios et al. 2007; Inagaki, Dutchak et al. 2007; Badman, Koester et al. 2009; Berglund, Li et al. 2009; Potthoff, Inagaki et al. 2009; Fisher, Estall et al. 2011). During this extended fasting state feeding occurs since without eventual feeding fasting leads to starvation and death. Upon feeding after fasting, FGF21 levels increase further (Sanchez, Palou et al. 2009; Oishi, Konishi et al. 2011; Dutchak, Katafuchi et al. 2012). The intake of fats from food leads to activation of PPARγ, FGF21 expression is increased by PPARγ activity and transcription of genes for fat storage in adipocytes is increased (Muise, Azzolina et al. 2008; Zhang, Yeung et al. 2008; Dutchak, Katafuchi et al. 2012). Also the increases in glucose subsequent to feeding result in activation of ChREBP and increased liver FGF21 levels (Iizuka, Takeda et al. 2009; Uebanso, Taketani et al. 2011). The role of FGF21 during feeding subsequent to fasting is to increase the ability to store energy sources through increased uptake of glucose and increased lipogenesis in WAT and gluconeogenesis in liver tissue (Kharitonenkov, Shiyanova et al. 2005; Arner, Pettersson et al. 2008; Berglund, Li et al. 2009; Li, Bao et al. 2009). The prominent role of FGF21 is not specific to either the feeding or fasting state, but rather FGF21 is important for signaling that extended fasting has recently occurred and thus upon re-feeding more energy should be stored in expectation of future fasting conditions. FGF21 is increased less substantially by feeding if fasting has not recently occurred and less of the current energy intake is stored for future use. Thus in my opinion, FGF21 acts as a tracking signal to indicate the amount of current energy source to be stored for future use somewhat like an investment broker handling a retirement account and indicating how much current income should be invested and in what manner for future use.

FGF21 Activity in BAT. BAT is similar to WAT in that it stores TGs, but the unique aspect of BAT is that it uncouples the production of ATP from oxidation and produces heat through the unique presence of thermogenin, a protein transcribed from the gene UCP1. PPARγ and PGC1α act in concert to increase expression of UCP1 in adaptive thermogenesis, which can occur during cold exposure or excess caloric intake (Puigserver, Wu et al. 1998). FGF21 transgenic mice have more BAT than their counterparts (Kharitonenkov, Shiyanova et al. 2005). Cold exposure induces BAT expression of FGF21 that may be released into the blood and also increases BAT PGC1α expression. This increased expression of FGF21 results from β-adrenergic stimulation by norepinephrine mediated by cAMP (Chartoumpekis, Habeos et al. 2011; Hondares, Iglesias et al. 2011). Increasing FGF21 increases UCP1 expression in BAT (Coskun, Bina et al. 2008). FGF21 injection increases thermogenic genes in BAT of neonatal mice, which rely more on heat production from BAT than adults, and causes increased body temperature. FGF21 also causes increases in thermogenic genes in cultured brown adipocytes (Hondares, Rosell et al. 2010). FGF21 increases mitochondrial gene and protein expression in brown adipocytes and BAT in mice. LKB1, AMPK, and SIRT1, and PGC1α are required for this activity of FGF21 (Chau, Gao et al. 2010). FGF21 treatment is also capable of inducing expression of UCP1 and increasing the protein concentration of PGC1α in some WAT depots, inducing the 'browning' of the WAT stores (Fisher, Kleiner et al. 2012).

FGF21 Response in other Tissues: Pancreas, Heart, and Muscle. FGF21 not only has effects in adipose and liver tissues, but activity has also been demonstrated in pancreatic cells, cardiac tissue, and muscle cells. In pancreatic cells FGF21 is capable of inducing signaling and increasing the mRNA and protein insulin content of the cells, but FGF21 does not affect the secretion of insulin or glucagon (Wente, Efanov et al. 2006; Xu, Stanislaus et al. 2009). In diabetic models but not control animals, FGF21 increases the glucose stimulated release of insulin from the pancreas (Wente, Efanov et al. 2006). Treatment of db/db mice with FGF21 preserves pancreatic β-cells, inducing pancreatitis increases FGF21 expression in pancreatic cells, and mice with overexpression of FGF21 have less damage from induced pancreatitis while FGF21 KO mice have more damage (Wente, Efanov et al. 2006; Johnson, Weston et al. 2009). FGF21 treatment increases the success of pancreatic cell transplant in mice (Uonaga, Toyoda et al. 2010). Thus FGF21 has a protective effect on pancreatic cells.

In addition to being protective of pancreatic cells, FGF21 may also be protective of cardiac endothelial cells. In response to injury of cardiac endothelial cells, FGF21 is increased and pharmacologically inducing increased expression of FGF21 reduces apoptosis while knockdown of FGF21 increases apoptosis of cardiac endothelial cells (Lu, Liu et al. 2010).

FGF21 expression has also been observed in muscle cells induced by insulin signaling through Akt1 (Izumiya, Bina et al. 2008). FGF21 treatment of muscle cells can induce GLUT1 mRNA and increase glucose uptake, but this effect was not observed in isolated muscle tissue (Mashili, Austin et al. 2011).

Hypothesis of the Relationship between FGF21 and Torpor. There are several similarities between the effects of increased FGF21 and the metabolic changes observed in a seasonal hibernator. Increases in FGF21 can result in a metabolic profile indicating increased lipolysis. This metabolic profile includes decreased liver weight and smaller adipocytes with increased FGF21 (Kharitonenkov, Shiyanova et al. 2005; Coskun, Bina et al. 2008). Subsequent to long-term fasting FGF21 liver mRNA and serum protein are increased through increased PPARα activity (Badman, Pissios et al. 2007; Inagaki, Dutchak et al. 2007; Lundasen, Hunt et al. 2007). Serum FA levels and serum BHB are increased with increased FGF21 (Inagaki, Dutchak et al. 2007). There are increased transcripts for lipases PTL and HSL, and HMGCS and CPT1 proteins. Increased FGF21 also increases PGC1α levels (Inagaki, Dutchak et al. 2007; Coskun, Bina et al. 2008).

During seasonal hibernation, animals are in a fasting state for several months and lipolysis provides energy during this long term fast. PPARα levels are increased during torpor (Kabine, El Kebbaj et al. 2004; El Kebbaj, Andreoletti et al. 2009). Over the hibernation season WAT volume decreases and liver color changes from pale, indicating high fat content, to dark brown, indicating less fat content (Dark 2005; and unpublished observations). Increased lipolysis during hibernation results in increased serum albumin, free FA, glycerol, and ketones (Baumber, South et al.

1971; Rauch and Behrisch 1981; Krilowicz 1985; Andrews, Russeth et al. 2009; Nelson, Otis et al. 2010; Epperson, Karimpour-Fard et al. 2011; Hampton, Melvin et al. 2011). There are increases in HSL and PTL expression, and increased CPT1, HMGCS, and PGC1α during hibernation (Steinberg and Khoo 1977; Wilson, Deeb et al. 1992; Andrews, Squire et al. 1998; Bauer, Squire et al. 2001; Epperson and Martin 2002; Squire and Andrews 2003; Squire, Lowe et al. 2003; Epperson, Dahl et al. 2004; El Kebbaj, Andreoletti et al. 2009; Shao, Liu et al. 2010). These similarities of the fasting state during hibernation and the effects of increased FGF21 in mice indicate that FGF21 has important role in the metabolic fasting response during hibernation.

There are also other effects of increased FGF21 that are observed in hibernators. PPARγ increases WAT expression of FGF21 and PPARγ protein levels are increased in WAT and BAT during torpor in squirrels and brown bats (Eddy and Storey 2003; Eddy, Morin et al. 2005; Muise, Azzolina et al. 2008; Zhang, Yeung et al. 2008; Dutchak, Katafuchi et al. 2012). Increased FGF21 expression in WAT increases adipocyte TG content, attenuates lipolysis, and reduces serum free FAs (Arner, Pettersson et al. 2008; Berglund, Li et al. 2009; Li, Bao et al. 2009). During the fall before hibernation occurs, hibernators increase adiposity and this occurs despite the amount of food available through reduced MR (Dark 2005). Increased FGF21 increases glucose uptake in WAT, lowers serum insulin levels, and increases pancreatic insulin content (Kharitonenkov, Shiyanova et al. 2005; Wente, Efanov et al. 2006; Kharitonenkov, Wroblewski et al. 2007). Similarly, during torpor serum glucose is decreased and pancreatic insulin content increases (Tashima, Adelstein et al. 1970; Bauman 1990; Buck, Squire et al. 2002; Andrews, Russeth et al. 2009). Serum insulin levels in hibernators are highest before torpor occurs and subsequently decrease (Lyman, Willis et al. 1982; Florant, Lawrence et al. 1985; Tokuyama, Galantino et al. 1991; Boswell, Woods et al. 1994; Buck, Squire et al. 2002). Mice with increased FGF21 levels have more BAT and the BAT has increased UCP1 content and increased thermogenic capacity (Kharitonenkov, Shiyanova et al. 2005; Coskun, Bina et al. 2008; Chau, Gao et al. 2010; Hondares, Rosell et al. 2010). This increase corresponds to increased levels of PGC1α (Chartoumpekis, Habeos et al. 2011; Hondares, Iglesias et al. 2011). BAT is essential during hibernation for warming and before hibernation occurs BAT volume increases, there is increased UCP1 content and increased thermogenic capacity. PGC1α levels are also increased in BAT of hibernators (Boyer, Barnes et al. 1998; Liu, Lin et al. 1998; Barger, Barnes et al. 2006; Yan, Burman et al. 2006; Kitao and Hashimoto 2012).

FGF21 activity is observed during the extremes of metabolic challenge in mice, both during long-term fasting and upon re-feeding. Naturally hibernators annually experience an extended fasting state and hibernators consume excess food to store as adipose tissue in preparation for hibernation. This natural dichotomy of metabolism observed in hibernators may involve FGF21 expression as part of the coordination between metabolic states.

Along with the similarities between hibernation and FGF21, increased levels of FGF21 cause increased sensitivity for fasted mice to enter torpor (Inagaki, Dutchak et al. 2007). This evidence prompted us to investigate the effect of increased FGF21 levels on the induction of torpor, metabolite response, and lipolysis-related gene expression in a seasonal hibernator. We have hypothesized that increased FGF21 sensitizes TLG squirrels to enter torpor and changes the metabolic and gene expression profile to indicate increased lipolysis.

CHAPTER 2

METHODS

Animal Maintenance and Surgery

General Animal Collection and Maintenance. All animal protocols were approved by the University of Minnesota Institutional Animal Care and Use Committee. Thirteen-lined ground squirrels were wild-caught in Southern Minnesota and transferred to Research Animal Resources at the University of Minnesota Duluth. Squirrels were kept at 23 ºC with a 12:12 light:dark schedule. Most squirrels were fed Laboratory Rodent Diet 5001 (PMI Nutrition International). If animals appeared very small and thin at the time of arrival to the facility, they were placed on Iams Chunks Dog Food with a higher fat content (at least 15%) to facilitate accumulation of adipose tissue in preparation for hibernation and enhance survival during the transition to a laboratory setting from the wild environment.

For experiments involving measurement of natural seasonal fluctuations of metabolites, mRNA, and proteins of interest to this study, squirrels were placed on a ambient temperature and light cycle schedule that replicates hibernation season conditions in the wild. The squirrels were maintained at 23 °C with a 12:12 l:d cycle and food and water available *ad libitum*. In November food was removed, the light cycle was changed to 24 h dark, and the hibernaculum temperature was reduced to 5 ºC where it remained until March. The squirrels remained in the hibernacula through the second week of March when the ambient temperature was increased to 23 ºC, light cycle was returned to 12:12 l:d, and food was supplied freely. All squirrels had access to water during the entire year. Samples were examined from active squirrels in August and March and from torpid and IBA squirrels from December through February (Fig 2.1, open arrows).

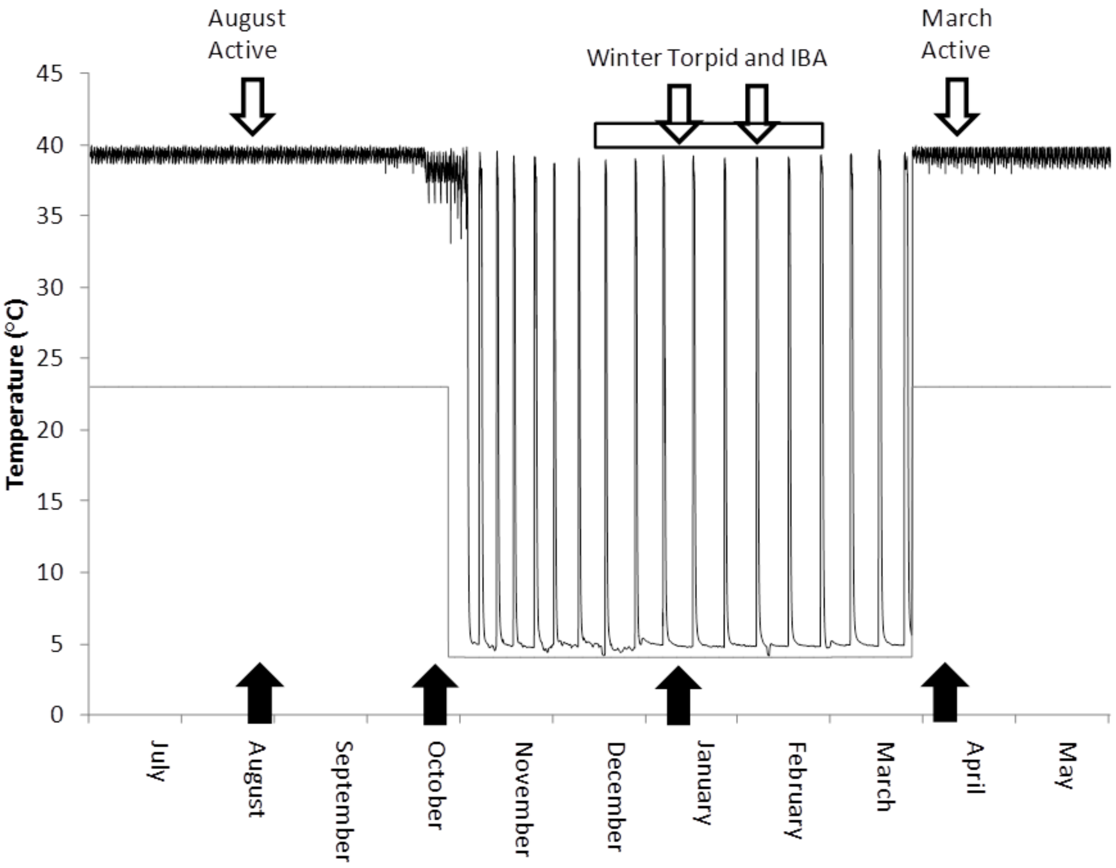

Figure 2.1: Illustration of experimental design. A schematic of thirteen-lined ground squirrel body temperature fluctuations (black line) and laboratory ambient temperature (gray line). Samples were collected without experimental interventions from August active, March active, and winter torpid and IBA squirrels (open arrows). Squirrels were injected with AdRR5 or AdFGF21 at times indicated by black arrows. Adenovirus administration in January was only done in pilot experiments and this experiment was discontinued due to lack of healing at the low body temperatures of torpor.

Pilot experiments involving increasing FGF21 levels using adenovirus mediated expression were done in August, October to November, January, and March to April (Fig 2.1, black arrows). Hibernating squirrels in January had poor surgical recovery and this experimental time point was discontinued after pilot experiments. In all future studies, squirrels receiving adenovirus were maintained at 23 ºC, 12:12 l:d, and fed freely until adenoviral administration. In one experimental set after the hibernation season at the end of March into the beginning of April, squirrels were maintained at 23 °C with a 12:12 l:d cycle and fed freely after receiving the adenoviral construct. In another experimental set after the hibernation season at the end of March and in the beginning of April and in the experimental sets performed in August, October, and January squirrels were maintained at 5 °C with a 24 h dark cycle and no food was available in order to allow typical deep torpor of the experimental squirrels to occur. One experimental set was done in November to determine the effect of fasting without changes in light cycle or temperature and the squirrels were maintained at 23 °C with a 12:12 l:d cycle without food available after administration of the adenoviral construct. Serum and tissue samples were collected in these experiments at 3, 5, 7, 10, or 12 days in pilot experiments in order to evaluate when the adenoviral construct administration resulted in increased levels of FGF21. Raised levels of FGF21 were apparent at all points between 3 and 12 days and the remaining experimental samples were collected at 7 days.

Preparation of Surgical Supplies. All surgical tools were sterilized by autoclaving at 28 psi, 270 °F, for 3 min with a 5 min pre-vacuum cycle and a 10 min post-vacuum cycle. CTA-F40 transmitters (Data Sciences International) were sterilized by soaking in Actril Cold Sterilant (Minntech) for 24 hours, rinsing 3 times with sterile water and soaking in sterile water for 24 hours to remove any sterilant before implant. Sterile surgical technique as detailed by Research Animal Resources at the University of Minnesota was used for all surgeries.

Anesthesia. Initial anesthesia was achieved by placing an isoflurane (Pheonix Pharmaceutical, Inc.) soaked gauze pad in a sealed cage with a squirrel. When anesthesia depth was observed by evaluating lack of movement and slowing of respirations, the squirrel was weighed and administered isoflurane through a nose cone with a vacuum system for flow of anesthetic and removal of isoflurane from the surgery suite. Isoflurane was mixed with breathing air (Praxair, 19.5% to 23.5% oxygen, less than 10 ppm carbon monoxide, less than 1000 ppm carbon dioxide, less than 24 ppm water) at a range of 0.5% to 5%. Anesthetic depth was evaluated using a toe pinch and the isoflurane dosage was monitored and adjusted according to the respiration rate and rectal body temperature (Physitemp, BAT-12) observed throughout the surgical procedure. On occasion, 5% isoflurane was not sufficient to maintain anesthesia throughout surgery. This was especially noted during the late fall and winter months when squirrels had notable white adipose tissue and were prepared to enter torpor. When 5% isoflurane was not sufficient to maintain anesthesia, a gauze pad dampened with isoflurane was placed inside the nose cone to maintain anesthesia.

Transmitter Implant. Before surgery the ventral surface was shaved, any loose fur was removed, and the squirrel was secured to the surgical table with tape. The skin was cleaned and disinfected using three alternating washes with betadine (Purdue Products L.P., povidone-iodine, 7.5%) and 70% ethanol (Aaper Alcohol and Chemical Co.). Each wash was started in the center of the abdomen and a spiral movement was used until the gauze came in contact with the outer edge of the shaved region. Before surgery began anesthetic depth was assured using a toe pinch and a rectal thermometer probe was inserted. The initial incision through the epidermis of approximately one inch was made along the bilateral line ventral to the intestines. A blunt tipped scissors was used to detach the connection between the epidermis and the abdominal muscle to expose the region around the incision site. A small pointed scissor was used to make a ¾ inch incision through the abdominal muscle, taking care not to puncture the intestines. A CTA-F40 transmitter capable of collecting body temperature, electrocardiogram (ECG), and activity data was placed inside the abdominal cavity ventral to the intestines and positioned so the ribs of the transmitter were aligned with the abdominal muscle incision. A 14 gauge needle (Kendall Monoject Hypodermic Needle, Aluminum Hub) was used to puncture the abdominal muscle near the anterior end of the abdominal incision on both sides. One milliliter of 0.9% sterile saline solution was injected into the abdominal cavity to prevent drying during the procedure. The negative ECG lead (clear) of the transmitter was thread through the needle on the dextral side of the incision and the positive ECG lead (pink) was thread through the needle on the sinister side of the incision. The negative lead was tunneled subcutaneously to the dextral pectoral muscle. A 4 inch, 14 gauge laboratory cannula (Becton, Dickenson and Company, #1789 1250NR) was ideal for tunneling and sterilization for reuse. A 1.5 cm region of the ECG lead was exposed using a razor blade to remove the casing. The end of the casing remaining on the ECG lead was closed by tying a piece of silk suture (Patterson Dental Supply, Inc., non-absorbable surgical suture, black braided type B) in a square knot around the casing. This prevented liquid from entering the transmitter and interfering with its electronic components. A 20 gauge needle (Kendall Monoject Hypodermic Needle Aluminum Hub, 200219) was tunneled through 1 cm of the pectoral muscle just below the surface of the muscle. The ECG lead was thread through the needle and the end of the ECG lead was capped with a section of the casing and secured with silk suture tied in a square knot. The exposed section of the ECG lead metal was adjusted to lie flat in the pectoral muscle and any excess lead was pulled into the abdominal cavity. The incisions were kept moist using 0.9% sterile saline solution throughout the procedure. The positive lead was tunneled subcutaneously to approximately 1 cm sinister to the xyphoid process and secured in the same manner as the negative lead. The exposed sections of the two ECG leads created a diagonal line crossing the heart. After securing the leads, the transmitter ribs were secured to the abdominal wall with polyamide monofilament, non-absorbable surgical suture (Black, 4/0, 18 inch, with DS19 3/8 19 mm needle, Veterinary Products Laboratories), and any open section of the abdominal incision was sutured. All incisions were closed using surgical staples (3M, Precise©, DS-25). Anesthesia was ceased and the squirrel was placed on a paper towel on bedding in a cage and monitored for anesthetic recovery. All animals were given 15 mg/kg ibuprofen in their water (2.35 ml in 500 ml water bottle, Children's Motrin, ibuprofen 100 mg per 5 ml) and fed freely during recovery from transmitter implant for at least 7 days.

Characterization of Ground Squirrel FGF21 Sequence. The sequencing of thirteen-lined ground squirrel FGF21 was kindly performed by Xunshan Ding, Ph.D. at University of Texas Southwestern Medical Center. The FGF21 DNA sequences from multiple species were aligned and primers that flanked a conserved region were selected. The primers selected were: primer A) 5' AAG CCC ACC TGG AGA TCA GG 3' (20 mer) and primer B) 5' TCT GAA ACT GCA GGC CTC AGG 3' (21 mer). These primers flanked an approximately 200 bp region of cDNA. Low-stringency PCR was performed with the following conditions: 94 °C 2 min; 40 cycles of 94 °C

30 sec, 53 °C 30 sec, 72 °C 1 min; then 72 °C 7 min; 4 °C hold. This was followed by 5' and 3' rapid amplification of cDNA ends (RACE). Primer B was used for 5' RACE with the following conditions: 94 °C 3 min; 40 cycles of 94 °C 30 sec, 64 °C 30 sec, 72 °C 1 min; then 72 °C 7 min; 4 °C hold. Primer A was used for 3' RACE with the following conditions: 94 °C 3 min; 40 cycles of 94 °C 30 sec, 60 °C 30 sec, 72 °C 1 min; then 72 °C 7 min; 4 °C hold.

Development of Ground Squirrel FGF21 Expressing Adenovirus. Adenoviruses were kindly produced by Robert D. Gerard, Ph.D. at the University of Texas Southwestern Medical Center. The cre-loxP method was used to produce recombinant adenoviruses as described by (Gerard and Meidell 1995). Briefly, the thirteen-lined ground squirrel FGF21 cDNA sequence was inserted into the *Xba*I and *Hind*III sites in the polylinker region of the pACCMVpLmP1(-)loxP-SSP plasmid. The FGF21 sequence was 645 Kb long, and the coding region was 627 bp (Fig 2.2). The adenoviruses were cloned by plaque assay and propagated on 911 cells. For *in vivo* use, crude stocks were purified sequentially by centrifugation on CsCl step gradients and gel filtration on Sepharose CL-4B columns equilibrated with Tris-buffered isotonic saline (137 mM NaCl, 5 mM KCl, 10 mM Tris-HCl pH 7.4, 1 mM $MgCl_2$). Absorbance at 260 nm ($1A_{260}$ equals $1x10^{12}$ particles/ml) was used to determine particle concentration. After the addition of 10% glycerol, viruses were stored frozen at -80 °C at concentrations between 10^{12} and 10^{13} particles/ml until use.

Thirteen-lined Ground Squirrel FGF21 Signaling. Thirteen-lined ground squirrel FGF21 signaling capability was kindly examined by Jamie Boney-Montoya, Ph.D. at University of Texas Southwestern Medical Center. Primary preadipocytes

```
tagtgacgtcagatccggtcgcgcgaattcgagctcggtacccggggatcctctagaaccaccatggact
gggtcaaggccaagttggagcccctgggactgtgggtcctggtgctggctgcccttgtgctgggagcctg
ccaggcgtaccccatccctgactcaagccccctcctccaatttgggggccaagtccggcagcggtacctg
tacacagatgatgcccaggagactgaggcccacctggagatcagggctgatggcaccgtggtgggggctg
cccatcaaagcccggaaagtctcttggaactgaaagccttgaagcctggggtcattcaaatcttgggggt
caaaacatccaggttcctgtgccagaggccagatggagtgctgtatggatcgctccactttgaccctgag
gcctgcagcttccgggagcagcttctggaggacgggtacaacgtttaccagtcagaatcccacggcctcc
ccgtgcgcctgccccctaactcaccataccgggacccagcgccgccaggaccagcccgcttccttccact
gccaggcctgcccccagcagccctggagccgccagggatcctgggccctgagcccccctgatgtgggctcc
tccgacccactcagcatggtggggcctttgcagggccgaagccccagttacgcttcctgaaagcttggga
tctttgtgaaggaaccttacttctgtggtgtgacataattggacaaactacctacagagatttaaagctc
taaggtaaatataaaatttttaagtgtataatgtgntaaactactgattctaattgtttgtgtattttag
attcacagtcccaaggctcatttcaggcccctcagtcctcacagtctgttcatgatcataatcagccata
```

Figure 2.2. Ground squirrel FGF21 sequence inserted into adenoviral vector pACCMVpLmP1(-)loxP-SSP between *Xba*I and *Hind*III sites.

were isolated from postnatal day 4 wild-type mice, grown to confluency in 6-well plates, and differentiated in media containing high-glucose DMEM plus 10% FBS, 5 μg/ml insulin, 0.5 mM isobutylmethylxanthine, and 1.0 μM dexamethasone (Detailed protocol available in (Dutchak, Katafuchi et al. 2012). After 2 days, differentiation was induced and media was replaced every other day for 6 more days with media containing high glucose DMEM plus 10% FBS and 5 ug/ml insulin. On day 10 of differentiation, media was replaced with serum-free high glucose DMEM for 24 h and adipocytes were treated with serum-free conditioned media from permissive 911 cells infected with adenovirus expressing either control, murine FGF21, or thirteen-lined ground squirrel FGF21 for 10 minutes. Cells were collected in 300 µl lysis buffer containing 10 mM Tris-HCl, pH 7.4, 5 mM EDTA, 5 mM EGTA, 150 mM NaCl, 10% Glycerol, 1% NP-40, 0.5% Triton X-100, with complete protease inhibitor cocktail (Roche) and phosphatase inhibitor cocktail (Roche) per well. Samples were centrifuged at 13,000 rpm for 30 minutes at 4 °C and supernatants were collected and diluted with 2X SDS sample buffer (Sigma), boiled for 3 minutes, and frozen at -20 °C until processed. Lysate samples of 50 ug were resolved on a 10% SDS-polyacrylamide gel and transferred to a nitrocellulose membrane (Bio-Rad). The membrane was blocked in 5% milk/TBS-T and probed with a specific P-ERK1/2 (thr202/tyr204) (Cell Signal) or total-ERK antibody (Cell Signal) at a 1:1000 dilution at 4 °C overnight followed by a secondary horseradish peroxidase-conjugated antibody. Proteins were resolved by Enhanced Chemiluminescence (ECL) western blotting substrate (Pierce) according to manufacturer's instructions. Primary antibodies were prepared in a 3% BSA/TBS-T solution and secondary antibodies in a 5% milk/TBS-T solution.

Adenovirus Injection. After recovery from surgical transmitter implant for at least 7 days, an anesthetized squirrel was weighed, the length was measured, and the left thigh and lower abdomen were shaved. The squirrel was placed under a dissecting microscope (Bauch and Lomb, 1X to 2.5X magnification) and anesthetic depth was determined by a toe pinch. A 1.5 cm incision was made through the epidermis at the anterior end of the thigh above the knee joint and excess adipose tissue was removed in order for observation of the blood vessels. The bifurcation of the femoral vein and artery in the thigh was located and the artery was gently lifted and connective tissue was removed by stripping with a micro-forceps. Silk suture was tied around the posterior end of the cleaned artery and a micro-hemostat was used to create tension on the artery by clamping the suture and placing the hemostat near the knee of the squirrel. A piece of silk suture was tied around the anterior end of the cleaned femoral artery section. A micro-scissors (Miltex, 18-1618) was used to make a diagonal incision approximately half-way through the artery. A cannula was composed of 3 cm of PE10 tubing (Polyethylene, Braintree Scientific) with a beveled tip inserted into 30 cm of PE50 tubing (Polyethylene, Braintree Scientific) with a 23 gauge needle (Kendall Monoject, Polypropylene Hub) in the other end of the PE50 tubing. The cannula was filled with heperanized saline (sterile saline containing 100 units USP per ml heparin sodium, AAP Pharmaceutical). The cannula was carefully inserted into the incision in the femoral artery without breaking the artery or puncturing the opposite side of the artery with the beveled cannula tip. While holding the cannula secure and clamping gently to the artery to prevent blood loss the anterior silk suture was loosened with the opposite hand. The cannula was gently threaded into the artery taking care to keep the artery intact and feeling for the connection to the iliac artery and not forcing past that connection until approximately 2 cm of the PE10 tubing was in the artery. The cannula was secured to the artery with silk suture and the squirrel was checked for any bleeding around the cannulation site. One ml of blood was removed through the cannula using a 1 ml syringe (Kendall Monoject Tuberculin Syringe, Without Needle) and placed in a 1.5 ml microfuge tube (Dot Scientific) on ice. The squirrel and dissection microscope were moved to a Biosafety Level-2 Cabinet.

Adenoviral solution was prepared at a concentration of 7.5×10^{12} particles per gram squirrel weight by dilution in 0.9% sterile saline. The diluted adenoviral solution was injected into the squirrel through the cannula using a 1 ml syringe followed by 1 ml of 0.9% sterile saline. The cannula was carefully removed from the femoral artery and the artery was securely closed using silk suture tied in a gentle double square knot above the incision to prevent breakage of the blood vessel. The hemostat was removed from the posterior silk suture and suture ends were trimmed. The incision was closed using surgical staples, and the squirrel was returned to a cage with pine shaving bedding on a paper towel. The squirrel was given 15 mg/kg ibuprofen in the water (2.35 ml in 500 ml water bottle, Children's Motrin, ibuprofen 100 mg per 5 ml) and recovery from anesthesia was monitored.

All waste contaminated by possible contact with adenovirus including any packaging or gauze that was in the biosafety cabinet and animal bedding was autoclaved at 270 °F, 28 psi, for 60 min with an exhaust rate of 0.5 psi/min before disposal. The inside of the biosafety cabinet, all surgical tools, and other reusable supplies were sprayed with 10% bleach water and allowed to sit for 10 minutes before cleaning.

Monitor and Collection of Physiological Parameters. Transmitters were calibrated by allowing them to come to a thermal equilibrium in stirred water at temperatures of 3, 20, 35, and 40 ºC and recording the mV reading on channel 2. The electrocardiogram collection was calibrated by Data Sciences International before the transmitters were shipped.

The Dataquest A.R.T. system was installed with hardware purchased from Data Sciences International. A Dell Optiplex GX520 PC with a Pentium 4, 3.2 GHz with HT, 800 MHz front side bus, 2 MB Cache processor, 1 GB RAM, 160 GB NTFS hard drive, and Windows XP Professional, Service Pack 2, and the Dataquest PCI Card installed was used for data collection. The COM jack from a Data Exchange Matrix (271-01117-001) was connected to the J1 jack on the Dataquest PCI card in the PC using an 8-pin, twisted pair communication cable. The COM jack from another Data Exchange Matrix was connected to a row A jack in the Data Exchange Matrix that was already connected to the PCI card. Four receivers (RPC-1, 272-6001-001) were connected to each receiver in the C jacks.

Dataquest A.R.T. 4.1, gold edition software had been installed on the PC connected to the physiological monitoring equipment. In the Acquisition program, a new configuration was set-up for each set of physiological monitoring experiments. For each transmitter the type, calibration values, and serial number were entered into Acquisition along with the animal ID that each transmitter was implanted in. Each transmitter ID was linked to the receiver ID upon which that squirrel was placed in the configuration set-up in Acquisition.

Squirrels given control adenovirus (AdRR5) or adenovirus that increased the expression of ground squirrel FGF21 (AdFGF21) were allowed to recover from anesthesia before the cage was placed on the receiver that was configured to detect the transmitter that had been implanted into that squirrel. For all squirrels, the data monitoring and collection was initiated at the time the squirrel was placed on the receiver and continued for a minimum of 7 days. All physiological data was temporarily stored on the hard drive of the collection PC until it could be transferred to two separate external hard drives (WD, 500 GB) to store all data in duplicate.

Tissue and Serum Collection. The squirrel was anesthetized, weighed, and a rectal body temperature was taken. The abdomen was shaved and loose hair was removed. An incision was made along the bottom of the rib cage and the diaphragm was disconnected from the inside of the ribcage. An incision was made through the ribs on the dextral side of the sternum and also through the lower sinister rib bones. The heart was exposed by lifting the sinister side of the rib cage and securing to a hemostat. A 14 gauge needle attached to a 6 ml syringe was used to puncture the heart, attempting to enter through the bottom of the left ventricle. Blood was aspirated into the syringe as the heart beat. In torpid animals the heart rate is very low and aspiration of blood was difficult. Special care was taken not to collapse the ventricle by aspiration in this case. The blood was put into a 15 ml centrifuge tube and stored on ice. The squirrel was decapitated with a rat guillotine and the head and body were placed on chilled aluminum blocks. Organs, including brain, heart, liver, brown adipose tissue, white adipose tissue, kidney, adrenal glands, skeletal muscle, and spleen were removed, trimmed, and snap frozen in liquid nitrogen in cryovials (Nunc Cryotube Vials, 1.8 ml, 368632). All tissues were stored in -80 ºC freezer or in liquid nitrogen as space allowed.

Hematocrit Determination. Following cardiac puncture and blood collection, a hematocrit tube (Fisherbrand Heparinized Micro-Hematocrit Capillary Tubes, 22-362-566) was placed at the opening in the cardiac tissue and blood wicked into the tube until it was approximately 2/3 full. One end of the tube was sealed with Critoseal (McCormick Scientific, 215003). Six tubes were prepared for each animal and centrifuged at 17,000 rpm for 5 min. The percentage of red blood cells in the whole blood was calculated by measuring the distances of each component from the clay sealant. Six replicate measurements were taken for one average value for each squirrel.

Serum Preparation. Blood was allowed to clot on ice after removal. If the blood sample was greater than 1 ml, the 15 ml centrifuge tube was centrifuged at 10,000 x g (Beckman) at 4 ºC for 10 min. The serum supernatant was aspirated and transferred to 1.5 ml microcentrifuge tubes. A second centrifugation was performed at 10,000 x g in a cold room at 4 ºC for 10 min. If the blood sample was 1 ml or less, the sample was centrifuged once at 10,000 x g in a cold room at 4 ºC for 10 min. The serum supernatant was aliquoted and stored at -80 ºC until analysis.

Metabolite Analysis

β-Hydroxybutyrate. Serum β-hydroxybutyrate was measured using β-Hydroxybutyrate LiquiColor Kit (Stanbio Laboratory, 2440-058). Serum aliquots were thawed on ice. In a 96-well plate 215 μl of Enzyme R1 (Stanbio Laboratory, 2441) was pipetted into each well. A standard curve was prepared by pipetting 6, 4.8, 3.6, 2.4, 1.2, and 0 μl of standard solution (1 mM Sodium D-3-hydroxybutyrate) in duplicate into 10 wells, and adding 0, 1.2, 2.4, 3.6, 4.8, and 6 μl, respectively, of distilled water to dilute to 6 μl per well. Serum samples (6 μl) were pipetted in duplicate into the remaining wells. The 96-well plate was incubated at 37 ºC for 3 minutes and blank absorbance was measured at 492 nm wavelength with a Multiskan plate-reader. Catalyst reagent (36 μl R2, Stanbio Laboratories, 2442) was rapidly pipetted into each well and the plate was incubated at 37 ºC for 3 minutes. Final absorbance was measured at 492 nm wavelength with a Multiskan plate-reader. β-hydroxybutyrate concentrations were calculated by averaging the duplicate blank and final measurements and subtracting the blank absorbance. A standard curve was calculated by plotting the absorbance against the known standard concentrations and solving for the slope and intercept of the linear equation. This equation was used to calculate the unknown concentrations of β-hydroxybutyrate in the serum samples.

Non-esterified Fatty Acids. Non-esterified fatty acids (NEFA) were measured in duplicate using HR Series NEFA-HR (2) kit (Wako). Color Reagent Solution A (0.53 U/ml Acyl-coenzyme A synthetase, 0.31 mM Coenzyme A, 4.3 mM Adenoxine triphosphate, 1.5 mM 4-aminoanitipyrine, 2.6 U/ml Ascorbate oxidase, and 0.062% Sodium azide, 50 mM phosphate buffer, pH 7.0) was prepared by adding one bottle of Solvent A (Wako, 995-34791) to one vial of Color Reagent A (Wako, 999-34691) and mixing gently until completely dissolved. This solution was stable at 4 ºC for 10 days and was used within that time. Color Reagent Solution B (12 U/ml Acyl-coenzyme A oxidase, 14 U/ml peroxidase, 2.4 mM 3-methyl-N-ethyl-N-(β-hydroxyethyl)-aniline) was prepared by adding one bottle of Solvent B (Wako, 993-35191) and mixing gently until completely dissolved. This solution was stable at 4 ºC for 3 weeks and was used within that time. Serum aliquots were thawed on ice. Standard NEFA samples were prepared by pipetting 5, 4, 3, 2, 1, and 0 µl of NEFA Standard Solution (1 mM Oleic acid, Wako, 276-76491) into duplicate wells in a 96-well plate and adding 0, 1, 2, 3, 4, and 5 µl of deionized water respectively. Aliquots of 5 µl of serum samples were pipetted into wells in duplicate and 200 µl of Color Reagent A Solution was added to standard and unknown sample wells. The 96-well plate was gently mixed and incubated at 37 ºC for 5 minutes. Blank absorbance was measured at 540 nm wavelength. A 100 µl aliquot of Color Reagent Solution B was pipetted into each sample well and the 96-well plate was gently mixed and incubated at 37 ºC for 5 minutes. Final absorbance was measured at a wavelength of 540 nm.

The mean blank absorbance was subtracted from the mean final absorbance for each sample. The absorbencies of the standard solutions were plotted against their known concentrations and the linear equation was solved. This equation was used to calculate the NEFA concentrations of the unknown serum samples.

Triglycerides. Serum triglyceride (TG) concentrations were measured using an L-Type TG H kit (Wako). Serum aliquots were thawed on ice. Standards (107 mg/dl TG, Lipids Calibrator, Wako, 464-01601) were pipetted in duplicate into wells of a 96-well plate at volumes of 5, 10, 15, 20, and 25 μl, and 5 μl of serum samples and deionized water were pipetted in duplicate into other wells. Enzyme Color A (80 μl, 50 mM Good's buffer, pH 7.0, 0.45 mM N-(2-hydroxy-3-sulfopropyl)-3, 5-dimehoxyaniline, 30 IU/ml glycerol kinase, 4.0 mM ATP, 3.8 IU/ml glycerol-3-phosphate oxidase, 4.0 IU/ml catalase, 2.4 IU/ml ascorbate oxidase, Wako, 997-37492) was pipetted into each well. The plate was gently mixed and incubated at 37 ºC for 5 minutes. The blank absorbance of samples was taken at a wavelength of 595 nm. Enzyme Color B (40 μl of 50 mM Good's buffer, pH 7.0 containing 150 IU/ml lipoprotein lipase, 13.5 IU/ml peroxidase, 3.4 mM 4-aminoantipyrine, 0.1% sodium azide, Wako, 993-37592) was added to each sample well, the plate was gently mixed, and incubated at 37 ºC for 5 minutes. The final absorbance of the samples was measured at a wavelength of 595 nm. The average blank absorbance was subtracted from the average final absorbance for all sample measurements. A standard calibration curve was made by plotting standard absorbance against volume adjusted known concentrations and the linear equation was solved. The linear equation was used to determine the TG concentrations of unknown serum samples.

Glucose. Serum glucose concentrations were measured using a Glucose LiquiColor kit (Stanbio Laboratories, 1070-125). Serum aliquots were removed from storage at -80 ºC and thawed on ice. Glucose standards (100 mg/dl glucose in aqueous benzoic acid, Stanbio, 1072) were aliquoted into duplicate wells in a 96-well plate at volumes of 3, 4, 5, 6, and 7 µl. An aliquot of 3 µl of serum samples and deionized water were pipetted in duplicate in the remaining wells. Aliquots of 300 µl of Glucose LiquiColor Reagent (0.2 mM 4-aminoantipyrine, 15.0 U/ml glucose oxidase, 1.2 U/ml peroxidase, 4.0 mM phenol, Stanbio Laboratories, 1071) were pipetted into each sample well. The plate was gently mixed and incubated at 37 ºC for 5 minutes. The absorbance of samples was measured at a wavelength of 492 nm. A standard curve was made by plotting absorbance against known concentration of the standards and the linear equation was solved. This equation was used to calculate the concentration of glucose in the serum samples.

Insulin. Serum insulin was measured using an Ultra Sensitive Mouse Insulin ELISA Kit (Crystal Chem Inc, 90080). All kit reagents were equilibrated to room temperature and serum aliquots that had been stored at -80 °C were thawed on ice. The mouse insulin standard was reconstituted with 100 µl of distilled water and wash buffer stock solution was diluted to 1 l with distilled water. Mouse insulin standards were prepared by diluting 50 µl of mouse insulin stock solution (25.6 ng/ml) to 200 µl with sample diluent and mixing to make a 6.4 ng/ml standard. Six more standards were prepared by diluting each 1:2 with sample diluent and one blank was prepared using sample diluent only. In each well of the antibody-coated microplate, 96 µl of sample diluent was dispensed. Standard and unknown serum sample aliquots of 5 µl were dispensed into wells in duplicate and the plate was incubated at 4 °C for 2 h. Well contents were aspirated and washed five times with 300 µl of wash buffer per well. Anti-insulin enzyme conjugate was prepared by mixing 3.6 ml of anti-insulin enzyme conjugate stock solution with 1.8 ml of enzyme conjugate diluent and mixed. In each well, 100 µl of anti-insulin enzyme conjugate was added. The plate was covered and incubated for 30 min at room temperature. All well contents were aspirated and wells were washed five times with 300 ul of wash buffer per well. Aliquots of 100 µl of enzyme substrate solution were added to each well and allowed to react for 40 min at room temperature in a dark drawer. After 40 min of reaction time, the reaction was stopped using 100 µl of enzyme reaction stop solution. The absorbances of samples were read at 450 nm and 630 nm using a plate reader. The absorbances at 630 nm were subtracted from absorbances at 450 nm. A standard curve with linear fit was calculated and the equation of the line was used to determine insulin concentrations of the unknown samples.

Gene Expression Analysis

RNA Extraction. RNA extraction was completed using RiboPure Kit (Ambion) as per directions. Briefly, squirrel tissue was removed from storage at -80 °C and placed in liquid nitrogen. The tissue was gently removed from the cryovial and 300 mg of liver tissue or 1 g of WAT was weighed. The tissue was crushed with a mortor and pestle in liquid nitrogen to a powder. Tissue was homogenized in 20X volume of TRI Reagent (Ambion) using short 30 s bursts. The homogenate was incubated at room temperature for 5 min and then centrifuged at 12,000 x g for 10 min at 4 °C. The supernatant was transferred to a new tube and the cell debris pellet was discarded. A 100 ul aliquot of bromochloropropane was added to each tube containing approximately 1 ml of supernatant and mixed vigorously for 15 s. The homogenate was incubated at room temperature for 5 min and then centrifuged at 12,000 x g for 10 min at 4 °C. The aqueous layer, approximately 500 µl, was transferred to a new tube. A 0.5X volume of ice cold 100% ethanol was added to the solution and mixed immediately. The RNA solution was passed through a RiboPure filter (Ambion) using centrifugation in a bench top mini-centrifuge for 30 s. The filter was washed 2X with 500 µl of wash solution provided with the filter (Ambion) and the filter was dried with an additional centrifugation. A 100 µl aliquot of elution buffer (Ambion) was added to the dried filter and incubated at room temperature for 2 min. The filter was centrifuged in a bench top mini-centrifuge for 30 s to elute the RNA and the RNA was mixed into solution. The concentration of RNA was determined by measuring the absorbance of the sample at 260 nm, and the integrity was confirmed using the absorbance at 260 to 280 nm ratio (Nanodrop).

RNA Quality Confirmation. RNA quality was confirmed by running 1 µg of RNA with 2 µl of 6X loading dye on a 1.5% agarose gel in 1X TAE buffer (Tris base 0.2 M, acetic acid 0.2 M, EDTA 0.01 M, pH 8.0) with < 1 µl of ethidium bromide solution (0.5 µg/µl) added to the gel. Electrophoresis was applied to the gel at 100 V until the loading dye reached 2/3 of the way to the end of the gel. A UV image was taken of the gel with a BioRad ChemiDoc XRS using Quantity One software. If the UV image of the gel contained 2 clear bands, the RNA quality was considered adequate for use. If a smear was present on the UV image of the gel, the

RNA sample was discarded and a new sample was prepared from tissue. The RNA solutions were aliquoted and stored at -80 °C.

Preparation of cDNA. Preparation of cDNA from the extracted RNA was done using QuantiTect Reverse Transcription Kit (Qiagen) as per directions. The template RNA, gDNA Wipeout Buffer, Quantiscript Reverse Transcriptase, Quantiscript RT Buffer, RT primer mix, and RNase-free water were thawed on ice. The primer mix provided in the QuantiTect Reverse Transcription kit was a mix of oligo-dT and random primers. The reverse transcriptase contains a mix of recombinant heterodimeric enzymes expressed in *E. coli* and RNase inhibitor. The RT buffer contained dNTPs in buffered solution. Each RNA sample concentration was read in triplicate on a Nanodrop 1000 Spectrophotometer. The mean concentration was used to calculate the volume of RNA sample that contained 500 ng of RNA and this was aliquoted into the PCR reaction tubes. RNase-free water was also added to the reaction tubes to a total volume of 6 µl. A 1 µl aliquot of gDNA Wipeout Buffer was added to each reaction tube. The tubes were mixed and briefly centrifuged. To eliminate any DNA contamination the reactions were incubated at 42 °C for 2 min and placed immediately on ice. A master mix was prepared using 0.5 µl Quantiscript Reverse Transcriptase, 2 µl Quantiscript RT Buffer, and 0.5 µl of RT primer mix per each reaction. A no-RT master mix was also prepared using RNase-free water in place of the reverse transcriptase. A 3 µl aliquot of master mix was added to each reaction tube. The reactions were incubated at 45 °C for 15 min for reverse transcription and then at 95 °C for 3 min to inactivate the reverse transcriptase. Each cDNA was diluted to 5 ng/µl for use in PCR and stored at -80 °C.

All cDNA preparations with no reverse transcriptase were run through a quantitative PCR cycle as per the directions that follow in order to detect any contamination. If no gene amplification was noted the cDNA was used for quantification of mRNA levels and if gene amplification was noted, the cDNA was discarded and the preparation of that sample was repeated.

Target Gene Quantification. Quantification of target gene RNA was done using the Rotor-Gene SYBR Green PCR Kit (Qiagen) as per the directions. The 2X Rotor-Gene SYBR Green Master Mix in the kit contained HotStar *Taq* Plus DNA Polymerase, Rotor-Gene SYBR Green PCR Buffer, and SYBR Green I. The template cDNA was thawed on ice and the PCR reagents and primers were thawed at room temperature. All reaction components were mixed and briefly centrifuged. A master mix was made including 12.5 µl 2X Rotor-Gene SYBR Green Master Mix, 0.25 µl of each primer, and 10 µl of RNase-free water per reaction. A 23 µl aliquot of master mix and 2 µl of cDNA were added to each 0.1 ml Rotor-Gene PCR reaction tube. The tubes were capped and loaded in the RotorGene 3000 PCR instrument (Corbett Research). The reactions were incubated at 95 °C for 5 min to activate the HotStar *Taq* Plus DNA Polymerase and cycled at 95 °C for 5 s and 60 °C for 15 s, 35 times.

Primer Design and Verification. To design primers for possible control genes and genes of interest, a gene sequence was searched in the BLAST database, the ENSEMBLE database, or from previously acquired sequences from the Andrews lab. The highest quality sequence available was used for primer design. Exons of the DNA sequences were determined by matching the thirteen-lined ground squirrel sequence to a reference sequence in the BLAST database. The primers were designed by using either OligoPerfect Designer (Invitrogen) or Primer Quest (IDT). The primer pairs, their melting temperatures, GC content, and amplicon size can be viewed in Table 2.1.

Table 2.1: Q-RT-PCR Primers

Target Gene	Amplicon Size (bp)	Primer Sequence	GC Content (%)	Melt Temp (°C)
βActin	135	F’: TTGCTGACAGGATGCAGAAG	50	60.14
		R’: GCTGGAAGGTGGACAGAGAG	60	59.99
GAPDH	84	F’: ATGCCTCCTGTACCACCAAC	55	59.85
		R’: TGGTCATGAGTCCTTCCACA	50	60.09
RPL13A	158	F’: CCTCCGCAAGAGGATGAATA	50	60.17
		R’: GTGGAATCCCATCAAACACC	50	60.03
SDHA	113	F’: TCTTTCCTACCCGGTCACAC	55	59.97
		R’: AGAGCCCTTCACAGTGTCGT	55	59.91
CycA	224	F’: GTTGGATGGCAAGCATGTGGTCTT	50	60.00
		R’: TGGGATATTGCGAGCAGATGGGAT	50	60.00
βKlotho	85	F’: TTGGTGAAGCTCTGGATCAC	50	60.02
		R’: CTGCCCTGTAGGTGTCGTTA	55	59.95
PTL	150	F’: TGAACTGCATCTGTGTGGACTGGA	50	60.00
		R’: TGACATGGACATTGGAAGGCGAGT	50	60.30
HMGCS	106	F’: AAGGCCTCCCTTTACCTTTCCACA	50	60.10
		R’: AGCCAAGTCCTGAGCAGAGTGATT	50	59.90
CPT1a	124	F’: TTTGACCTGGAGAGGAACCCAGAA	50	59.50
		R’: AGGAGACGTGGAAGTGGATGAAGT	50	59.40
HSL	166	F’: AGATGAGAAGGCACTGGGCATGAT	50	60.10
		R’: ACTGCGTCGCATTGACTCTACTGT	50	60.00

The efficiency and accuracy of designed primers was verified. If the amplicon region for a primer pair doubles in quantity during PCR amplification, the primer pair has 100% efficiency. The semi-log regression of a plot of the cycle threshold value (C_T) versus the log input of cDNA concentration with a slope of -3.32 indicates a reaction of 100% efficiency. This slope is calculated with the following equation:

$$E = (10^{-\frac{1}{slope}} - 1) \times 100$$

Dilutions of the cDNA sample were prepared making dilutions of 50 ng/µl, 5 ng/µl, 0.5 ng/µl, 50 pg/µl, 5 pg/µl, and 0.5 pg/µl. Quantitative PCR was performed according to the method stated above with a melt curve following the amplification cycles. The fluorescence of the melt curve was checked for indication of any primer dimers and the slope of the C_T versus log concentration plot was calculated using the above equation. If the amplification efficiency was between 90% and 110%, the primer pair was considered acceptably efficient. It was determined that an input of 10 ng of cDNA had an acceptable cycle threshold of amplification. The PCR product was run on a 2% agarose gel in TAE buffer as described previously. The UV image of the gel was used to verify there was only one amplicon of the appropriate size for each primer pair.

CHAPTER 3

FIBROBLAST GROWTH FACTOR 21 IN THE THIRTEEN-LINED GROUND SQUIRREL (*ICTIDOMYS TRIDECEMLINEATUS*) DURING HIBERNATION

FGF21 in Thirteen-lined Ground Squirrels

The levels of FGF21 protein and mRNA levels in active, torpid, and aroused thirteen-lined ground squirrels were evaluated to determine if they fluctuated in a way that was complimentary to the hypothesis that FGF21 is involved in torpor induction in a seasonal hibernator. Measurements of FGF21 levels were performed using samples collected from four of the main activity states of a hibernator. August active squirrels are in the process of storing excess adipose tissue for the upcoming hibernation season. Torpid and IBA squirrels are in the middle of the hibernation season (December through February) and are cycling through long torpor bouts with IBAs approximately every 10 days and have not consumed food since the end of October. March active squirrels have awakened from hibernation for the season and are prepared to reproduce. If FGF21 is involved in inducing torpor, the highest concentrations are expected during IBAs just before torpor bouts, and into the torpor bouts themselves, with lower concentrations found in active animals.

Several tissues were examined in order to determine what tissues expressed FGF21 mRNA. Samples of RNA were extracted from liver, brain, heart, kidney, adrenal gland, skeletal muscle, spleen, and WAT from 6 squirrels. Two squirrels were selected from each August active, winter torpid, and winter IBA activity states. FGF21 mRNA was found to be exclusive to liver tissue with a mean mRNA level of 2.8 relative to 18S and mRNA levels below 0.005 in all other tissues examined (Fig 3.1). Recently, the lack of FGF21 expression in heart, skeletal muscle, BAT and WAT was confirmed by 454 analysis (Hampton, Melvin et al. 2011).

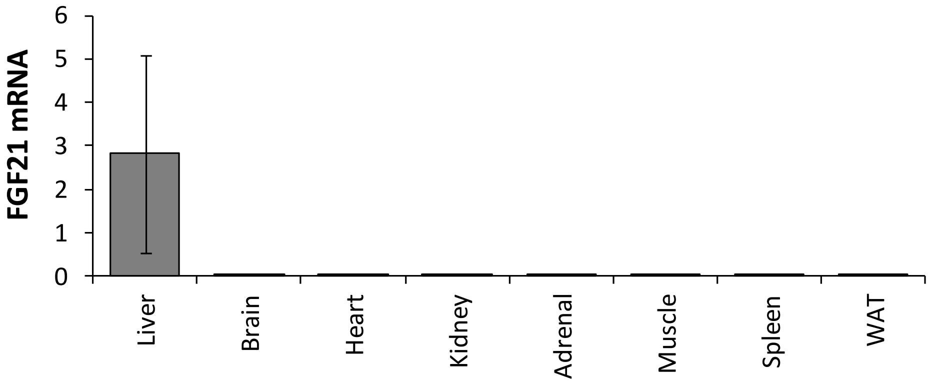

Figure 3.1: Relative mRNA expression of FGF21 in thirteen-lined ground squirrel tissues. The mRNA level of FGF21 was examined in 8 tissues from 2 active squirrels, 2 torpid squirrels, and 2 squirrels from IBA for a total of 6 squirrels. The mRNA of FGF21 was detected in liver tissue, but not the other tissues examined. Standard error bars are shown.

The relative level of FGF21 mRNA in liver tissue collected during multiple activity states was determined to measure if FGF21 mRNA levels were different in different activity states. Liver RNA was extracted from tissue and quantitative real-time PCR (Q-RT-PCR) was performed. The mRNA levels of FGF21 relative to 18S in August active, winter torpid, winter IBA, and March active were 1.2, 3.2, 9.8, and 1.7 respectively with 6 samples in each group (Fig 3.2). The mRNA levels were compared by ANOVA followed by Tukey's HSD ($p < 0.01$) and the FGF21 mRNA level was significantly higher during IBA than during any other activity state. If bars in Figure 3.2 do not have the same letter above them this indicates significant difference as tested by Tukey's HSD. The liver FGF21 mRNA level from IBA squirrels was 7.9-fold higher than August active squirrels.

Serum samples were prepared from whole blood by centrifugation and used for FGF21 concentration measurements by enzyme-linked immunosorbent assay (ELISA). The FGF21 protein concentrations in August active (AUG), winter torpid (TOR), winter IBA (IBA), and March active (MAR) squirrel serum samples were

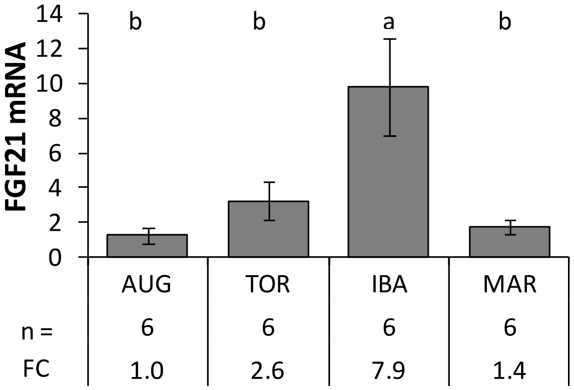

Figure 3.2: Relative mRNA expression of FGF21 in liver tissue of thirteen-lined ground squirrels in multiple activity states. Liver tissue from multiple squirrels was collected and the FGF21 mRNA expression relative to 18S was measured. The mRNA level of FGF21 during IBA is significantly higher than the other activity states (ANOVA followed by Tukey's HSD, $p < 0.01$). Abbreviations: FC is fold change, AUG is August active, TOR is winter torpid, IBA is winter IBA, and MAR is March active. Standard error bars are shown.

1.09, 3.64, 9.45, and 0.86 ng/ml respectively (Fig 3.3). Serum samples from 8 squirrels were measured for each group except winter torpid, where serum samples were measured from 9 squirrels. The protein concentrations were compared by ANOVA, followed by Tukey's HSD. The IBA squirrel serum FGF21 protein concentration was 8.7-fold higher than August active squirrel levels. The winter torpid squirrel serum had a higher level of FGF21 protein than in active animal serums from March or August, but the difference was not statistically significant. Thus, there were higher serum FGF21 protein concentrations in squirrels that were about to enter torpor (IBA) and a trend toward higher concentrations in torpid squirrels relative to active squirrels. Serum FGF21 protein concentrations are increased during IBA and this corresponds to the liver mRNA levels of FGF21. Significantly increased FGF21 during IBA and a trend toward higher FGF21 during torpor is consistent with the hypothesis that increased FGF21 signaling precedes the induction of torpor in squirrels during hibernation.

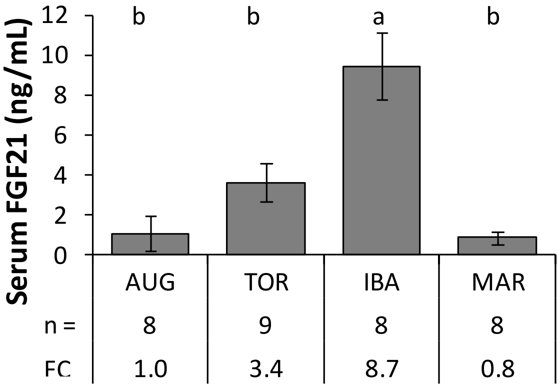

Figure 3.3: Thirteen-lined ground squirrel serum FGF21 concentration. Serum was prepared from blood withdrawn from ground squirrels in multiple activity states. The concentration of FGF21 was measured using a mouse ELISA. The serum concentration of FGF21 is significantly higher in inter-bout arousal (IBA) squirrels than other activity states (ANOVA followed by Tukey's HSD, *p* < 0.01). Abbreviations: n is number of squirrels, FC is fold change relative to AUG, AUG is August active, TOR is winter torpid, IBA is winter IBA, and MAR is March active. Standard error bars are shown.

FGF21 Signaling Components in Thirteen-lined Ground Squirrels

FGF21 signals most effectively through FGFR1 and requires the small transmembrane protein βKlotho for signaling (Kurosu, Choi et al. 2007; Ogawa, Kurosu et al. 2007; Kharitonenkov, Dunbar et al. 2008; Suzuki, Uehara et al. 2008; Adams, Astapova et al. 2010). Activity of FGF21 has been detected in liver and WAT in mice and cell culture. The presence of transcripts encoding for FGF21 signaling components were measured in multiple tissues. βKlotho was present in liver and WAT with relative mRNA levels of 11.9 and 19.5 respectively. Relative levels of βKlotho mRNA were below 1 in brain, heart, kidney, adrenal gland, skeletal muscle, and spleen (Fig 3.4A). The presence of βKlotho mRNA in WAT and lack of βKlotho mRNA in heart and muscle tissue were confirmed by 454 transcriptome analysis (Hampton, Melvin et al. 2011). FGFR1 was ubiquitously expressed at a low level in liver, brain, heart, kidney, adrenal gland, skeletal muscle, spleen and WAT with mRNA levels of 0.1, 1.9, 0.4, 0.3, 0.3, 0.4, 0.2 and 0.5 respectively. The highest mRNA level was in WAT (Fig 3.4 B). FGFR1 mRNA presence in heart, skeletal muscle, and WAT were confirmed by 454 and Illumina analysis (Hampton, Melvin et

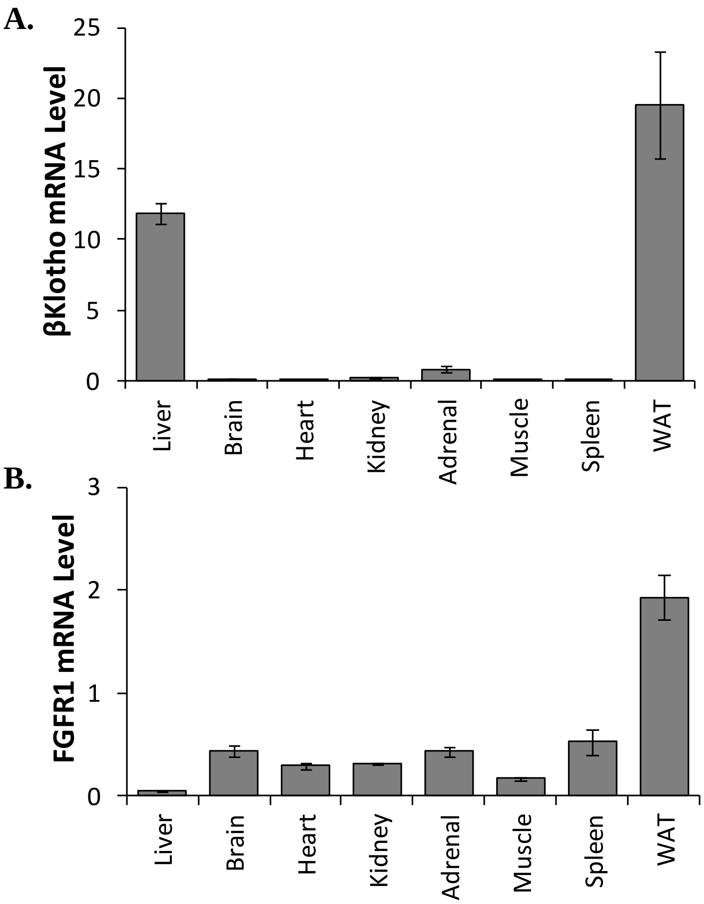

Figure 3.4: FGF21 signaling component mRNA levels in thirteen-lined ground squirrel tissues. The relative levels of mRNA were measured in 8 tissues from ground squirrels with 2 squirrels in August active state, 2 squirrels in winter torpid state, and 2 squirrels in IBA state for a total of 6 squirrels. **(A)** βKlotho mRNA was detected in liver and white adipose tissue (WAT). **(B)** FGFR1 mRNA was detected in all tissues at a low level with the highest expression in WAT. Standard error bars are shown.

al. 2011). The transcripts for βKlotho and FGFR1 were found in liver and WAT indicating that FGF21 is capable of signaling in both liver tissue and WAT.

Reductions in energy expenditure through reduced MR result in decreased gene expression during hibernation (van Breukelen and Martin 2001; van Breukelen and Martin 2002). The mRNA levels of βKlotho and FGFR1 were measured during hibernation and activity to determine if these transcripts were present during torpor and activity. The relative mRNA level of βKlotho in squirrel liver tissue was the highest in August active squirrels at 1.1 the mRNA level decreased through the hibernation season to the lowest level in March active squirrels at 0.5 (Fig 3.5 A). As determined by ANOVA followed by Tukey’s HSD, August active squirrels had a significantly higher βKlotho mRNA level than March active squirrels (*p* = 0.0311).

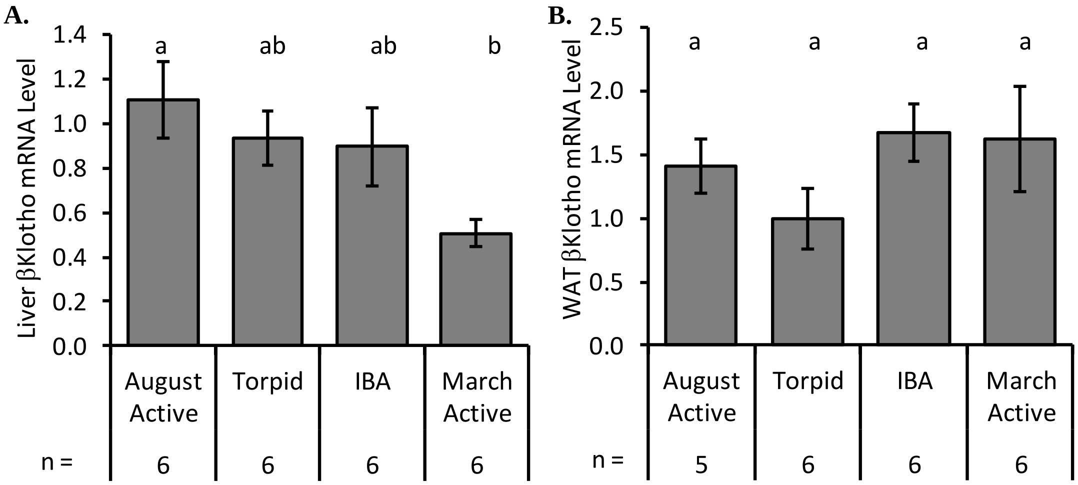

Figure 3.5: Relative levels of βKlotho mRNA in thirteen-lined ground squirrels during various activity states. **(A)** In liver tissue relative levels of βKlotho mRNA were determined to be significantly higher during August activity than during March activity by ANOVA followed by Tukey's HSD (*p* = 0.0311). **(B)** In WAT there was not a significant difference in βKlotho levels seasonally as tested by ANOVA. Standard error bars are shown.

In WAT of squirrels the relative mRNA expression of βKlotho did not significantly differ between activity states as determined by ANOVA with values of 1.41, 0.99, 1.68, and 1.62 for August active, torpid, IBA, and March active respectively (Fig 3.5 B).

The relative mRNA level of FGFR1 in liver was found to have significant variation between specific activity states (Fig 3.6 A). The FGFR1 mRNA levels in August active, 3.26, and IBA, 3.33, were the lowest with increased levels during torpor, 4.22, and significantly higher levels during March activity, 5.41, as determined by ANOVA followed by Tukey's HSD (*p* = 0.025). The level of FGF21 mRNA in WAT did not have significant variation between activity states with mRNA levels of 1.29, 1.49, 1.99, and 1.09 in August active, torpid, IBA, and March active respectively (Fig 3.6 B).

In summary, mRNA levels of βKlotho and FGFR1 did not significantly differ in WAT. The βKlotho mRNA level was higher in liver tissue in the August active

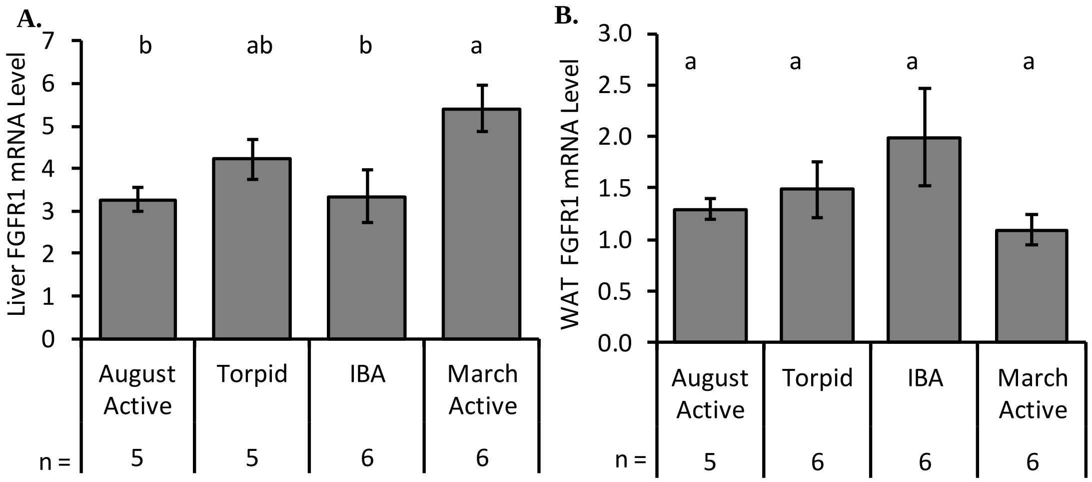

Figure 3.6: Relative mRNA level of FGFR1 in thirteen-lined ground squirrels in various activity states. **(A)** In liver tissue the relative level of FGFR1mRNA was significantly higher during March activity compared to August activity or IBA as determined by ANOVA followed by Tukey's HSD (p = 0.025). **(B)** There was no significant difference in mRNA levels of WAT FGFR1 as determined by ANOVA (F = 1.70). Standard error bars are shown.

state compared to March active. Liver FGFR1 mRNA was increased during March active state compared to winter torpid and August active. Reduced βKlotho in March active squirrels and increased FGFR1 levels in liver tissue may affect the signaling responsiveness in this activity state relative to the August active state. Yet, these necessary components of FGF21 signaling were detectable at the mRNA level in all activity states, including torpor. The FGF21 signaling system is present and FGF21 is capable of inducing metabolic change during torpor when the levels of many transcripts that are not necessary for limited metabolic activity are greatly decreased.

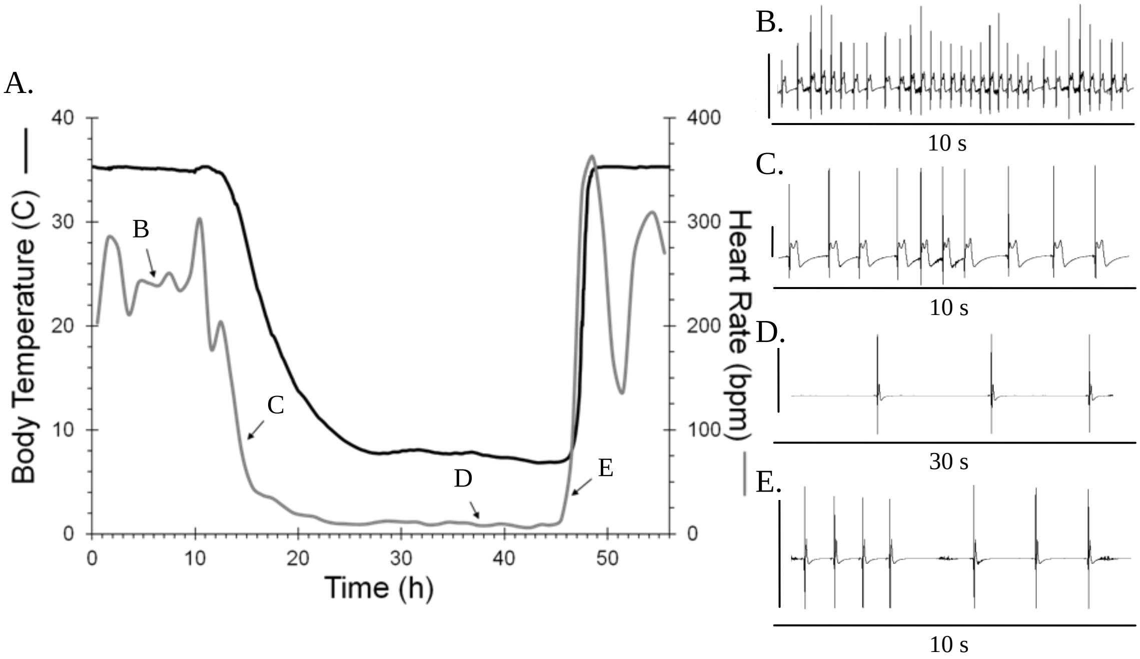

Figure 3.7: Example of a thirteen-lined ground squirrel torpor bout. **(A)** Simultaneous tracing of heart rate (gray line; 1 h moving average) and core body temperature (black line) collected with an implanted transmitter during the initial seasonal torpor bout (November) at an ambient temperature of 5 °C. ECG readings from the indicated points on the heart rate tracing show 10 s interval where the heart rate was ~240 bpm **(B)**; entry into torpor over 10 s at a heart rate of ~80 bpm **(C)**; 30 s during torpor to show multiple beats at a heart rate of 8 bpm **(D)**; arousal ECG where the heart rate is 15 bpm **(E)**. In B-E the vertical line on the left side of the ECG equals 1 mV to indicate the changes in the height of the R peak.

Physiological Parameters of Torpor in Thirteen-lined Ground Squirrels

FGF21 is increased during torpor and FGFR1 and βKlotho transcripts are present in liver and WAT during hibernation. To test the hypothesis that FGF21 induces torpor, naturally occurring torpor bouts were evaluated. The evaluation of natural torpor bouts provided a definition of when torpor occurs in TLG squirrels and a baseline for comparison of torpor bouts in squirrels with increased FGF21. Physiological transmitters capable of recording T_b, ECG, and movement resulting from change of location were implanted in 8 squirrels (CTA-F40 transmitters, Data Sciences International, St. Paul, MN). Squirrels were monitored for 2 months beginning in November in an environmental chamber set at 5 °C, 24 h darkness, with no food and water *ad libitum*. These conditions allow deep torpor to occur in captivity during the hibernation season.

Torpor occurs when physiological activity is lower than normal. Hibernators experience three phases of torpor: 1) *entrance*, consisting of decreasing physiological activity; 2) *maintenance*, consisting of steady, low level physiological activity; and 3) *arousal*, consisting of physiological activity increasing to normal, active levels. Figure 3.7 shows the core T_b and 1 h mean HR during a torpor bout from squirrel with insets of ECG activity exhibiting arrhythmias.

Defining Torpor in Thirteen-lined Ground Squirrels. Torpor occurs when physiological parameters are below the normal, active level. The T_b and HR of active squirrels were examined to define the range of these values during activity and determine the point at which they indicate torpor. The analysis of active squirrel data was based on 24 hours of T_b data from 8 clearly active squirrels kept in an environmental chamber at 5 °C in 24 hours darkness with no food available in early November. A 24 hour sample was used so that the circadian variations in resting and active temperatures were included in the analysis. Squirrels were put in the cold chamber in darkness and without food so the effect of these environmental conditions would be accounted for in determining lower limits of active T_b and HR. Data points were recorded every 30 seconds and a 5 minute running average of T_b data and a 1 hour running average of HR data was used for analysis. During the active state the T_b ranged from 33.7 to 35.4 °C with a mean T_b of 35.0 °C. The HR during the active state ranged from 174 to 451 bpm with a mean HR of 254 bpm. The changes in T_b were less variabile than the changes in HR and the value used to define the beginning of torpor was based on T_b. Based on the minimum active T_b of 33.7 °C, torpor was defined to occur at least 1 °C below this minimum at a T_b less than 32.0 °C. The minimum HR detected during activity was 174 bpm with a standard deviation of 21 bpm, and a HR of 150 bpm was below the active level.

Maintenance of torpor was defined by analyzing steady sections of T_b data from 7 torpid squirrels. The average continuous T_b sample length used for analysis was 34.2 hours. During torpor the maximum T_b detected was 8.5 °C, the T_b minimum was 5.0 °C, and the mean T_b was 6.1 °C with a standard deviation of 0.94. Based on these characteristics maintenance was defined to begin at a T_b of 9 °C or approximately the mean T_b plus 3 standard deviations. The HR detected in this data sample ranged from 3 bpm to 13 bpm. The mean HR was 6 bpm with a standard deviation of 1.7. The HR was defined to be maintained at steady low levels below 12 bpm, or approximately the average HR during steady torpor plus 3 standard deviations.

Table 3.1. Physiological Values during Initial Torpor Bout Progression
(t = 0 at T_b < 32 °C)

Phase of Torpor	Event	Time (h)	T_b (°C)	HR (bpm)
Activity	Movement stops	-1.1	31.1	180.0
	HR drop begins	-0.7	33.7	< 150.0
Entrance	T_b drop begins	0.0	< 32.0	106.9
	HR at low level	7.1	12.8	< 12.0
Maintenance	T_b at low levels	10.5	< 9.0	7.3
	HR begins to rise	58.8	6.0	> 12.0
Arousal	T_b begins to rise	60.5	> 9.0	159.5
	HR at active level	60.5	8.9	> 150.0
IBA	T_b at active level	61.5	> 32.0	386.1
	Movement starts	63.6	35.2	355.0

The entrance phase, or transition into deep torpor, was defined to start at a T_b below 32 °C and continue until a squirrel reached a $T_b < 9$ °C. The transition out of torpor, or arousal phase, was defined to begin when maintenance of torpor ended at a $T_b > 9$ °C and continue until torpor ended at a $T_b > 32$ °C. At the end of arousal, the active IBA period began and lasted until the next entrance into torpor occurred.

Physiological Characteristics of Torpor in Thirteen-lined Ground Squirrels. After defining the beginning of torpor at a $T_b < 32$ °C and maintenance of torpor below a T_b of 9 °C, the characteristic pattern of initial torpor bouts of 7 squirrels in November at an ambient temperature of 5 °C with constant darkness and no food available was examined. Movement of squirrels stopped 1.1 hours before torpor began at a mean T_b of 31.1 °C and HR of 180 bpm, although movement was detected after the initiation of torpor where T_b and HR were below active levels in some squirrels. During torpor entrance HR dropped below the active level of 150 bpm at a mean T_b of 33.7 °C. The HR began to drop 0.7 hours before the drop in T_b below 32 °C and took 7.8 hours to reach below 12 bpm. The drop in T_b below 32 °C occurred at a HR of 107 bpm and dropped to less than 9 °C in 10.5 hours (Fig 3.7). The HR dropped below 12 bpm at a T_b of 12.8 °C, and reached low levels 3.3 hours before the T_b maintained low levels below 9 °C at a HR of 7.3 bpm. The mean minimum T_b detected during torpor was 5.6 °C and the mean minimum HR was 4.6 bpm. During the first torpor bout at 5 °C in darkness, low T_b was maintained below 9 °C for a mean of 48.3 hours with a range of 22.4 to 79.6 hours. Low HR was maintained below 12 bpm for a similar amount of time with a mean of 47.9 hours and a range of 20.8 to 78.9 hours. Upon arousal from torpor HR rose above 12 bpm at a

T_b of 6.0 °C and this occurred 1.6 hours before the rise in T_b. The T_b rose above 9.0 °C at a HR of 160 bpm. The HR increased to active levels in 1.7 hours and reached above 150 bpm at a T_b of 8.9 °C. The T_b rose to active levels in 1.0 hours and reached above 32 °C at a HR of 386 bpm, and this HR is near the mean maximum HR detected during activity of 352 bpm. The HR reached active levels 1.0 hours before the T_b reached active levels. Movement began 1.5 hours after completing a torpor bout. The length of the torpor bouts averaged 61.5 hours with a range of 34.2 to 96.3 hours. The physiological parameters of initial torpor bout analysis are summarized in Table 3.1.

The torpor bout lengths measured early in the hibernation season were compared to the parameters of torpor bouts in the middle of the hibernation season measured in January. The middle season squirrels were kept in the same environmental conditions with an ambient temperature of 5 °C, no light, water *ad libitum* and no food available. The torpor bout entrance lengths were not significantly different as tested by Student's t-test during early-season and mid-season torpor bouts with 10.5 and 9.2 hours respectively ($p = 0.2086$). The arousal lengths were longer in early-season torpor bouts with a value of 1.1 hours a mid-season length of 0.7 hours ($p = 0.0031$). The length of torpor bouts during mid-season, 193.6 hours, were longer than the torpor bouts in early season, 61.5 hours ($p < 0.001$). Thus, during the middle of the hibernation season squirrels maintained torpor for longer periods and T_b rose to active levels faster during arousal than during early season torpor, but the entrance into torpor did not differ.

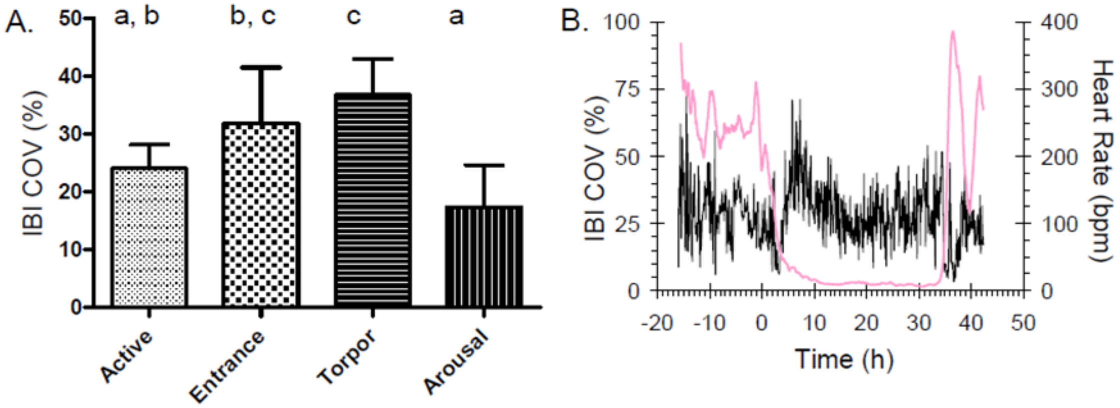

Figure 3.8: Occurrence of arrhythmias during torpor bouts in thirteen-lined ground squirrels. The level of arrhythmias was measured by calculating the interbeat interval (IBI) coefficient of variation (COV) for 8 squirrels during the first seasonal torpor bout at 5 °C. **(A)** Arrhythmic patterns occurred more frequently as squirrels entered and maintained a torpor bout and less frequently during the arousal phase. (**B)** example of the changes in IBI COV (black) relative to the changes in heart rate (pink). For comparison, the same animal is used as in Figure 3.7.

Arrhythmias and Torpor. Before the occurrence of torpor bouts arrhythmias were noticeable on ECGs examined. It was hypothesized that arrhythmias increased just before a torpor bout occurred and could be used to signify an upcoming torpor bout. Figure 3.7 shows arrhythmic ECG samples from just before torpor occurred (B), during entrance (C), during maintenance (D) and during arousal (E). Note that the period shown during maintenance of torpor is 30 seconds rather than 10 seconds to allow multiple heartbeats to be displayed (D). The coefficient of variation (COV) of the inter-beat interval (IBI) was calculated to analyze arrhythmias. The COV of the IBI provides a numerical value of the variation of the time between heartbeats relative to the mean time between heartbeats. As shown in Figure 3.8, there was a higher frequency of arrhythmias during maintenance of torpor (36.7%, SD 6.2), than during active (24.0%, SD 4.1) and arousal (17.4%, SD 7.2) states. During entrance (31.8%, SD 9.6) there was a higher incidence of arrhythmia than during arousal, which had the lowest frequency of arrhythmias. The arrhythmias noted before torpor bouts were not indicative of an impending bout of torpor (Hampton, Nelson et al. 2010).

If FGF21 induces torpor in TLG squirrels in a similar manner to naturally occurring torpor bouts in early hibernation season, T_b will reduce from 32 °C to less than 9 °C in approximately 10 hours. The drop in HR below 150 bpm will occur before the drop in T_b below 32 °C and the rise in HR above 12 bpm will occur before the rise in T_b above 9 °C.

CHAPTER 4

EFFECTS OF INCREASED FGF21 IN THIRTEEN-LINED GROUND SQUIRRELS

Development of Thirteen-lined Ground Squirrel FGF21 Adenoviral Construct

Determination of Thirteen-lined Ground Squirrel FGF21 Sequence. The TLG squirrel FGF21 sequence was isolated by low stringency PCR followed by 3’ and 5’ rapid amplification of cDNA ends using primers from conserved FGF21 sequences from multiple species. Figure 4.1 shows the TLG squirrel FGF21 sequence. A BLAST search of the FGF21 sequence produced a top result of NM_019113.2 [*Homo sapiens* fibroblast growth factor 21, mRNA] with a score of 795 bits and an expect score of 0.0 with 676/793 (85%) identities and 24/793 (3%) gaps (Zhang, Schwartz et al. 2000). The sequence was translated using ExPASy translate tool from the first methionine sequence to the poly-A tail (Artimo, Jonnalagedda et al. 2012). The resulting protein sequence contained 208 amino acids (Fig 4.1) and was entered in a protein-protein BLAST search that resulted in a top hit of [gb|AAH18404.1| Fibroblast growth factor 21 [*Homo sapiens*]] with a score of 321 bits and an expect score of 3*e*-86 (Altschul, Madden et al. 1997; Altschul, Wootton et al. 2005). There were 178/209 (85%) identities and 187/209 (89%) positives and 1/209 (0%) gaps. The translated sequence was aligned to FGF21 sequences from *Homo sapiens* (UniProt ID Q9NSA1), *Myotis lucifigus* (little brown bat, UniProt ID G1P6U5), *Rattus norvegicus* (Rat, UniProt ID Q8VI80), *Xenopus tropicalus* (western clawed frog, UniProt ID B7U4G3), *Gallus gallus* (Chicken, UniProt ID F1NYA6), and *Danio rario* (Zebrafish, UniProt ID F1QR52) using CLUSTAL W from the UniProt database (UniProt 2012) (Fig. 4.2). When comparing the alignment of FGF21 from multiple species there are few substitutions noted that have the potential to affect the structure or function of TLG squirrel FGF21. The

A.
AAGAGTCCTGGGTGTCCTGTCAGCTGGGGATCCACAGGTAGGAGGACGCAAGCTCCTG
GATGATCTGAGCCACAGTGCTGTCCCGGACAAGCACATCTGGAATTGATTCAGGACTG
CTCACCTCCTCGGACCCCATACTCCAGACCCTGCACTCTGGACCCCGCCTGAGGACAA
GAACCATTGATGGACTGGGTCAAGGCCAAGTTGGAGCCCCTGGGACTGTGGGTCCTGG
TGCTGGCTGCCCTTGTGCTGGGAGCCTGCCAGGCGTACCCCATCCCTGACTCAAGCCCC
CTCCTCCAATTTGGGGGCCAAGTCCGGCAGCGGTACCTGTACACAGATGATGCCCAGG
AGACTGAGGCCCACCTGGAGATCAGGGCTGATGGCACCGTGGTGGGGGCTGCCCATC
AAAGCCCGGAAAGTCTCTTGGAACTGAAAGCCTTGAAGCCTGGGGTCATTCAAATCTT
GGGGGTCAAAACATCCAGGTTCCTGTGCCAGAGGCCAGATGGAGTGCTGTATGGATCG
CTCCACTTTGACCCTGAGGCCTGCAGCTTCCGGGAGCAGCTTCTGGAGGACGGGTACA
ACGTTTACCAGTCAGAATCCCACGGCCTCCCCGTGCGCCTGCCCCCTAACTCACCATAC
CGGGACCCAGCGCCGCCAGGACCAGCCCGCTTCCTTCCACTGCCAGGCCTGCCCCCAG
CAGCCCTGGAGCCGCCAGGGATCCTGGGCCCTGAGCCCCCTGATGTGGGCTCCTCCGA
CCCACTCAGCATGGTGGGGCCTTTGCAGGGCCGAAGCCCCAGTTACGCTTCCTGAAGC
CATGGGCCCTTCATTTTGGGGTCTCCTCTTATTTATTGGGGTATTTATCTTATTTATTTTT
TTATTTTTTTCTATCTTGGGATAATAAAGAGTCTGAGAGAGGAGTAAAAAAAAAAAAA
AAAAAAAAAAA

B.
MDWVKAKLEPLGLWVLVLAALVLGACQAYPIPDSSPLLQFGGQVRQRYLYTDDAQETEA
HLEIRADGTVVGAAHQSPESLLELKALKPGVIQILGVKTSRFLCQRPDGVLYGSLHFDPEA
CSFREQLLEDGYNVYQSESHGLPVRLPPNSPYRDPAPPGPARFLPLPGLPPAALEPPGILGPE
PPDVGSSDPLSMVGPLQ GRSPSYAS

Figure 4.1: Thirteen-lined ground squirrel FGF21 sequence. **(A)** The ground squirrel cDNA sequence with the proposed start and stop codons are highlighted and the sequence ending poly-A tail included. **(B)** The amino acid sequence translated by ExPASy from the cDNA sequence.

hydrophobic leucine residue in human, brown bat and rat sequences is substituted with a polar glutamine residue at position 126 in the TLG squirrel sequence. This substitution is in β-strand 8 in the predicted structure of FGF21 (Fig 4.3). Although the other mammalian species have a hydrophobic residue at this site, the *Xenopus*, chicken, and zebrafish have charged residues at this site (Fig 4.2). The polar serine at site 139 in the TLG squirrel FGF21 sequence aligns with a small, hydrophobic alanine in human, brown bat, and rat sequences. In the *Xenopus*, chicken, and zebrafish sequences there is a large, basic lysine amino acid at this site. Another notable difference in the TLG squirrel FGF21 sequence is the proline at site 158. This substitution aligns with a basic, large arginine in human and rat sequences and

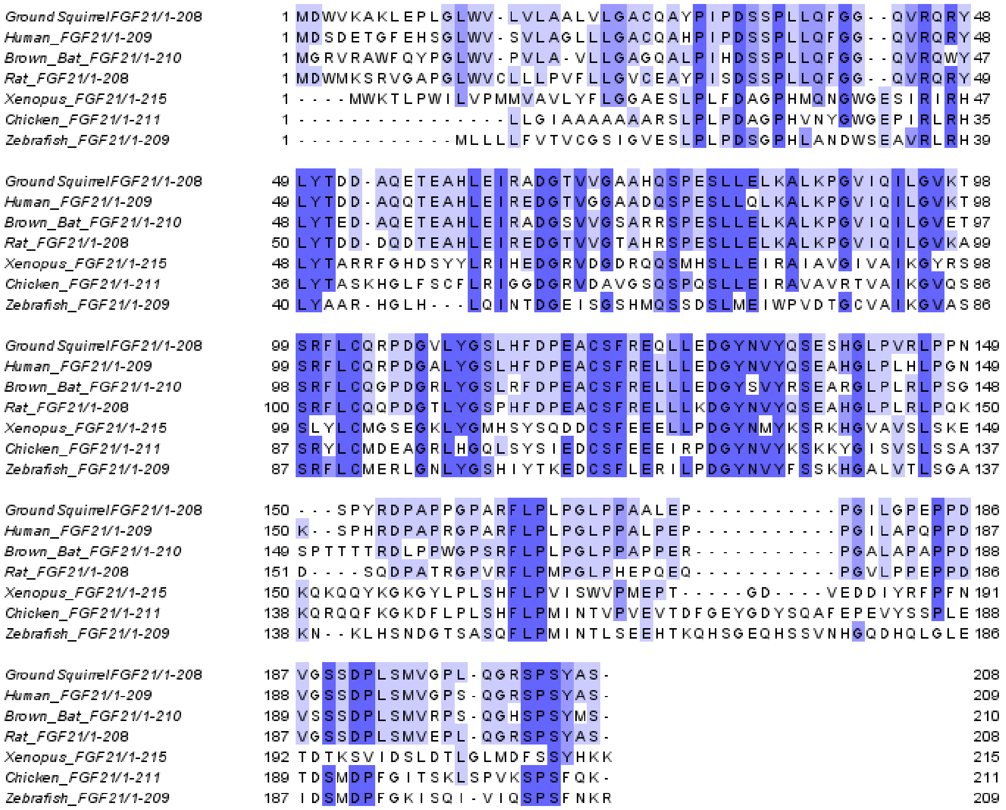

```
Ground SquirrelFGF21/1-208    1 MDWVKAKLEPLGLWV-LVLAALVLGACQAYPIPDSSPLLQFGG--QVRQRY 48
Human_FGF21/1-209             1 MDSDETGFEHSGLWV-SVLAGLLLGACQAHPIPDSSPLLQFGG--QVRQRY 48
Brown_Bat_FGF21/1-210         1 MGRVRAWFQYPGLWV-PVLA-VLLGAGQALPIHDSSPLLQFGG--QVRQWY 47
Rat_FGF21/1-208               1 MDWMKSRVGAPGLWVCLLLPVFLLGVCEAYPISDSSPLLQFGG--QVRQRY 49
Xenopus_FGF21/1-215           1 ----MWKTLPWILVPMMVAVLYFLGGAESLPLFDAGPHMQNGWGESIRIRH 47
Chicken_FGF21/1-211           1 ----------------LLGIAAAAAAARSLPLPDAGPHVNYGWGEPIRLRH 35
Zebrafish_FGF21/1-209         1 ------------MLLLLFVTVCGSIGVESLPLPDSGPHLANDWSEAVRLRH 39

Ground SquirrelFGF21/1-208   49 LYTDD-AQETEAHLEIRADGTVVGAAHQSPESLLELKALKPGVIQILGVKT 98
Human_FGF21/1-209            49 LYTDD-AQQTEAHLEIREDGTVGGAADQSPESLLQLKALKPGVIQILGVKT 98
Brown_Bat_FGF21/1-210        48 LYTED-AQETEAHLEIRADGSVVGSARRSPESLLELKALKPGVIQILGVET 97
Rat_FGF21/1-208              50 LYTDD-DQDTEAHLEIREDGTVVGTAHRSPESLLELKALKPGVIQILGVKA 99
Xenopus_FGF21/1-215          48 LYTARRFGHDSYYLRIHEDGRVDGDRQQSMHSLLEIRAIAVGIVAIKGYRS 98
Chicken_FGF21/1-211          36 LYTASKHGLFSCFLRIGGDGRVDAVGSQSPQSLLEIRAVAVRTVAIKGVQS 86
Zebrafish_FGF21/1-209        40 LYAAR-HGLH---LQINTDGEISGSHMQSSDSLMEIWPVDTGCVAIKGVAS 86

Ground SquirrelFGF21/1-208   99 SRFLCQRPDGVLYGSLHFDPEACSFREQLLEDGYNVYQSESHGLPVRLPPN 149
Human_FGF21/1-209            99 SRFLCQRPDGALYGSLHFDPEACSFRELLLEDGYNVYQSEAHGLPLHLPGN 149
Brown_Bat_FGF21/1-210        98 SRFLCQGPDGRLYGSLRFDPEACSFRELLLEDGYSVYRSEARGLPLRLPSG 148
Rat_FGF21/1-208             100 SRFLCQQPDGTLYGSPHFDPEACSFRELLLKDGYNVYQSEAHGLPLRLPQK 150
Xenopus_FGF21/1-215          99 SLYLCMGSEGKLYGMHSYSQDDCSFEEELLPDGYNMYKSRKHGVAVSLSKE 149
Chicken_FGF21/1-211          87 SRYLCMDEAGRLHGQLSYSIEDCSFEEEIRPDGYNVYKSKKYGISVSLSSA 137
Zebrafish_FGF21/1-209        87 SRFLCMERLGNLYGSHIYTKEDCSFLERILPDGYNVYFSSKHGALVTLSGA 137

Ground SquirrelFGF21/1-208  150 ---SPYRDPAPPGPARFLPLPGLPPAALEP-----------PGILGPEPPD 186
Human_FGF21/1-209           150 K--SPHRDPAPRGPARFLPLPGLPPALPEP-----------PGILAPQPPD 187
Brown_Bat_FGF21/1-210       149 SPTTTTRDLPPWGPSRFLPLPGLPPAPPER-----------PGALAPAPPD 188
Rat_FGF21/1-208             151 D----SQDPATRGPVRFLPMPGLPHEPQEQ-----------PGVLPPEPPD 186
Xenopus_FGF21/1-215         150 KQKQQYKGKGYLPLSHFLPVISWVPMEPT-----GD----VEDDIYRFPFN 191
Chicken_FGF21/1-211         138 KQRQQFKGKDFLPLSHFLPMINTVPVEVTDFGEYGDYSQAFEPEVYSSPLE 188
Zebrafish_FGF21/1-209       138 KN--KLHSNDGTSASQFLPMINTLSEEHTKQHSGEQHSSVNHGQDHQLGLE 186

Ground SquirrelFGF21/1-208  187 VGSSDPLSMVGPL-QGRSPSYAS-                            208
Human_FGF21/1-209           188 VGSSDPLSMVGPS-QGRSPSYAS-                            209
Brown_Bat_FGF21/1-210       189 VSSSDPLSMVRPS-QGHSPSYMS-                            210
Rat_FGF21/1-208             187 VGSSDPLSMVEPL-QGRSPSYAS-                            208
Xenopus_FGF21/1-215         192 TDTKSVIDSLDTLGLMDFSSYHKK                            215
Chicken_FGF21/1-211         189 TDSMDPFGITSKLSPVKSPSFQK-                            211
Zebrafish_FGF21/1-209       187 IDSMDPFGKISQI-VIQSPSFNKR                            209
```

Figure 4.2: CLUSTALW (1.81) multiple sequence alignment of proposed thirteen-lined ground squirrel translated cDNA sequence to FGF21 protein sequences from multiple species. Sequences colored according to percentage identity with > 80% dark blue, > 60% medium blue, > 40% light blue, and <= 40% white.

with large, hydrophobic amino acids in the brown bat, *Xenopus*, chicken, and zebrafish sequences. This substitution is in the predicted heparin binding region of canonical FGFs, where FGF21 is expected to have a divergent sequence. Considering the comparison of FGF21 sequences the isolated TLG squirrel sequence was determined to be FGF21.

The TLG squirrel FGF21 amino acid sequence was also aligned with the following human FGFs: FGF21 (GenBank ID AAQ89444), FGF19 (GenBank ID AAQ88669), FGF23 (GenBank ID AAG09917), FGF2 (GenBank ID EAX05222), FGF9 (GenBank ID BAA03572.1), and FGF10 (GenBank ID CAG46489) (Figure

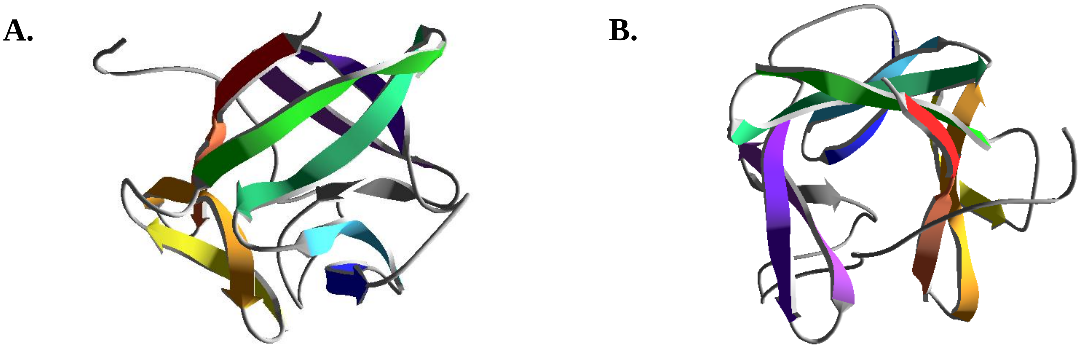

C.

```
                                                    αN
FGF21 gs 1      -----------------------------MDWVKAKLEPLGLWVLV-LAALVLGACQAYP
FGF21 hu 1      -----------------------------MDSDETGFEHSGLWVSV-LAG-LLGACQAHP
FGF19 hu 1      --------------------------------MRSGCVVVHVWILAGLWLAVAGRPLAFS
FGF23 hu 1      ----------------------------------MLGARLRLWVCALCSVCSMSVLRAYP
FGF2  hu 1      -----------------------------MAAGSITTLPALPEDG-----------GSGA
FGF9  hu 1      -----MAPLGEVGNYFG-----------VQDAVPFGNVPVLPVDSPVLLSDHLGQSEAGG
FGF10 hu 1      MWKWILTHCASAFPHLPGCCCCCFLLLFLVSSVPVTCQALGQVMVSPEATNSSSSSFSSP

                                   β1              β2      β3            β4
FGF21 gs 31     IPDS---SPLLQFGGQVRQRYLYTDDAQ-ETEAHLEIRADGTVVGAAHQ-SPESLLELKA
FGF21 hu 30     IPDS---SPLLQFGGQVRQRYLYTDDAQ-QTEAHLEIREDGTVGGAADQ-SPESLLQLKA
FGF19 hu 29     DAGP---HVHYGWGDPIRLRHLYTSGPHGLSSCFLRIRADGVVDCARGQ-SAHSLLEIKA
FGF23 hu 27     NASP---LLGSSWGG---LIHLYTATAR--NSYHLQIHKNGHVDGAPHQ-TIYSALMIRS
FGF2  hu 21     FPPG-------HFK---DPKRLYCKNGG----FFLRIHPDGRVDGVREKSDPHIKLQLQA
FGF9  hu 45     LPRGPAVTDLDHLKGILRRRQLYCRTG-----FHLEIFPNGTIQGTRKDHSRFGILEFIS
FGF10 hu 61     SSAGRHVRSYNHLQGDVRWRKLFSFTK-----YFLKIEKNGKVSGTKKENCPYSILEITS

                      β5         β6      β7            β8        β9
FGF21 gs 86     LKPGVIQILGVKTSRFLCQRPDGVLYGSLHFDPEACSFREQLLEDGYNVYQSESHG----
FGF21 hu 85     LKPGVIQILGVKTSRFLCQRPDGALYGSLHFDPEACSFRELLLEDGYNVYQSEAHG----
FGF19 hu 85     VALRTVAIKGVHSVRYLCMGADGKMQGLLQYSEEDCAFEEEIRPDGYNVYRSEKHR----
FGF23 hu 78     EDAGFVVITGVMSRRYLCMDFRGNIFGSHYFDPENCRFQHQTLENGYDVYHSPQYH----
FGF2  hu 67     EERGVVSIKGVCANRYLAMKEDGRLLASKCVT-DECFFFERLESNNYNTYRSRKYT----
FGF9  hu 100    IAVGLVSIRGVDSGLYLGMNEKGELYGSEKLT-QECVFREQFEENWYNTYSSNLYKHVDT
FGF10 hu 116    VEIGVVAVKAINSNYYLAMNKKGKLYGSKEFN-NDCKLKERIEENGYNTYASFNWQHN--

                    β10     β OR α11   g11   β12                   αC
FGF21 gs 142    ---LPVRLPPN---SPYRDPA-PPGPARFLPLPGLPPAALE-----PPGILGPEPPDVGS
FGF21 hu 141    ---LPLHLPGN--KSPHRDPA-PRGPARFLPLPGLPPALPE-----PPGILAPQPPDVGS
FGF19 hu 141    ---LPVSLSSAKQRQLYKNRG-FLPLSHFLPMLPMVPEEPEDLRGHLESDMFSSPLETDS
FGF23 hu 134    ---FLVSLGRA--KRAFLPGMNPPPYSQFLSRRNEIPLIHFNTPIPRRHTRSAEDDSERD
FGF2  hu 122    --SWYVALKRTGQYKLGSKTGPGQKAILFLPMSAKS------------------------
FGF9  hu 159    GRRYYVALNKDGTPREGTRTKRHQKFTHFLPRPVDPDKVPELYKDILSQS----------
FGF10 hu 173    GRQMYVALNGKGAPRRGQKTRRKNTSAHFLPMVVHS------------------------
```

Figure 4.3: **(A** and **B)** Homology model of thirteen-lined ground squirrel FGF21 structure based on human FGF19. FGF21 adopts the beta-trefoil structure with beta-strand ribbons shown in color. **(C)** Multiple sequence alignment of thirteen-lined ground squirrel (gs) FGF21 with human (hu) FGFs. The beta-strands are underlined in the alignment and labeled above.

4.3 C). This multiple sequence alignment was compared to the sequence alignment in Goetz, *et al* and structural information for each of the FGFs was added to the alignment (Goetz, Beenken et al. 2007). FGF proteins form a beta-trefoil structure containing 12 anti-parallel beta-strands in a barrel-like formation. FGF19 and FGF21 have the highest structural identity with a 40% similarity. A homology model of TLG squirrel FGF21 was solved using human FGF19 as the analogous protein (PDB ID 2P23B) using Swiss Model Software (Peitsch, Wells et al. 1995; Arnold, Bordoli et al. 2006; Kiefer, Arnold et al. 2009) (Fig 4.3). The FGF21 homology model adopts the same beta-trefoil structure of the other FGFs. The predicted beta-strands in FGF21 are underlined in the sequence and numbered above the alignment (Fig 4.3 C). Traditional FGFs have paracrine signaling and contain a heparin binding region between beta-strands 10 and 12. Upon release from a cell they bind to HS molecules in the extracellular matrix. The heparin binding regions of the endocrine acting FGFs; including FGF19/15, FGF23, and FGF21; have distinct structural differences compared to the traditional FGFs that appear to allow endocrine activity by preventing heparin binding (Goetz, Beenken et al. 2007). The region between beta-strands 10 and 12 has low amino acid identity in the alignment of multiple FGFs and the alignment of FGF21 sequences from multiple species (Fig 4.2 and Fig 4.3C). As a result this region of the homology model of FGF21 is not accurate and the predicted beta-strand in this region is colored in gray in Figure 4.3.

Thirteen-lined Ground Squirrel FGF21 Adenoviral Construct. The TLG squirrel FGF21 sequence was inserted into the *Xba*I and *Hin*dIII sites in the polylinker region of the pACCMVpLmP1(-)loxP-SSP plasmid. The FGF21 cDNA

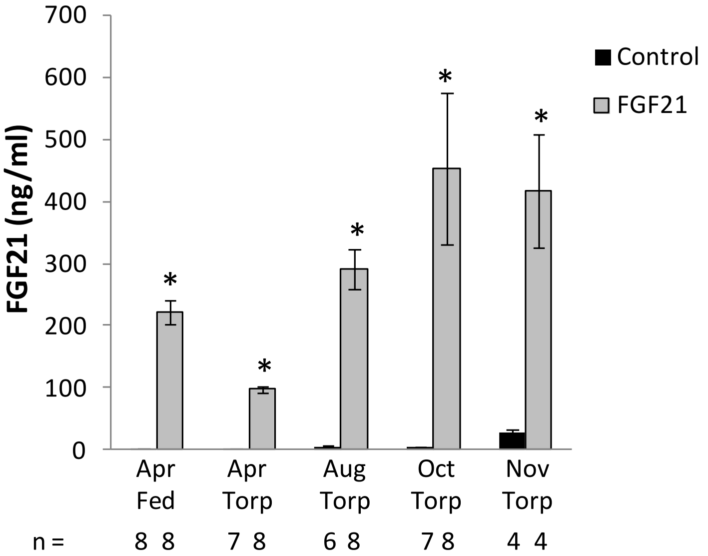

Figure 4.4: Thirteen-lined ground squirrel serum FGF21 concentrations after injection of FGF21 or control adenoviral vector. The injection of adenoviral vector containing the thirteen-lined ground squirrel FGF21 sequence significantly increased FGF21 protein concentration in serum samples as compared for each experimental group by Student's t-test as indicated by *. Apr fed experiments were done after the hibernation season in fed squirrels kept at 23 °C with a 12:12 l:d cycle and food freely available. Torpor (Torp) experiments were done in April, August, and October in squirrels kept at 5 °C in 24 h darkness and no food available for 7 days. In the November torpor experiments squirrels were maintained at 23 °C in a 12:12 l:d cycle with no food available for 7 days. All serum samples were collected 7 days after adenoviral injection. Standard error bars are shown.

sequence was 645 bp long, and the coding region was 627 bp (Fig 4.1A). The resulting adenoviral vector (AdFGF21) was purified and injected into squirrels to increase the expression of FGF21. As a control, squirrels were injected with the RR5 adenoviral construct that did not contain an insert (AdRR5). Serum samples were collected and the concentration of FGF21 was determined by ELISA (Fig 4.4). AdFGF21 increased the concentration of serum FGF21 significantly as compared to serum from AdRR5-injected squirrels for each experimental group as tested by Student's t-test. The TLG squirrel FGF21 adenoviral vector was effective in increasing FGF21 serum protein in wild squirrels.

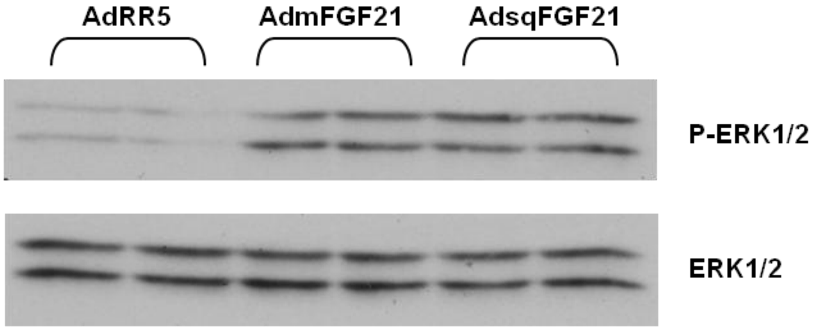

Figure 4.5: Adenoviral-mediated expression of thirteen-lined ground squirrel FGF21 was capable of signaling in primary mouse adipocytes. Downstream of FGF21 activation of FGFR, the MAPK pathway is initiated and this involves phosphorylation of ERKs 1 and 2. The phosphorylation of ERK1/2 resulting from thirteen-lined ground squirrel FGF21 was similar to the positive control using mouse FGF21.

Thirteen-lined Ground Squirrel FGF21 Signaling Capability. As noted previously the TLG squirrel FGF21 sequence is similar to FGF21 sequences from other species and other FGF sequences, but there were some amino acid substitutions present (Fig 4.2 and Fig 4.3). The FGF21 protein expressed using the adenoviral vector was tested for its capability to signal in a cellular system. Primary pre-adipocytes were isolated from mice and differentiated. The adipocytes were treated with conditioned media from 911 cells infected with adenovirus with no insert (AdRR5), adenovirus expressing mouse FGF21 (AdmFGF21), or adenovirus expressing TLG squirrel FGF21 (AdsqFGF21). The phosphorylation of ERK downstream of FGF signaling was measured by western blotting. TLG squirrel FGF21 expressed using an adenoviral construct resulted in similar phosphorylation of ERK compared to mouse FGF21 (Fig 4.5). This demonstrates that adenoviral-mediated expression of TLG squirrel FGF21 results in a signaling competent protein.

Physiological Response to Increased FGF21 in Thirteen-lined Ground Squirrels

Increased FGF21 during IBAs is consistent with the hypothesis that FGF21 is involved in induction of natural torpor bouts in TLG squirrels. Our published evaluation of physiological parameters of natural torpor bouts provided a guideline for evaluating induction of torpor with increased FGF21 (Hampton, Nelson et al. 2010). Next serum FGF21 concentrations in squirrels were increased to determine if higher concentrations of FGF21 induce torpor. FGF21 concentrations were increased using an adenoviral construct containing the TLG squirrel FGF21 sequence and injecting this recombinant adenovirus into squirrels. Pilot experiments were done in August when squirrels are fattening in preparation for hibernation, in October to November when squirrels are prepared to begin hibernation, in January when squirrels have been hibernating since November, and in March to April after the end of hibernation (Fig 2.1, black arrows). Endogenous gene expression differs at each of these annual times and FGF21 could affect the physiology of squirrels differently with different endogenous gene expression. Hibernating squirrels in January had poor recovery from the surgical manipulations involved in adenoviral injection and this experimental time point was discontinued after pilot experiments. In all other studies squirrels were maintained at 23 ºC, with a 12:12 l:d cycle, and fed freely until after adenoviral injection. In one experimental set after the hibernation season at the end of March into the beginning of April, squirrels were maintained at 23 °C with a 12:12 l:d cycle and fed freely after receiving the adenoviral construct. In another experimental set after the hibernation season at the end of March into the beginning of April and in the experimental sets performed in August, October, and January squirrels were maintained at 5 °C with a 24 h dark cycle and no food was available in order to allow typical deep torpor bouts to occur. Another experimental set was done in November to determine the effect of fasting without changes in light cycle or temperature and the squirrels were maintained at 23 °C with a 12:12 l:d cycle without food available after injection of the adenoviral construct. Serum and tissue samples were collected in pilot experiments at 3, 5, 7, 10, and 12 days to evaluate when the adenoviral injection resulted in increased FGF21. FGF21 was increased in all serum samples collected between 3 and 12 days and the remaining experimental samples were collected at 7 days.

The weight, T_b, HR, and movement of squirrels were monitored using implanted transmitters capable of detecting T_b, ECG, and movement. A selection of mean measurements from each experimental group is presented. Torpor occurred if minimum T_b is below 32 °C as defined in Chapter 3 and lower mean minimum T_b or mean minimum HR indicate deeper torpor bouts. A lower mean T_b or mean HR indicate more time spent with decreased physiological activity during the experiment.

April Fed Squirrels. In mid-April, after the end of hibernation, squirrels were kept at 23 °C in a 12:12 l:d cycle with food available for 2 to 4 weeks, and serum protein levels of FGF21 were raised using AdFGF21 in 8 squirrels. AdRR5 was administered to 8 squirrels as a control. The squirrels were kept at 23 °C with a 12:12 l:d cycle and given food and water *ad libitum* for 7 days after injection of the viral construct, when serum and tissues were collected. Serum concentration of FGF21 in control squirrels was 2 ng/ml and 222 ng/ml in squirrels given AdFGF21, a 111 fold increase, as measured by ELISA ($p < 0.0001$, Fig 4.6A). No squirrels

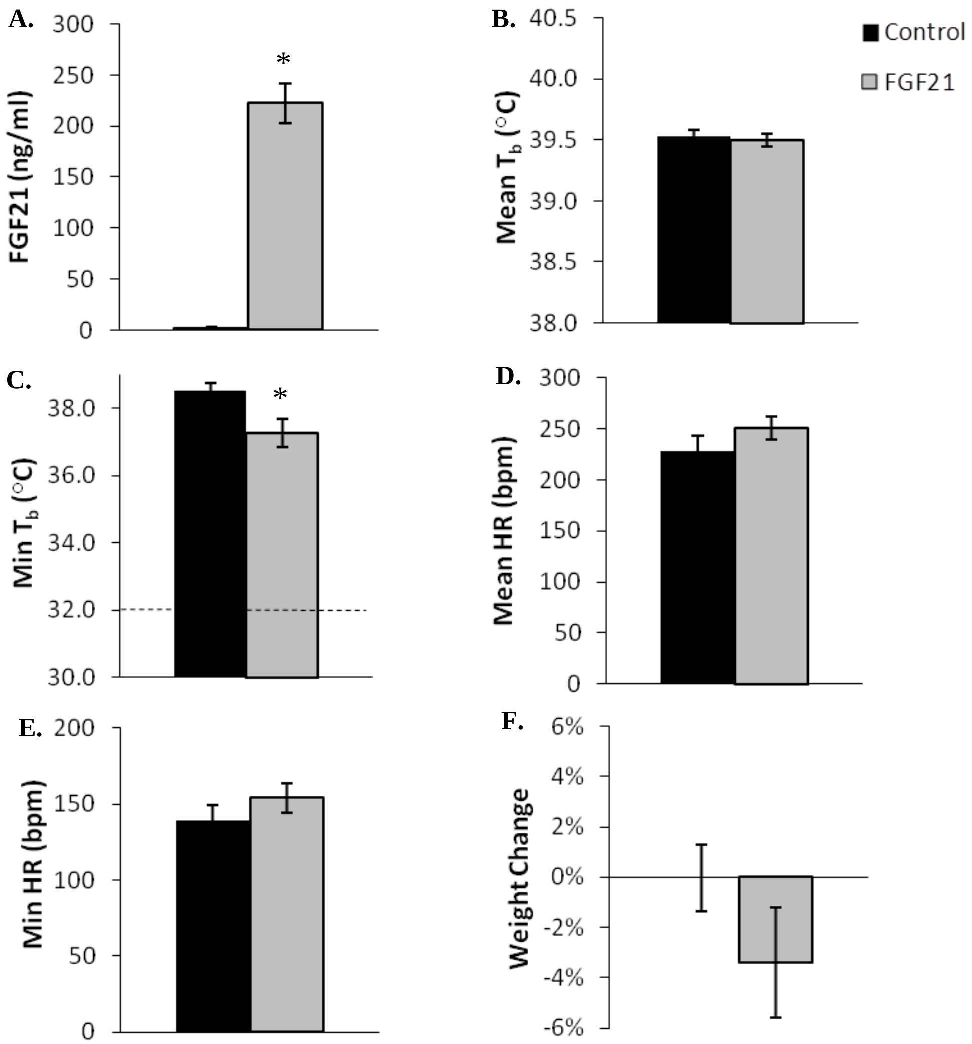

Figure 4.6: T_b, HR, and weight changes in fed thirteen-lined ground squirrels with raised levels of FGF21 (n = 8) and control squirrels (n = 8) during April. The squirrels were kept at 23 °C with a 12:12 light:dark cycle and fed *ad libitum* for 7 days. **(A)** The serum concentration of FGF21 measured by ELISA was significantly increased with administration of AdFGF21 ($p < 0.0001$). **(B)** The mean T_b of ground squirrels with raised levels of FGF21 did not differ from control squirrels. **(C)** The minimum T_b reached was significantly lower in squirrels with raised levels of FGF21 as tested by Student's t-test ($p = 0.012$). The dotted line indicates T_b necessary to be considered torpid. **(D and E)** The mean and minimum HR of squirrels with raised FGF21 did not differ from control squirrels. **(F)** The change in weight over 7 days was not different for squirrels with increased FGF21. Standard error bars are shown and (*) indicates significant difference.

entered torpor as defined by a T_b less than 32 °C. The mean minimum T_b of squirrels with increased FGF21 of 37.3 °C was significantly lower than that of control squirrels of 38.5 °C as tested by a Student's t-test ($p = 0.012$, Fig. 4.6C). Squirrels with increased FGF21 had a mean T_b of 39.5 °C, a mean HR of 251 bpm, a minimum HR of 154 bpm, and lost 3% body weight. There were no significant differences as tested by Student's t-test in these values when compared to control squirrels with a mean T_b of 39.5 °C ($p = 0.354$), a mean HR of 228 bpm ($p = 0.122$), a mean minimum HR of 139 bpm ($p = 0.155$), and a 0% change in body weight ($p = 0.108$, Fig. 4.6 B through F). FGF21 may sensitize squirrels to lower T_b as indicated increased FGF21 in fed squirrels kept at 23 °C in April lowering mean minimum T_b by 1.3 °C, but FGF21 did not induce torpor. FGF21 did not cause any significant differences in HR or weight changes over 7 days of monitoring of fed squirrels in April.

Hibernation Conditions. In captivity, squirrels do not maintain torpor without favorable environmental conditions to encourage hibernation. The effect of increased FGF21 was examined at an ambient temperature of 5 °C with 24 h darkness and no food available to allow full torpor bouts to occur. Serum protein levels of FGF21 were raised in squirrels during the end of March and early April, during August, and during October. The significance of differences was tested using Student's t-test.

March and April, Hibernation Conditions. After the completion of the hibernation season at the end of March and in early April, AdFGF21 was injected into 8 squirrels and AdRR5 was injected into 7 squirrels. The serum FGF21 concentration of control squirrels was 0.82 ng/ml and squirrels injected with AdFGF21 had a significantly higher concentration at 98.10 ng/ml, a 119 fold increase ($p < 0.0001$, Fig 4.7 A). The control squirrel mean minimum T_b was 22.6 °C and 20.2 °C for squirrels with increased FGF21. There were no significant differences in T_b, HR, or weight changes between control squirrels and squirrels with increased FGF21 (Fig 4.7).

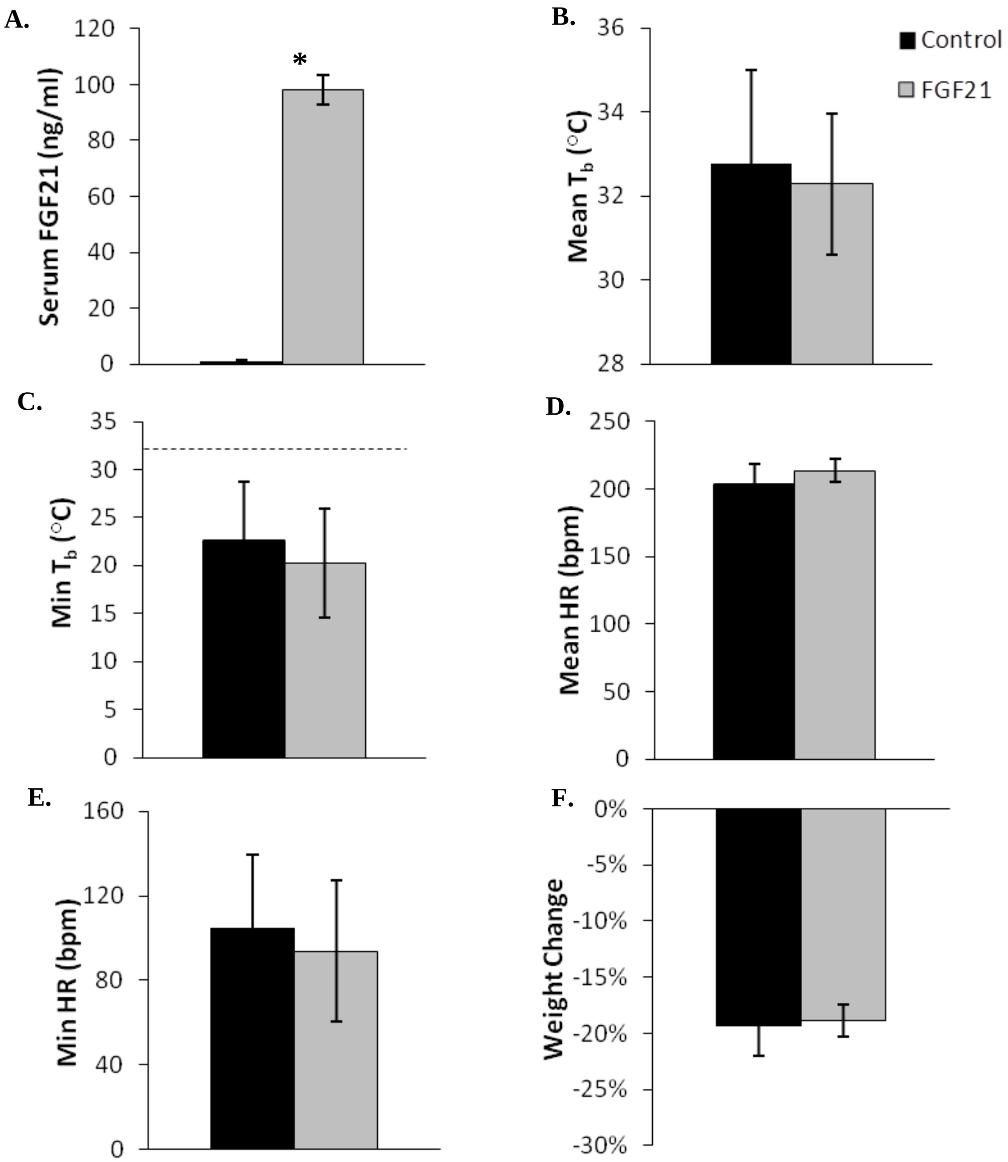

Figure 4.7: Physiological parameters of thirteen-lined ground squirrels with raised FGF21 in April. Control adenoviral vector was administered to 7 squirrels and the adenoviral vector that significantly raised levels of FGF21 was given to 8 squirrels **(A)**. Squirrels were kept at 5 °C, in 24 h darkness, without food and monitored for 7 days. There were no significant differences in T_b, HR, or weight changes between groups as tested by Student's t-test. The dashed line in **(C)** indicates torpid T_b. Standard error bars are shown.

Of the 15 squirrels approximately half entered torpor, including 4 given AdFGF21 and 3 given AdRR5. There was a significant difference in weight loss between squirrels that entered torpor (17%) and those that did not enter torpor (24%) regardless of adenovirus construct ($p = 0.0016$). The parameters of torpor bouts of the 3 control squirrels and 4 squirrels with increased FGF21 that entered torpor were compared. Squirrels with increased FGF21entered torpor 82.9 hours after injection and control squirrels entered torpor 81.5 hours after injection (*p* = 0.8874). The 3 control squirrels that entered torpor spent 58.5 hours in torpor and the 4 squirrels with increased FGF21 that entered torpor spent 58.8 hours in torpor (*p* = 0.9894). The lengths of entrance (control = 8.1 h, FGF21 = 7.8 h, *p* = 0.8167), maintenance (control = 27.5 h, FGF21 = 27.2 h, *p* = 0.9830) and arousal (control = 1.1 h, FGF21 = 1.5 h, *p* = 0.2454) phases of torpor did not differ between control squirrels and squirrels with increased FGF21. The HR began to drop an average of 0.8 hours before torpor began in squirrels with increased FGF21 and in control squirrels (*p* = 0.6039). In control squirrels HR began to rise 3.7 hours before the end of torpor and in squirrels with increased levels of FGF21 HR began to increase 3.6 hours before the end of torpor (*p* = 0.9048). The movement of control squirrels stopped 2.0 hours before the beginning of torpor and in squirrels with increased FGF21 3.2 hours before the beginning of torpor (*p* = 0.6565).

In summary, in April with hibernation conditions, squirrels with increased FGF21 did not enter torpor more readily or have deeper torpor bouts. There were no physiological differences observed in squirrels with increased FGF21. Regardless of the adenoviral construct used, squirrels that entered torpor during the 7-day experiment predictably lost significantly less weight than squirrels that did not enter torpor.

August, Hibernation Conditions. In August the experiment was repeated with 7 squirrels receiving AdRR5 and 8 squirrels receiving AdFGF21. The squirrels

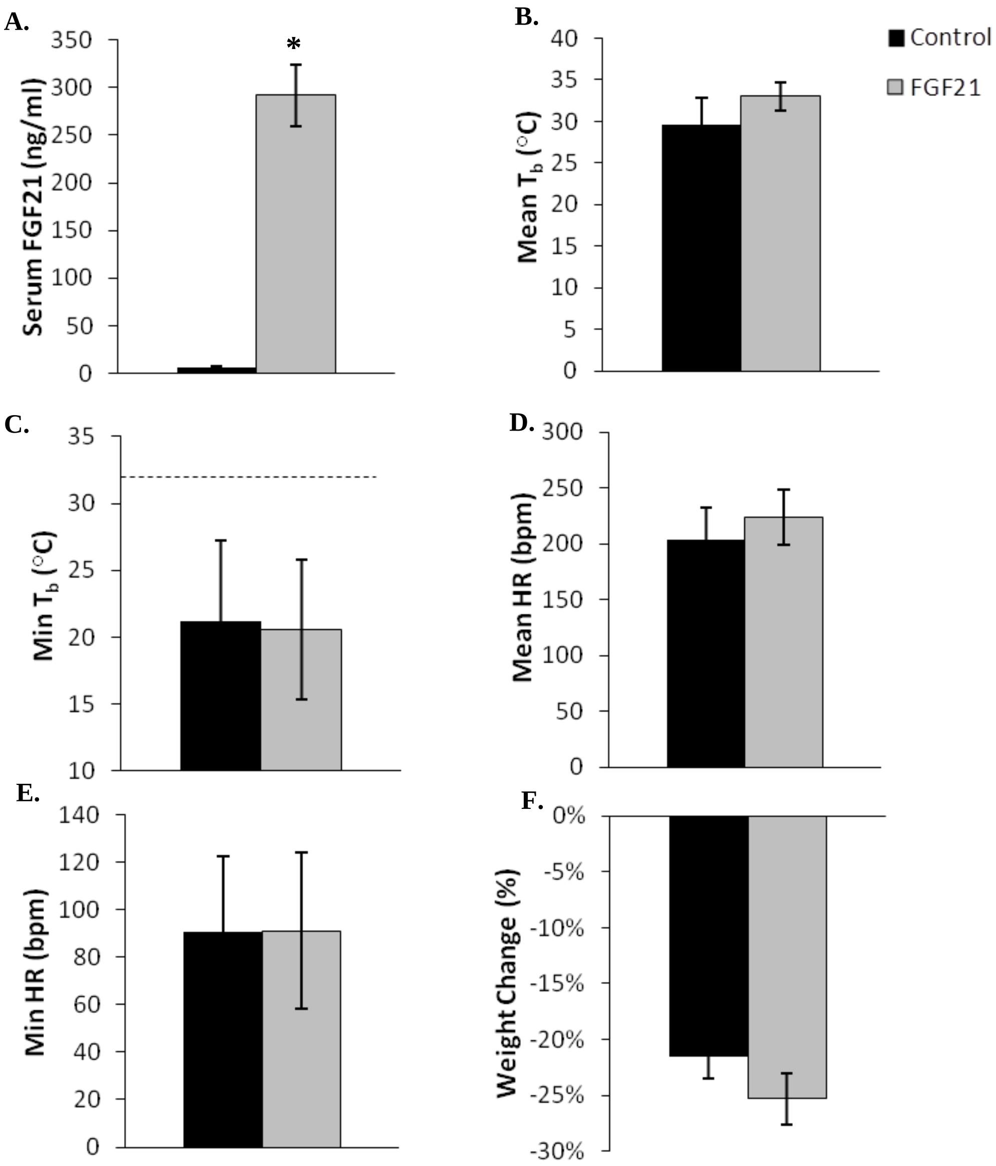

Figure 4.8: Physiological measurements in thirteen-lined ground squirrels with raised levels of FGF21. In August, 7 squirrels were given AdRR5 and 8 were given AdFGF21 **(A)**. The squirrels were placed in an environmental chamber at 5 °C, in 24 h darkness with no food and monitored for 7 days. The physiological parameters shown are **(B)** the mean T_b; **(C)** the minimum T_b; **(D)** the mean HR; **(E)** the minimum HR; and **(F)** the weight change. There were no significant differences in physiological parameters of the control and FGF21 groups as tested by Student's t-test. Standard error bars are shown.

were monitored for 7 days at 5 °C with no food in 24 h darkness. Control squirrels had a serum FGF21 concentration of 5.62 ng/ml and squirrels that received the AdFGF21 had a significantly higher concentration of 291.92 ng/ml ($p < 0.0001$, Fig

4.8). There were no significant differences in the T_b, HR, or weight changes between control squirrels and squirrels with increased FGF21 (Fig 4.8).

An analysis including only squirrels that entered torpor was done to evaluate if FGF21 affected the torpor bouts of squirrels. Of the 15 squirrels, 3 control squirrels and 4 squirrels with increased FGF21 entered torpor. Control squirrels entered torpor 34.1 hours after injection of adenovirus and squirrels with increased FGF21 entered torpor 75.8 hours into the experiment ($p = 0.116$). Although squirrels with increased FGF21 entered torpor later on average than control squirrels, the sub-sample size of squirrels that entered torpor was not sufficient for statistical significance. The mean minimum T_b reached during torpor was 4.1 °C for control squirrels and 7.0 °C for squirrels with raised FGF21 ($p = 0.274$). Control squirrels spent 93.6 hours in torpor and squirrels with increased FGF21 spent 43.6 hours in torpor ($p = 0.0533$). The lengths of entrance (control = 9.3, FGF21 = 9.8, $p = 0.7394$), maintenance (control = 35.1, FGF21 = 41.2, $p = 0.7331$), and arousal (control = 1.5, FGF21 = 1.6, $p = 9669$) did not differ with increased FGF21. The HR began to decrease 0.6 hours before the beginning of torpor for control squirrels and 0.2 hours before torpor for squirrels with increased FGF21 ($p = 0.6015$). HR began to rise 5.6 hours before the end of torpor in control squirrels and 3.5 hours before the end of torpor in squirrels with increased FGF21 ($p = 0.3659$). Squirrels stopped moving 2.0 hours before torpor began in the control group and 3.7 hours before torpor began in squirrels with increased FGF21 ($p = 0.3319$). The weight loss of all squirrels with increased FGF21 (25%) was not significantly different from control squirrels (21%, $p = 0.2263$) nor was there a significant difference if only torpid squirrels from each group were evaluated (*p* = 0.4380). Squirrels that entered torpor despite which adenoviral construct received (loss of 19%, n = 6), lost less weight than the squirrels that remained active for 7 days without food available (loss of 27%, n = 7, *p* = 0.0058). In summary, in August with hibernation conditions squirrels with increased FGF21 showed no significant differences in physiological parameters measured. Elevated levels of FGF21 did not affect weight loss in fasted squirrels during August, but there was significantly less weight loss in squirrels that entered torpor during fasting compared to squirrels that remained active.

October, Hibernation Conditions. In October, squirrels have acquired excess adipose tissue and are prepared to begin hibernation. The experiment was repeated giving 8 squirrels AdFGF21 and 7 squirrels AdRR5. All squirrels were placed in an environmental chamber at 5 °C, with 24 hours darkness with water *ad libitum* and fasted for 7 days. Control squirrels had a serum FGF21 concentration of 4.25 ng/ml and squirrels that received AdFGF21 had a significantly higher concentration of 452.68 ng/ml, a 106 fold increase (*p* = 0.0044, Fig 4.9). All 15 squirrels entered torpor despite which adenoviral construct they received. The mean T_b of 22.6 °C in squirrels with increased FGF21 was significantly higher than the mean T_b of 16.4 °C in control squirrels (*p* = 0.0384). The mean HR was also significantly higher in squirrels with increased FGF21 at 155 bpm compared to 96 bpm in control squirrels (*p* = 0.0356, Fig 4.9). The higher mean HR and T_b can be attributed to control squirrels entering torpor an average of 31.3 hours into the experiment and squirrels with raised levels of FGF21 entering torpor an average of 50.1 hours into the experiment (*p* = 0.0633). The mean minimum T_b during torpor

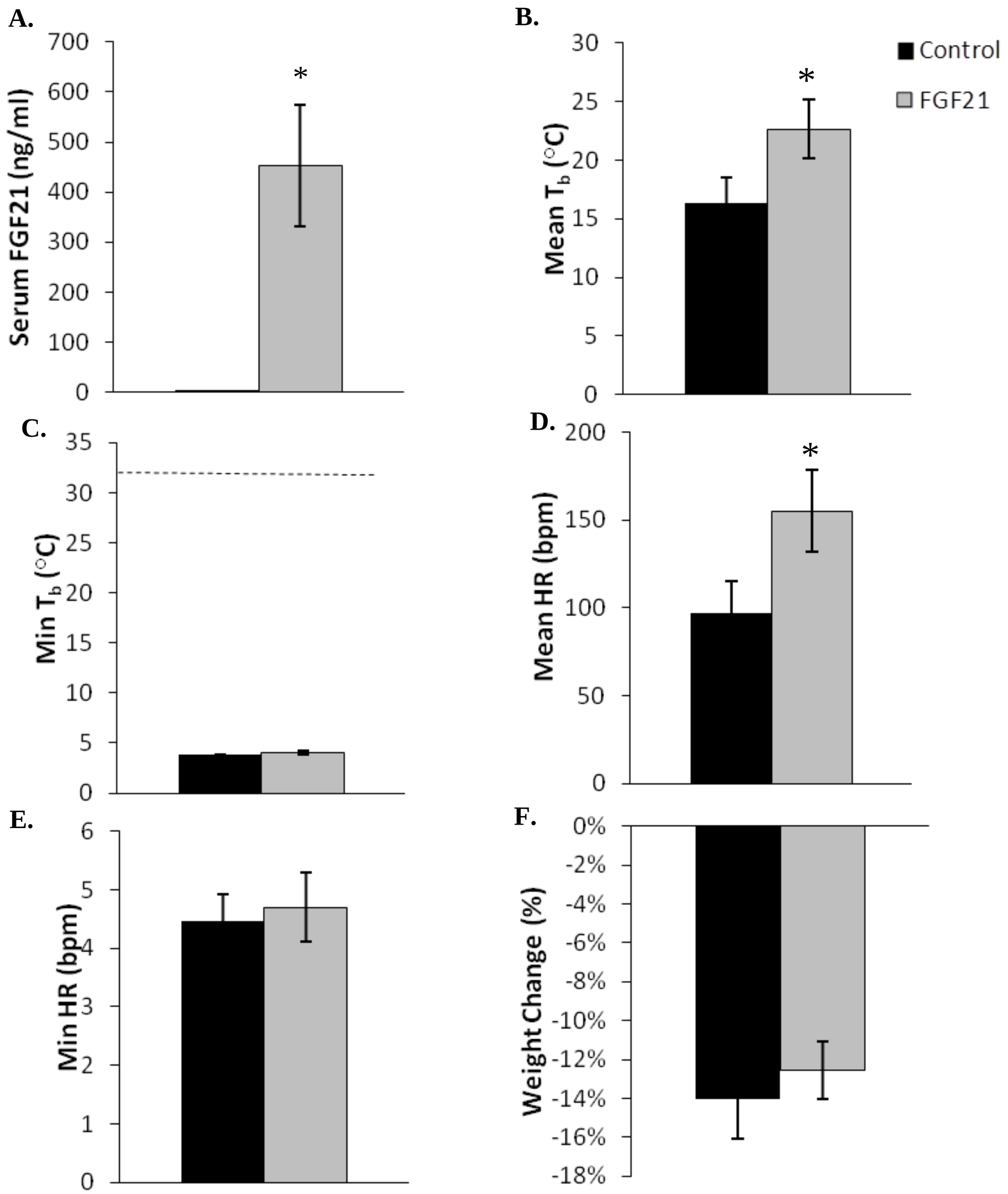

Figure 4.9: Physiological measurements of thirteen-lined ground squirrels with increased FGF21 in October. There were 7 squirrels that received AdRR5 and 8 squirrels that received AdFGF21 **(A)**. The squirrels were kept at 5 °C, in 24 h darkness with no food and monitored for 7 days. The mean T_b **(B)** and the mean HR **(D)** were significantly higher in squirrels with increased levels of FGF21 as tested by Student's t-test. There were no significant differences in minimum T_b **(C)**, minimum HR **(E)**, or weight change **(F)**. Standard error bars are shown and (*) indicates significant difference.

was 3.8 °C for control squirrels was not significantly different from the mean minimum T_b of 4.0 °C for squirrels with increased FGF21 ($p = 0.2447$). Control squirrels spent an average of 108.1 hours in torpor and squirrels with increased

FGF21 spent an average of 83.6 hours in torpor ($p = 0.1598$). The lengths of entrance (control 6.8 h, FGF21 7.9 h, $p = 0.1012$), maintenance (control 53.9 h, FGF21 57.4 h, $p = 0.7423$), and arousal (control 1.3 h, FGF21 1.2 h, $p = 0.7172$) phases of torpor did not differ significantly for squirrels with increased FGF21 compared to control squirrels. The HR of control squirrels dropped a mean of 1.1 hours before torpor began and 1.0 hours before torpor in squirrels with increased FGF21 ($p = 0.8185$). At the end of torpor the HR began to rise 4.2 hours before torpor ended in control squirrels and 3.2 hours before the end of torpor for squirrels with increased FGF21 ($p = 0.1414$). The movement of control squirrels stopped 4.5 hours before torpor and for squirrels with increased FGF21 movement stopped 3.6 hours before torpor ($p = 0.4181$). Control squirrels had a 14% weight loss over the 7-day fasting period and squirrels with elevated FGF21 had a 12% weight loss during this period ($p = 0.488$).

In summary squirrels with increased FGF21 kept at 5 °C in 24 hours darkness and fasted for 7 days during October had significantly increased mean T_b and mean HR compared to control squirrels. Squirrels with increased FGF21 entered torpor later and spent less time in torpor during the 7-day experiment than control squirrels, and although these differences were not statistically significant, this caused significantly increased mean T_b and HR. All squirrels entered torpor and the other physiological parameters measured did not differ between groups.

November, Fasted with 12:12 Light Cycle at 23 °C. The effect of fasting and increased FGF21 without changes in light cycle and ambient temperature were tested before the hibernation season began in November. After the completion of the October experiments, 4 squirrels were injected with AdRR5 and 4 squirrels were

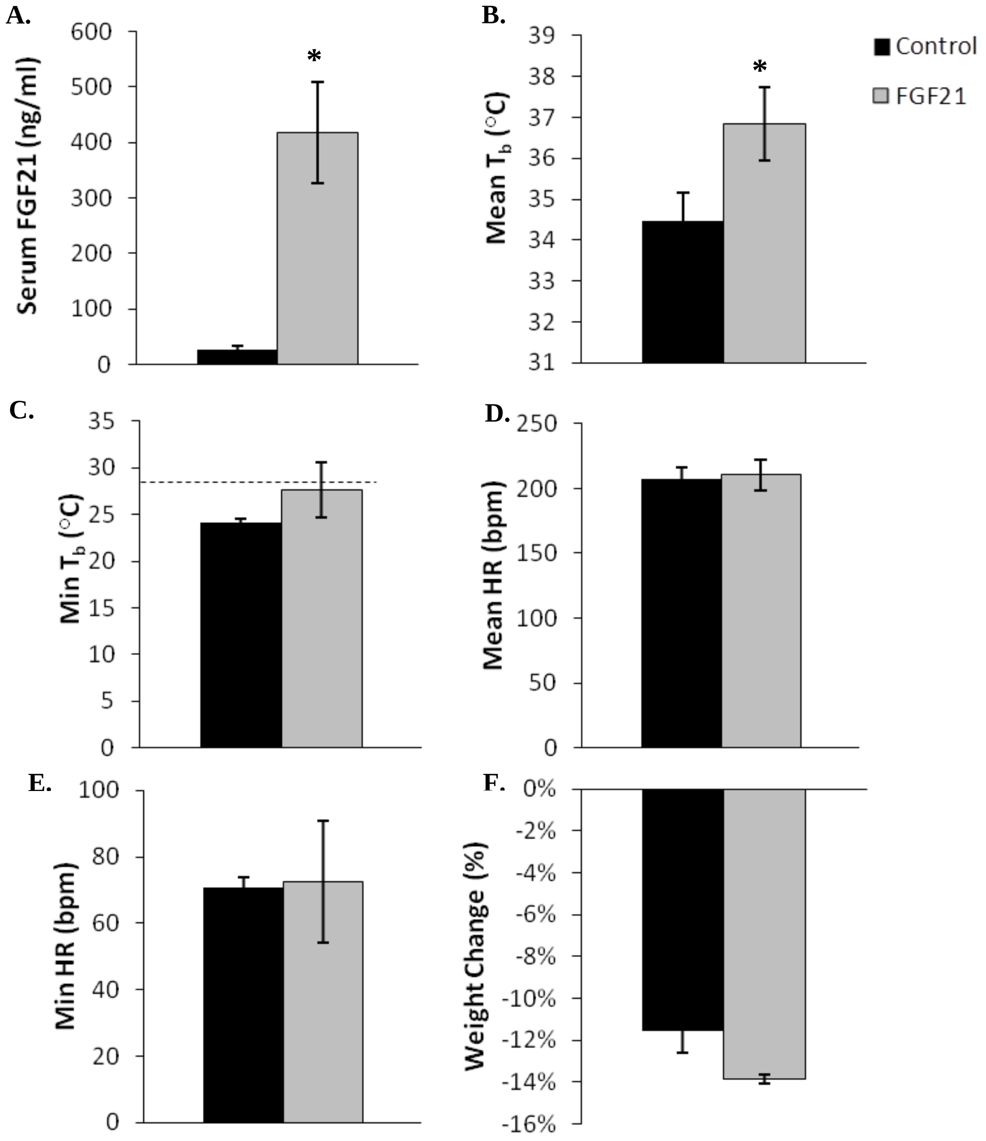

Figure 4.10: Physiological measurements in thirteen-lined ground squirrels in November with a 12:12 light cycle. There were 4 squirrels administered the control adenovirus and 4 squirrels given adenoviral construct that increased FGF21 **(A)**. The squirrels were kept at 23 °C with a 12:12 l:d cycle and no food and monitored for 7 days. The mean body temperature of squirrels with increased FGF21 was significantly higher than control squirrels **(B),** but no other measured parameters showed a significant difference as measured by Student's t-test. The dashed line in minimum T_b indicates torpid T_b and standard error bars are shown.

injected with AdFGF21. All squirrels were placed in an environmental chamber at 23 °C, with a 12:12 light dark cycle, water a*d libitum* and fasted for 7 days. Control squirrels had a serum FGF21 concentration of 26.63 ng/ml and squirrels given AdFGF21 had a significantly higher serum FGF21 concentration of 416.98 ng/ml (*p*

= 0.0053, Fig 4.10A). All 4 control squirrels entered torpor bouts with the minimum T_b limited by the ambient temperature of 23 °C. Of the 4 squirrels given AdFGF21, 3 entered ambient temperature limited torpor bouts and 1 did not. The mean T_b over 7 days was significantly higher in the group with increased FGF21, due to one squirrel with elevated FGF21 remaining active (Fig 4.10). The other physiological parameters measured did not differ significantly with elevated FGF21 (Fig 4.10).

The physiological parameters of the 4 control and 3 FGF21 squirrels that entered torpor were examined. The mean minimum T_b of the 4 control squirrels that entered torpor was 24.1 °C and the mean minimum T_b of the 3 FGF21 squirrels that entered torpor was 24.7 °C ($p = 0.370$). Due to the limits of an ambient temperature of 23 °C, torpid squirrels remained above this temperature and did not maintain deeper torpor bouts. Control squirrels began torpor a mean of 68.3 hours and squirrels with increased FGF21 began torpor a mean of 76.8 hours ($p = 0.6292$). Control squirrels spent 92.2 h and squirrels with increased FGF21 spent 80.6 h torpid during the 7-day experiment ($p = 0.8569$). HR of control squirrels dropped 2.9 hours before torpor occurred and 2.7 hours before torpor for squirrels with increased FGF21 ($p = 0.7469$). Movement stopped 2.7 hours before torpor began in control squirrels and 4.5 hours before torpor for squirrels with increased FGF21 ($p = 0.6917$). Control squirrels lost 12% body weight during the 7-day fast and squirrels with increased FGF21 lost 14% body weight ($p = 0.0803$). In summary there were no physiological differences noted in squirrels with increased FGF21 that entered torpor in November with a 12:12 l:d cycle at 23 °C and fasted for 7 days.

Summary of Physiological Experiments. None of the April fed squirrels kept at 23 °C with a 12:12 light cycle entered torpor, but squirrels with increased FGF21 had a lower mean minimum T_b. This is similar to the effect of elevated FGF21 in fasted mice (Inagaki, Dutchak et al. 2007). In fasting conditions, approximately half of the squirrels entered torpor in April and in August. The squirrels with elevated FGF21 did not enter torpor more frequently nor was there a difference in the measured parameters of torpor. In October fasting conditions, all squirrels entered torpor and the measured parameters of torpor were similar with increased FGF21 relative to control with the exception that squirrels with increased FGF21 had a significantly higher mean T_b and mean HR due to spending less time in torpor. In November fasting conditions during a 12:12 l:d cycle at 23 °C the measured parameters of torpor were also similar in squirrels with increased FGF21, with the exception of one squirrel with increased FGF21 not entering torpor. In conclusion increased FGF21 did not induce torpor in TLG squirrels, nor did it cause longer or deeper torpor bouts. In April fed squirrels increased FGF21 lowered mean minimum T_b and in October and November increased FGF21 reduced time spent torpid.

Metabolic Effects of FGF21 in Thirteen-Lined Ground Squirrels

The effect of FGF21 on serum metabolites was evaluated by measuring serum glucose, BHB, TG, and free FA, in addition to the metabolic hormone insulin. Serum was collected from squirrels the end of each pilot and full experiment. The experiments were performed during different months of the year under various environmental conditions of food availability (fed or fasted), ambient temperature

(°C), and l:d cycles. One experiment was conducted in conditions conducive to normal activity: April – fed, 23 °C, 12:12 l:d over 7 days. Six experiments were performed to examine the effect of elevated FGF21 under conditions conducive to torpor: 1) March-April – fasted, 5 °C, 24 h dark, 7 days; 2) March-April – fasted, 5 °C, 24 h dark, 10 days; 3) August – fasted, 5 °C, 24 h dark, 7 days; 4) October – fasted, 5 °C, 24 h dark, 7 days; 5) October – fasted, 5 °C, 24 h dark, 5 days; 6) January – fasted, 5 °C, 24 h dark, 12 days. Also one experiment was performed in November with 7 days of fasting at 23 °C and a 12:12 l:d cycle. The serum metabolite and insulin measurements were also done on that did not receive any injections to evaluate seasonal fluctuations of metabolites that occur in a hibernator.

Glucose. Glucose is the primary source of energy for cellular respiration in animals. It is derived from food sources and also is a common metabolic intermediate. Squirrels have decreased serum glucose during torpor and serum glucose concentrations are significantly below September-October active levels in December-February torpor ($p = 0.0015$) and March torpor ($p = 0.0005$) as compared by ANOVA followed by Tukey's HSD. The glucose concentration during IBA is similar to the concentrations during activity despite fasting (Fig 4.11, (Andrews, Russeth et al. 2009).

In April fed squirrels the serum glucose concentration was 9.0 mM for control squirrels and 9.1 mM for squirrels with increased FGF21 ($p = 0.48$, Fig 4.12 A). Control squirrels fasted for 7 days in hibernation conditions in April had a serum glucose concentration of 7.0 mM and squirrels with increased FGF21 had 6.6 mM ($p = 0.41$, Fig 4.12 B). Squirrels fasted for 10 days in hibernation conditions in April

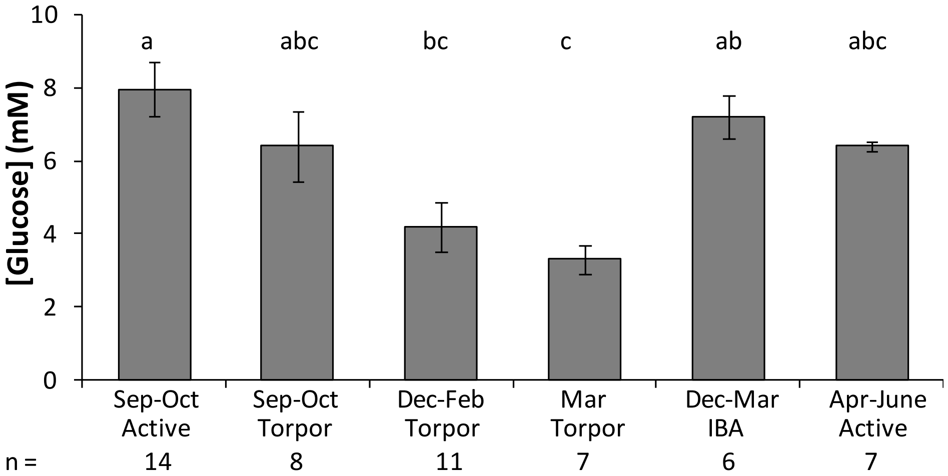

Figure 4.11: Seasonal fluctuations of serum glucose in thirteen-lined ground squirrels. Torpid squirrels had lower serum concentrations of serum glucose compared to active or IBA squirrels. This difference was significant between March torpid and the active and IBA states. This data was adapted from (Andrews, Russeth et al. 2009).

had a glucose concentration of 7.8 mM and with increased FGF21 the glucose concentration was 10.6 mM (*p* = 0.19, Fig 4.12 C). In August after 7 days of fasting in hibernation conditions the serum glucose concentration was 5.9 mM and 7.2 mM for squirrels with increased FGF21 (*p* = 0.14, Fig 4.12D). In October after 7 days of fasting in hibernation conditions the glucose concentration was 7.3 mM and for squirrels with increased FGF21 the glucose concentration was 9.6 mM (*p* = 0.11, Fig 4.12 E). In October after 5 days of fasting in hibernation conditions control squirrels had a serum glucose concentration of 9.6 mM and the squirrels with raised FGF21 had a serum glucose concentration of 9.3 mM (*p* = 0.47, Fig 4.12 F). After fasting for 7 days in November with a 12:12 l:d cycle at 23 °C the serum glucose concentration was 8.9 mM for control squirrels and squirrels with increased FGF21 (*p* = 0.49, Fig 4.12 G). In January after 12 days of fasting in hibernation conditions the serum glucose concentration was 8.1 mM and the serum glucose concentration was 4.9 mM with increased FGF21 (*p* = 0.23, Fig 4.12 H). Increased FGF21 did not significantly

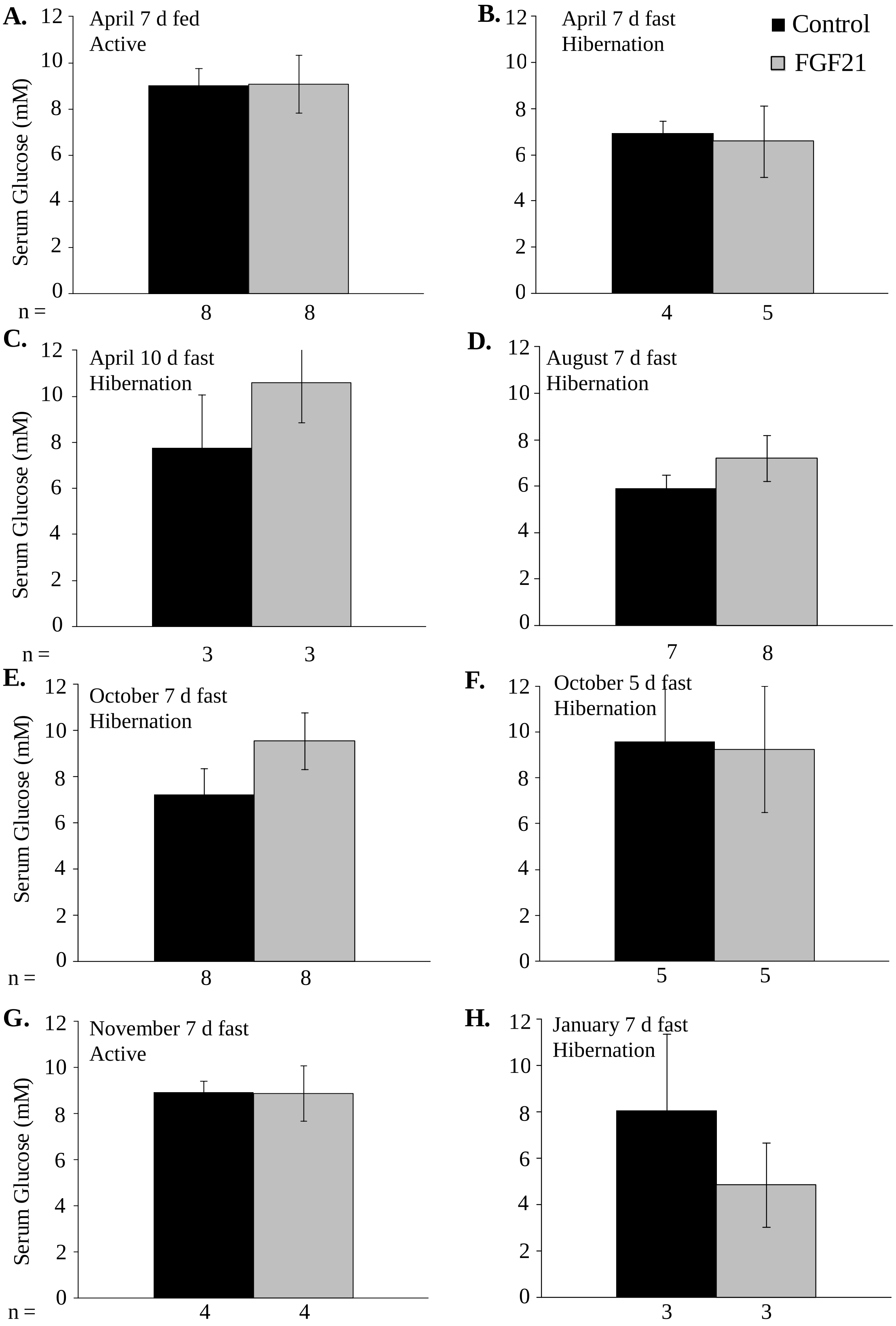
A.
April 7 d fed
Active
B.
April 7 d fast
Hibernation
■ Control
▨ FGF21
C.
April 10 d fast
Hibernation
D.
August 7 d fast
Hibernation
E.
October 7 d fast
Hibernation
F.
October 5 d fast
Hibernation
G.
November 7 d fast
Active
H.
January 7 d fast
Hibernation
Serum Glucose (mM)
0
2
4
6
8
10
12
n =
8 8
4 5
3 3
7 8
8 8
5 5
4 4
3 3

Figure 4.12: Serum glucose in thirteen-lined ground squirrels with increased FGF21. Glucose measurements were taken after each experiment including: fed for 7 days in April at 23 °C and 12:12 l:d **(A)**, fasted for 7 days in April in hibernation conditions **(B)**, fasted for 10 days in April in hibernation conditions **(C)**, fasted for 7 days in August in hibernation conditions **(D)**, fasted for 7 days in October in hibernation conditions **(E)**, fasted for 5 days in October in hibernation conditions **(F)**, fasted for 7 days in November at 23 °C and 12:12 l:d **(G)**, and fasted for 12 days in January in hibernation conditions **(H)**. There were no significant effects of increased FGF21 on serum glucose in thirteen lined ground squirrels as tested by Student's t-test.

affect the serum glucose concentration in squirrels in any of the conditions tested. This is in contrast to the lowering of serum glucose observed in mice (Kharitonenkov, Shiyanova et al. 2005).

Beta-hydroxybutyrate. Beta-hydroxybutyrate (BHB) is a ketone body that results from the breakdown of fatty acids and is transported through the bloodstream to tissues for use as fuel. Increased serum levels of BHB are expected in circumstances where lipid breakdown has increased, as in fasting states and when a high-fat diet is consumed. Squirrel serum BHB concentrations are increased during torpor relative to active and IBA states (Fig 4.13, (Andrews, Russeth et al. 2009). It is of interest that BHB concentrations are not significantly increased during an IBA despite the long-term fasting state of the squirrel. Combined with the previously described glucose concentrations during hibernation these results exemplify that squirrels rely on BHB for metabolic fuel during torpor and glucose during activity and IBAs.

In April fed squirrels 7 days after administration of the viral vector the mean serum BHB concentration of control squirrels was 0.17 mM and in squirrels with increased FGF21 was 0.16 mM (*p* = 0.39, Fig 4.14 A). Squirrels fasted for 7 days in hibernation conditions at the end of March and in the beginning of April had higher serum concentrations of BHB than fed squirrels. Control squirrels had a mean BHB

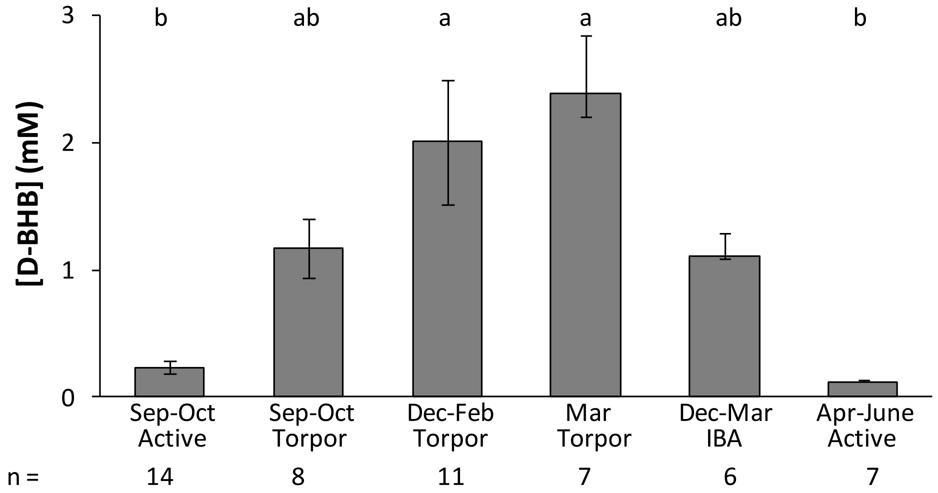

Figure 4.13: Thirteen-lined ground squirrel serum BHB during differing states of activity. Serum concentrations of BHB are increased during torpid states relative to activity in ground squirrels. Adapted from (Andrews, Russeth et al. 2009).

serum concentration of 2.1 mM and squirrels with increased FGF21 had a mean BHB serum concentration of 2.2 mM (*p* = 0.48, Fig 4.14 B). After 10 days of fasting at the end of March and in the beginning of April in hibernation conditions the mean serum BHB concentration from control squirrels was 2.1 mM and from squirrels with increased FGF21 was 0.6 mM (*p* = 0.22, Fig 4.14 C). In August after 7 days of fasting in hibernation conditions the mean BHB concentration of control squirrels and squirrels with increased FGF21 was 1.2 mM (*p* = 0.49, Fig 4.14 D). The mean serum BHB concentration measured in October after 7 days of fasting in hibernation conditions was 5.3 mM in control squirrels and 3.0 mM for squirrels with increased FGF21(*p* = 0.08, Fig 4.14 E). The BHB concentration in serum samples collected after 5 days of fasting in hibernation conditions in October were 3.8 mM in control squirrels and 0.9 mM in squirrels with increased FGF21. This difference was statistically significant as tested by Student's t-test with $p < 0.01$ (Fig 4.14 F). In November serum samples collected from squirrels fasted for 7 days and kept at 23 °C

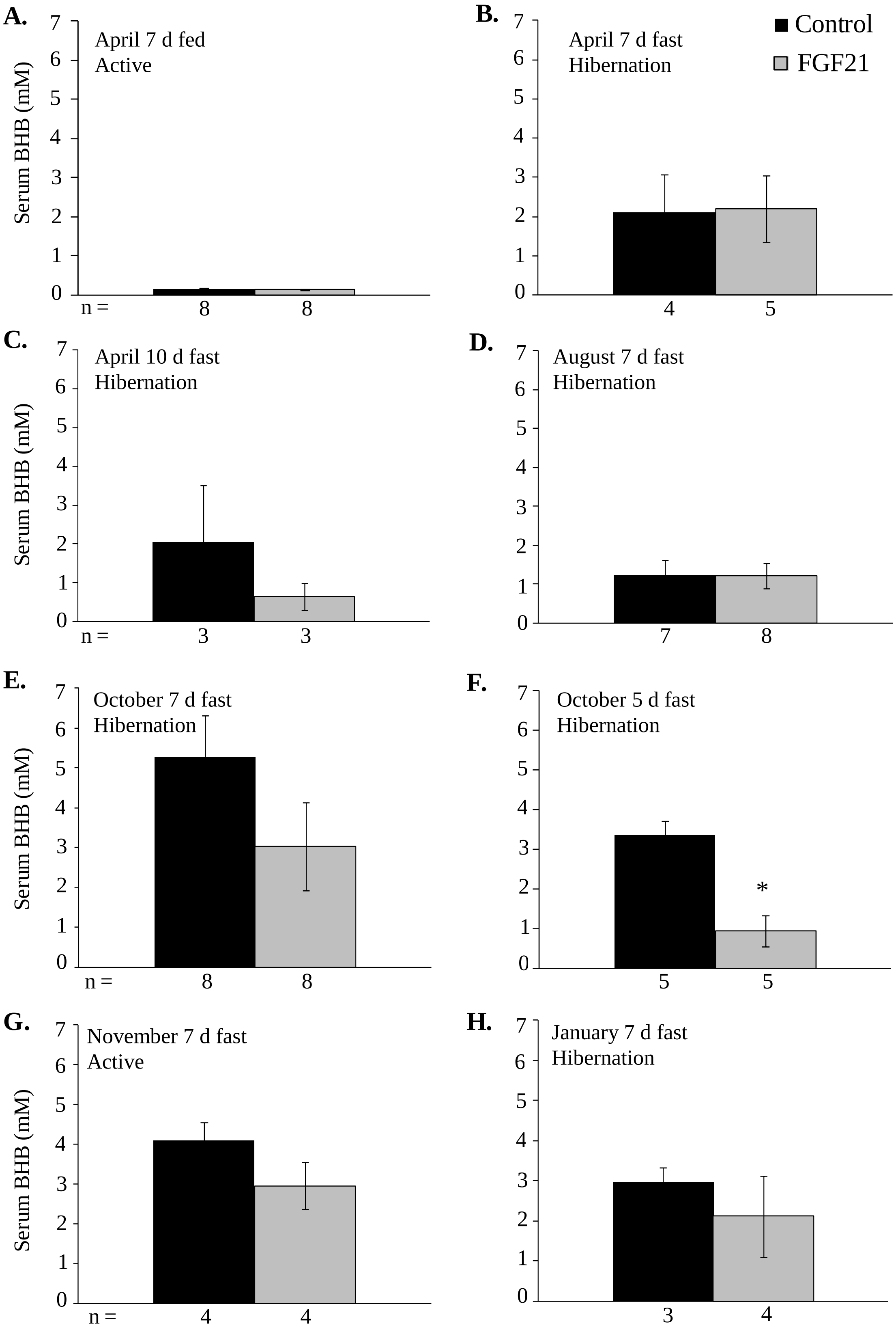
A.
April 7 d fed
Active
B.
April 7 d fast
Hibernation
■ Control
▨ FGF21
C.
April 10 d fast
Hibernation
D.
August 7 d fast
Hibernation
E.
October 7 d fast
Hibernation
F.
October 5 d fast
Hibernation
*
G.
November 7 d fast
Active
H.
January 7 d fast
Hibernation
Serum BHB (mM)
0
1
2
3
4
5
6
7
n = 8 8
4 5
n = 3 3
7 8
n = 8 8
5 5
n = 4 4
3 4

Figure 4.14: Thirteen-lined ground squirrel serum BHB with increased FGF21. BHB measurements were taken after each experiment including: fed for 7 days in April at 23 °C and 12:12 l:d **(A)**, fasted for 7 days in April in hibernation conditions **(B)**, fasted for 10 days in April in hibernation conditions **(C)**, fasted for 7 days in August in hibernation conditions **(D)**, fasted for 7 days in October in hibernation conditions **(E)**, fasted for 5 days in October in hibernation conditions **(F)**, fasted for 7 days in November at 23 °C and 12:12 l:d **(G)**, and fasted for 12 days in January in hibernation conditions **(H)**. Fasted squirrels had increased serum BHB concentrations (compare A to B). Increased FGF21 significantly attenuated this increase of BHB in October at 5 days of fasting (F). Standard error bars are shown.

with a 12:12 l:d cycle the mean serum BHB concentration in control squirrels was 4.1 mM and in squirrels with increased FGF21 was 3.0 mM ($p = 0.09$, Fig 4.14 G). After 12 days of fasting in January in squirrels kept in hibernation conditions the mean serum BHB concentration of control squirrels was 3.0 mM and of squirrels with increased FGF21 was 2.1 mM ($p = 0.23$, Fig 4.14 H). Increasing FGF21 in squirrels caused a trend toward a smaller increase in serum BHB during fasting. Increased FGF21 did not consistently cause a significant difference in the serum BHB concentration, but the serum BHB was significantly lower in squirrels with increased FGF21 after 5 days of fasting in October. In contrast to the attenuated increase in BHB in squirrels, FGF21 has been shown to increase serum BHB concentrations in mice (Inagaki, Dutchak et al. 2007).

Fatty Acids. Fatty acids (FA) are derived from the breakdown of triglycerides that are either stored in the body or consumed and absorbed through the intestine. Serum free FA concentrations were measured in in varying activity states throughout the year. Serum samples were collected from 8 August active, 8 winter torpid, 8 winter IBA, and 6 spring active squirrels. Winter torpid squirrels had significantly higher serum concentrations of FA with a mean of 2.2 mM as compared to 0.8 mM for IBA, 0.1 mM for August active and 0.5 mM for spring active (Fig

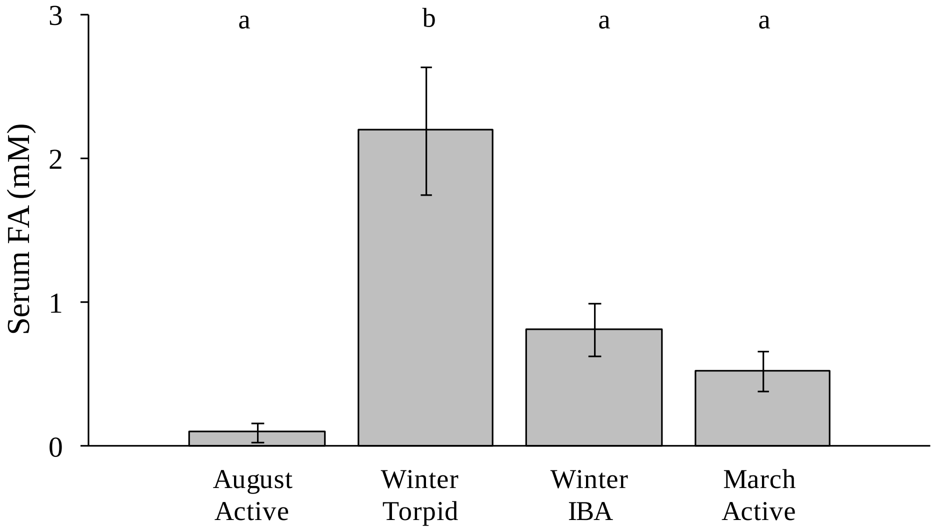

Figure 4.15: Thirteen-lined ground squirrel serum fatty acids (FA) in multiple activity states. The concentration of serum FA is significantly increased in torpid squirrels as compared to active and IBA squirrels as tested by ANOVA followed by Tukey's HSD. Standard error bars are shown.

4.15). The significance of these differences was tested by an ANOVA followed by Tukey's HSD.

In April fed squirrels the 7-day serum free FA concentration of was 0.2 mM and for squirrels with increased FGF21 was 0.1 mM (Fig 4.16 A). The significance of the difference of the serum free FA concentration was tested with a Student's t-test and the *p*-value was 0.02. Squirrels fasted for 7 days and kept in hibernation conditions in the end of March and the beginning of April had a mean serum free FA concentration of 0.7 mM and the mean serum free FA concentration squirrels with increased FGF21 was 0.4 mM ($p = 0.18$, Fig 4.16 B). Serum sampled after 10 days of fasting in hibernation conditions at the end of March and in the beginning of April had a mean free FA concentration of 0.4 mM and squirrels with increased FGF21 was 0.3 mM ($p = 0.15$, Fig 4.16 C). In August after 7 days of fasting in hibernation conditions control squirrels and squirrels with increased FGF21 had a mean serum free FA concentration of 0.6 mM ($p = 0.41$, Fig 4.16 D). In October after 7 days of

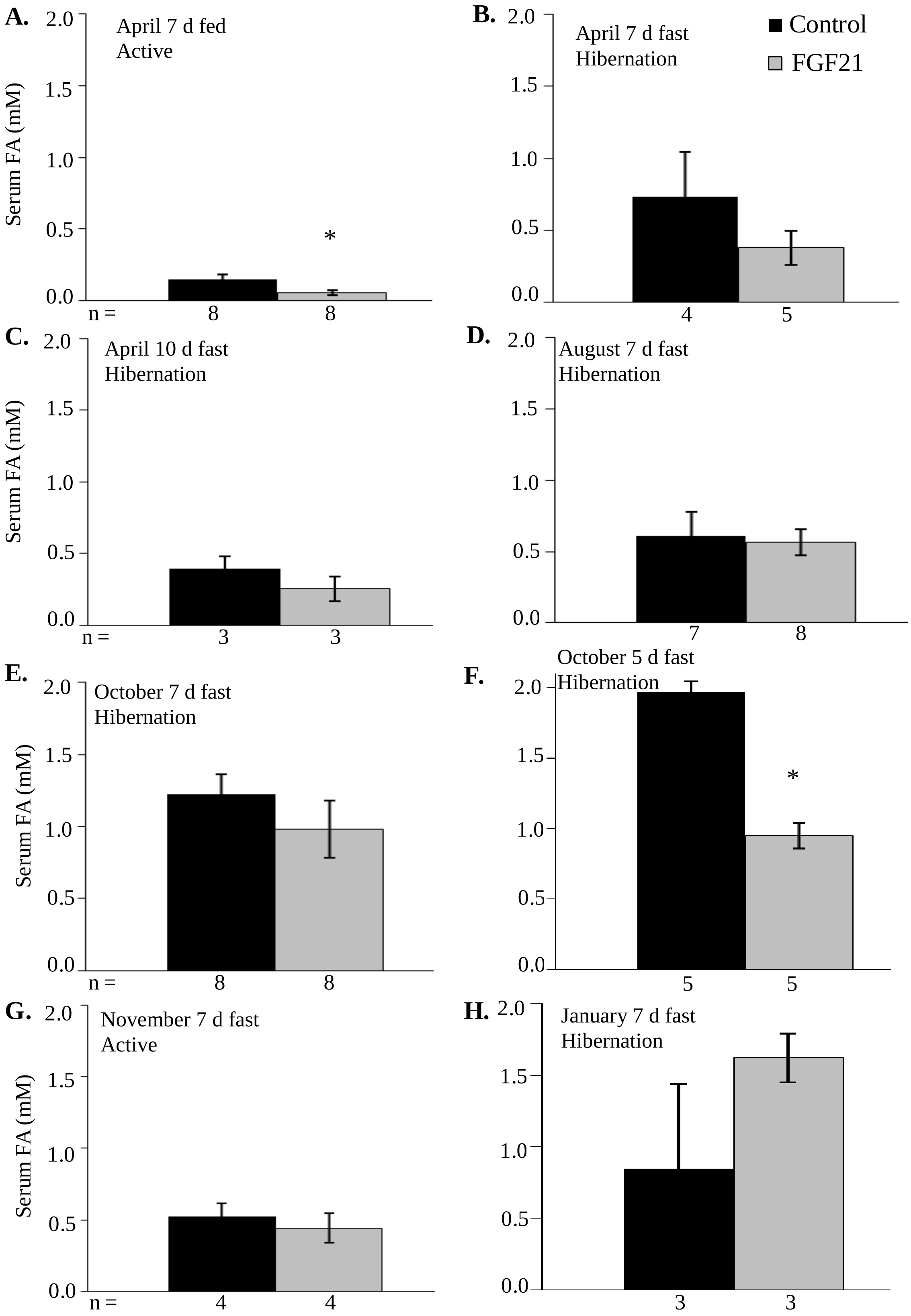
A.
April 7 d fed
Active
B.
April 7 d fast
Hibernation
■ Control
▨ FGF21
C.
April 10 d fast
Hibernation
D.
August 7 d fast
Hibernation
E.
October 7 d fast
Hibernation
F.
October 5 d fast
Hibernation
G.
November 7 d fast
Active
H.
January 7 d fast
Hibernation
Serum FA (mM)
2.0
1.5
1.0
0.5
0.0
*
n =
8
8
4
5
3
3
7
8
8
8
5
5
4
4
3
3

Figure 4.16: Thirteen-lined ground squirrel serum free fatty acids (FA) with increased FGF21. FA measurements were taken after each experiment including: fed for 7 days in April at 23 °C and 12:12 l:d **(A)**, fasted for 7 days in April in hibernation conditions **(B)**, fasted for 10 days in April in hibernation conditions **(C)**, fasted for 7 days in August in hibernation conditions **(D)**, fasted for 7 days in October in hibernation conditions **(E)**, fasted for 5 days in October in hibernation conditions **(F)**, fasted for 7 days in November at 23 °C and 12:12 l:d **(G)**, and fasted for 12 days in January in hibernation conditions **(H)**. Squirrels with increased FGF21tended to have lower serum FA, but this difference was only significant in April fed squirrels (**A**) and October 5-day fasted squirrels (**F**). Standard error bars are shown. (*) indicates significant difference.

fasting in hibernation conditions squirrels had a mean serum free FA concentration of 1.2 mM and squirrels with increased FGF21 had a mean of 1.0 mM (*p* = 0.17, Fig 4.16 E). After 5 days of in hibernation conditions in October, control squirrels had a significantly higher serum free FA concentration of 2.0 mM than squirrels with increased FGF21 with a mean of 1.0 mM (*p* = 0.04, Fig 4.16 F). At 23 °C in a 12:12 l:d cycle after 7 days of fasting in November, control squirrels had a mean serum free FA concentration of 0.5 mM and squirrels with increased FGF21 had a mean of 0.4 mM (*p* = 0.29, Fig 4.16 G). After 12 days of fasting in hibernation conditions in January, control squirrels had a mean serum free FA concentration of 0.8 mM and 3 squirrels with increased FGF21 had a mean of 1.6 mM (*p* = 0.17, Fig 4.16 H). Squirrels with increased FGF21 tended to have lower serum concentrations of free FA. This difference was only significant in April fed squirrels and in October fasted squirrels at 5 days. In January, squirrels with increased FGF21 had higher mean serum free FA but this was not significant.

Triglycerides. Triglycerides (TG) are composed of three fatty acids each in an ester linkage with a single glycerol. TG store energy, provide insulation, and can be absorbed from food through the intestine. Serum TG concentrations were measured in 8 squirrels in each of four activity states. August active squirrels had a mean serum TG concentration of 3.8 mM, winter torpid squirrels had a concentration

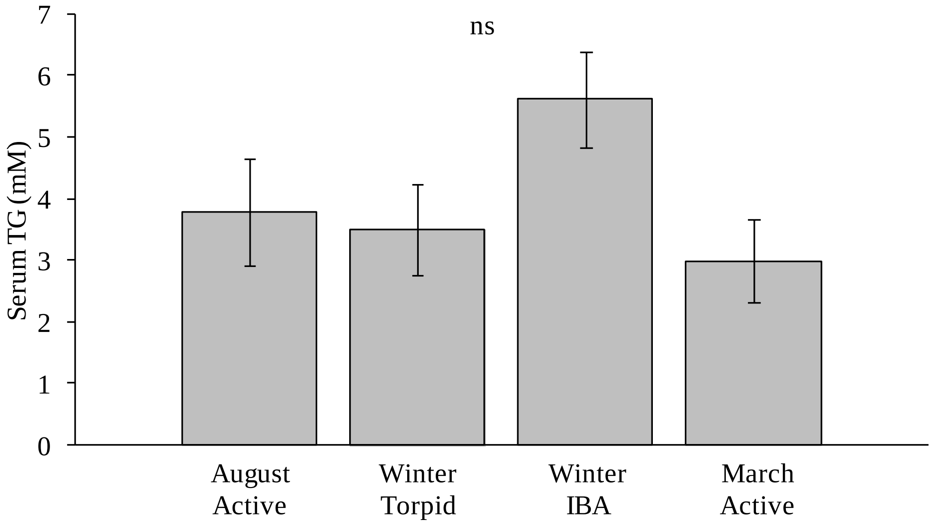

Figure 4.17: Thirteen-lined ground squirrel serum triglycerides (TG) during multiple activity states. There was no significant difference in serum TG seasonally in thirteen-lined ground squirrels as tested by ANOVA. Standard error bars are shown.

of 3.5 mM, winter IBA squirrels had a mean of 5.6 mM and April active squirrels had a mean of 3.0 mM (Fig 4.17). There was no significant difference in the means as tested by an ANOVA.

In April fed squirrels 7 days after adenoviral vector injection the mean serum TG concentration of control squirrels was 4.0 mM and in squirrels with increased FGF21 was 4.3 mM ($p = 0.36$, Fig 4.18 A). After 7 days of fasting in hibernation conditions at the end of March and in the beginning of April, control squirrels had a mean serum TG concentration of 2.2 mM and squirrels with increased FGF21 of 1.4 mM ($p = 0.14$, Fig 4.18 B). After 10 days of fasting in hibernation conditions at the end of March and in the beginning of April, control squirrels had a mean serum TG concentration of 5.0 mM and squirrels with increased FGF21 had a concentration of 4.1 mM ($p = 0.31$, Fig 4.18 C). In August after 7 days of fasting in hibernation conditions control squirrels had a mean serum TG concentration of 5.0 mM and squirrels with increased FGF21 had a concentration of 4.9 mM ($p = 0.48$,

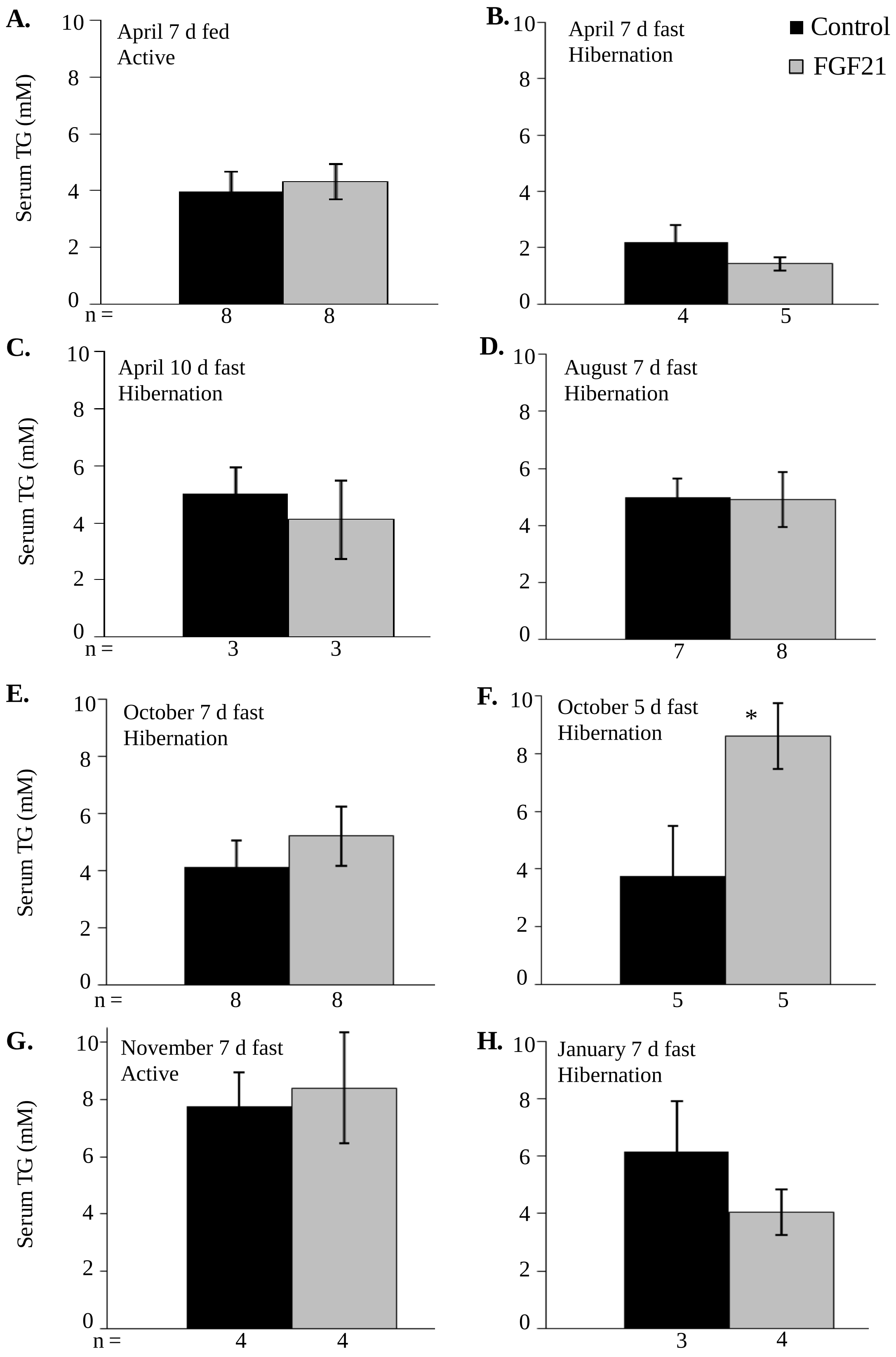
A.
Serum TG (mM)
10
8
6
4
2
0
April 7 d fed
Active
n =
8
8
B.
April 7 d fast
Hibernation
4
5
■ Control
□ FGF21
C.
April 10 d fast
Hibernation
n =
3
3
D.
August 7 d fast
Hibernation
7
8
E.
October 7 d fast
Hibernation
n =
8
8
F.
October 5 d fast
Hibernation
*
5
5
G.
November 7 d fast
Active
n =
4
4
H.
January 7 d fast
Hibernation
3
4

Figure 4.18: Thirteen-lined ground squirrel serum triglycerides (TG) with increased FGF21. TG measurements were taken after each experiment including: fed for 7 days in April at 23 °C and 12:12 l:d **(A)**, fasted for 7 days in April in hibernation conditions **(B)**, fasted for 10 days in April in hibernation conditions **(C)**, fasted for 7 days in August in hibernation conditions **(D)**, fasted for 7 days in October in hibernation conditions **(E)**, fasted for 5 days in October in hibernation conditions **(F)**, fasted for 7 days in November at 23 °C and 12:12 l:d **(G)**, and fasted for 12 days in January in hibernation conditions **(H)**. The effect of increased FGF21 on thirteen-lined ground squirrel serum TG did not have a clear trend. There was a significantly higher level of TG in squirrels with increased FGF21 in October after 5 days of fasting. Standard error bars are shown. (*) indicates significant difference.

Fig 4.18 D). In October after 7 days of fasting in hibernation conditions control squirrels had a mean serum TG concentration of 4.1 mM and squirrels with increased FGF21 had a concentration of 5.2 mM ($p = 0.23$, Fig 4.18 E). After 5 days of fasting in hibernation conditions control squirrels had a mean serum TG concentration of 3.8 mM and squirrels with increased FGF21 had a significantly higher concentration of 8.6 mM ($p = 0.03$, Fig 4.18 F). In November after 7 days of fasting at 23 °C in a 12:12 l:d cycle control squirrels had a mean serum TG concentration of 7.8 mM and squirrels with increased FGF21 had a concentration of 8.4 mM ($p = 0.40$, Fig 4.18 G). In January after 12 days of fasting in hibernation conditions control squirrels had a mean serum TG concentration of 6.1 mM and squirrels with increased FGF21 had a mean serum TG concentration of 4.1 mM ($p = 0.18$, Fig 4.18 H). There was not a clear trend in the affect of FGF21 on serum TG in fed or fasted squirrels. After 5 days of fasting in October squirrels with increased FGF21 had a higher serum TG concentration, but this effect was not observed at 7 days.

Insulin. Insulin is a metabolic hormone that is released when blood glucose concentrations are high. Insulin promotes uptake and storage of excess glucose and suppresses the breakdown of lipids for fuel. In fed squirrels insulin levels are significantly increased during September and October in both active and torpid states

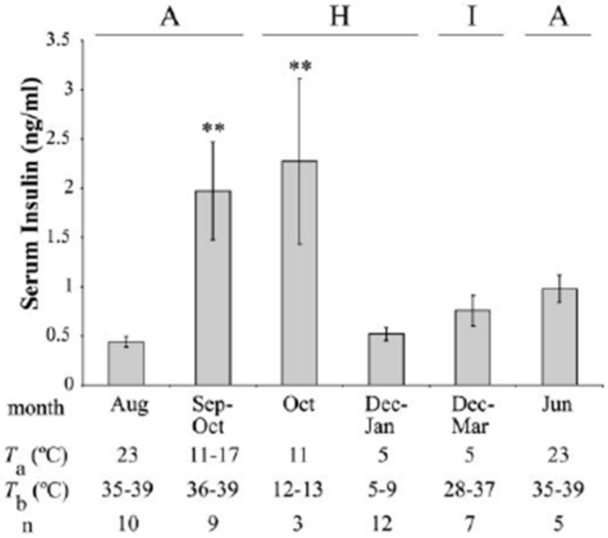

Figure 4.19: Serum insulin concentrations in thirteen-lined ground squirrels in multiple activity states. Serum insulin levels were significantly higher in September and October squirrels in both active (A) and hibernating (H) states compared to August active, December – January hibernating, December – March IBA (I), and June active. Figure from Buck, 2002.

(Fig 4.19,(Buck, Squire et al. 2002).

In April fed squirrels the serum insulin concentration was 1.0 ng/ml and in squirrels with increased FGF21 there was a significantly lower serum insulin concentration of 0.6 ng/ml ($p = 0.04$, Fig 4.20 A). After 7 days of fasting in hibernation conditions at the end of March and in the beginning of April, squirrels had a mean serum insulin concentration of 1.0 ng/ml and with increased FGF21 the concentration was 1.4 ng/ml ($p = 0.26$, Fig 4.20 B). After 10 days of fasting in hibernation conditions at the end of March and in the beginning of April, squirrels had a mean serum insulin concentration of 0.6 ng/ml and with increased FGF21 there was a mean concentration of 0.8 ng/ml ($p = 0.33$, Fig 4.20 C). In August after 7 days of fasting in hibernation conditions squirrels had a mean serum insulin concentration of 0.4 ng/ml and with increased FGF21 had a concentration of 0.6 ng/ml ($p = 0.28$,

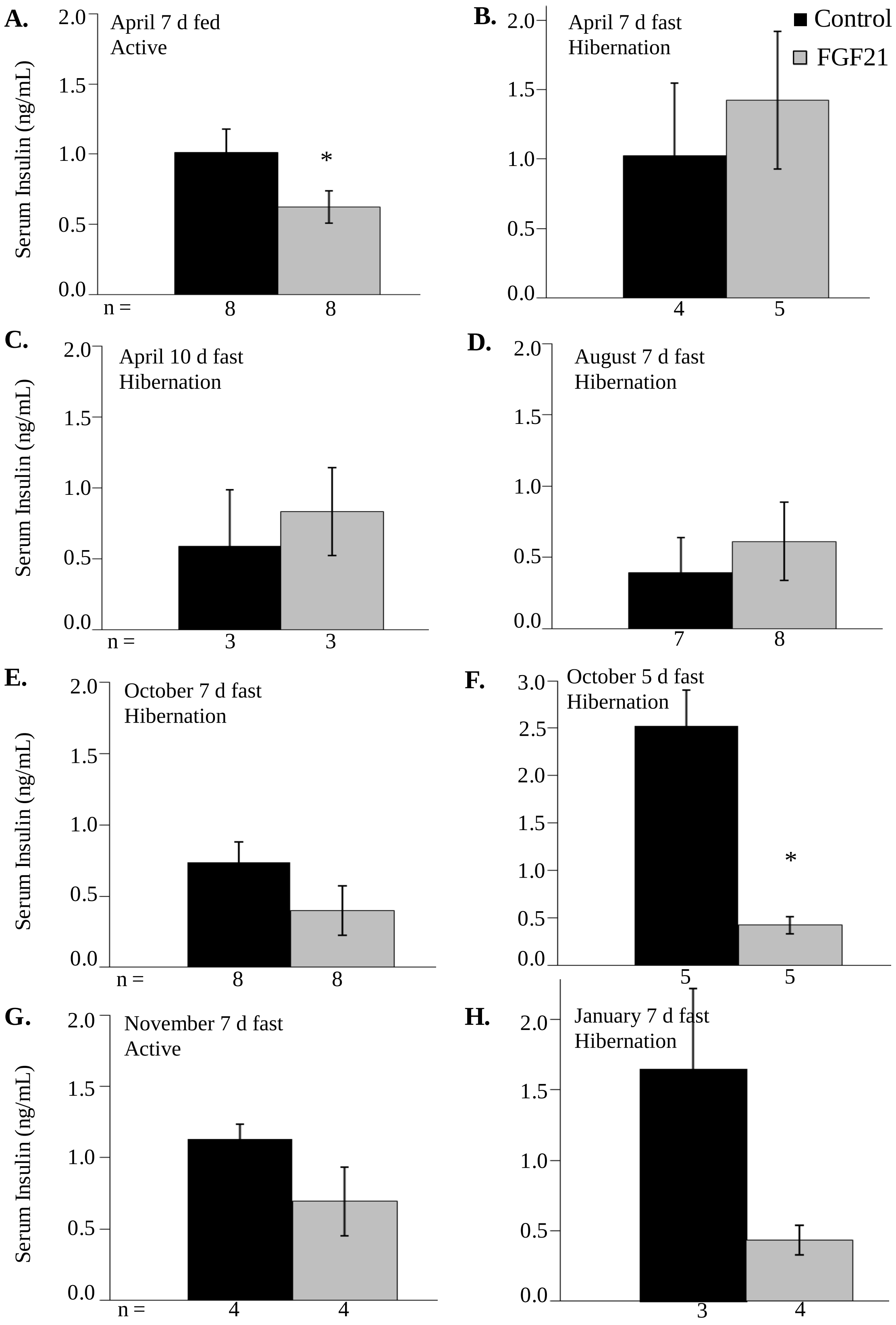
A.
April 7 d fed
Active
B.
April 7 d fast
Hibernation
■ Control
▨ FGF21
C.
April 10 d fast
Hibernation
D.
August 7 d fast
Hibernation
E.
October 7 d fast
Hibernation
F.
October 5 d fast
Hibernation
G.
November 7 d fast
Active
H.
January 7 d fast
Hibernation
Serum Insulin (ng/mL)
0.0
0.5
1.0
1.5
2.0
2.5
3.0
*
n =
8 8
4 5
3 3
7 8
8 8
5 5
4 4
3 4

Figure 4.20: Thirteen-lined ground squirrel serum insulin with raised levels of FGF21. Insulin measurements were taken after each experiment including: fed for 7 days in April at 23 °C and 12:12 l:d **(A)**, fasted for 7 days in April in hibernation conditions **(B)**, fasted for 10 days in April in hibernation conditions **(C)**, fasted for 7 days in August in hibernation conditions **(D)**, fasted for 7 days in October in hibernation conditions **(E)**, fasted for 5 days in October in hibernation conditions **(F)**, fasted for 7 days in November at 23 °C and 12:12 l:d **(G)**, and fasted for 12 days in January in hibernation conditions **(H)**. Increased levels of FGF21 led to decreased serum insulin in April fed squirrels **(A)** and October 5-day fasted squirrels **(F)**. There was a trend toward lower serum insulin with raised FGF21 in October 7-day fasted **(E)**, November 7-day fasted **(G)**, and January 12-day fasted **(H)** squirrels that was not statistically significant. April 7-day fasted **(B)**, April 10-day fasted **(C)**, and August 7-day fasted squirrels did not have lower serum insulin with increased FGF21. Standard error bars are shown. (*) indicates significant difference.

Fig 4.20 D). In October after 7 days of fasting in hibernation conditions squirrels had a mean serum insulin concentration of 0.7 ng/ml and with increased FGF21 had a concentration of 0.4 ng/mL ($p = 0.05$, Fig 4.20 E). After 5 days of fasting in hibernation conditions in October, squirrels had a mean serum insulin concentration of 2.5 ng/ml and with increased FGF21 had a significantly lower concentration of 0.4 ng/ml ($p < 0.01$, Fig 4.20 F). After 7 days of fasting in a 12:12 l:d cycle at 23 °C in November, control squirrels had a mean serum insulin concentration of 1.1 ng/ml and with increased FGF21 had a concentration of 0.7 ng/ml ($p =0.09$, Fig 4.20 G). After 12 days of fasting in January in hibernation conditions squirrels had a mean serum insulin concentration of 1.7 ng/ml and squirrels with increased FGF21 had a concentration of 0.4 ng/ml ($p = 0.09$, Fig 4.20 H). Increased FGF21 in squirrels led to significantly lower serum insulin concentrations in April fed and in October squirrels fasted for 5 days. There was not a significant effect of FGF21 on serum insulin in October squirrels fasted for 7 days, April fasted squirrels or August fasted squirrels. It is characteristic of FGF21 to lower serum insulin concentrations in multiple mouse models (Kharitonenkov, Shiyanova et al. 2005; Wente, Efanov et al. 2006; Kharitonenkov, Wroblewski et al. 2007).

Effect of FGF21 on mRNA Levels in Thirteen-lined Ground Squirrels

The effect of increased FGF21 on gene expression was evaluated using quantitative-real time- polymerase chain reaction (Q-RT-PCR). RNA was extracted from squirrel liver and WAT tissue collected after the 7-day fed experiments performed during April with a 12:12 l:d at 23 °C and 7-day fasting experiments performed during the end of March and beginning of April, during August, and during October with 24 h darkness at 5 °C. A cDNA sample was made from each RNA sample and gene amplification from the polymerase chain reaction was detected using SYBR green.

Control gene. In order to evaluate gene expression variation, a control gene that does not have variable expression between experimental groups was determined. The candidate control genes selected were β-actin, cyclophilin-a (CycA), glyceraldehyde-3-phosphate dehydrogenase (GAPDH), 60s ribosomal protein 13A (RPL13a), and succinate dehydrogenase complex subunit A (SDHA). The standard deviation of the natural log of the cycle number where the fluorescence of gene amplification crossed the detection threshold, or C_t value, for each gene was compared. RNA samples from 6 control squirrels and from 6 squirrels with increased FGF21 were compared for each candidate control gene. The standard deviations from the mean of the mRNA measurements from the 12 squirrels were similar for each candidate control gene (Table 3). The least significant number, or the number of observations that would produce a specified *p*-value $\alpha = 0.05$ from data with the same characteristics as the sampled data, was much larger for CycA compared to the other candidate control genes. It was determined with 16 observations of the experimental data CycA was the least likely to be significantly different between our experimental groups as identified by its large least significant number of 65.3.

Table 4.1: Variation of candidate control genes for Q-RT-PCR analysis of gene expression in thirteen-lined ground squirrels with increased FGF21

	Standard Deviation of C_t	**Least Significant Number ($\alpha = 0.05$)**
β-actin	0.047	14.0
CycA	0.040	65.3
GAPDH	0.044	17.2
RPL13a	0.047	17.6
SDHA	0.039	13.8

Ground Squirrel Liver βKlotho mRNA with Increased FGF21. βKlotho is a necessary component for FGF21 binding to FGF receptors (Kurosu, Choi et al. 2007; Ogawa, Kurosu et al. 2007; Kharitonenkov, Dunbar et al. 2008; Suzuki, Uehara et al. 2008). It was evaluated whether βKlotho mRNA was present in the experimental squirrels to confirm that FGF21 binding resulting in a signaling cascade to increase the expression of downstream target genes was possible in the experiments. The April fed control squirrel βKlotho mRNA level was set to 1 for

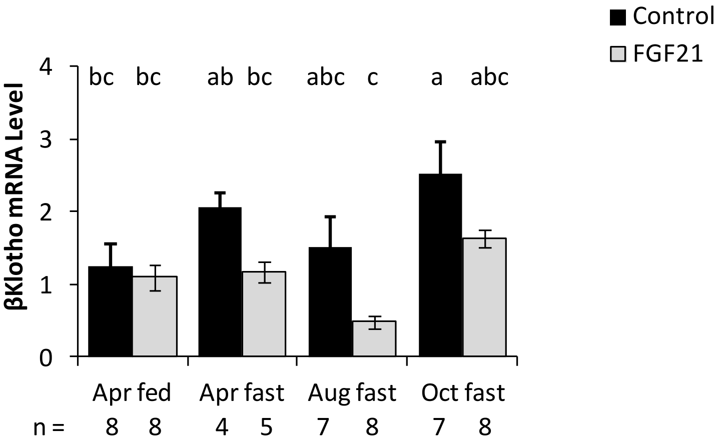

Figure 4.21: Thirteen-lined ground squirrel liver βKlotho mRNA levels with increased FGF21. βKlotho was detected in all samples and available for FGF21 signaling. Standard error bars are shown.

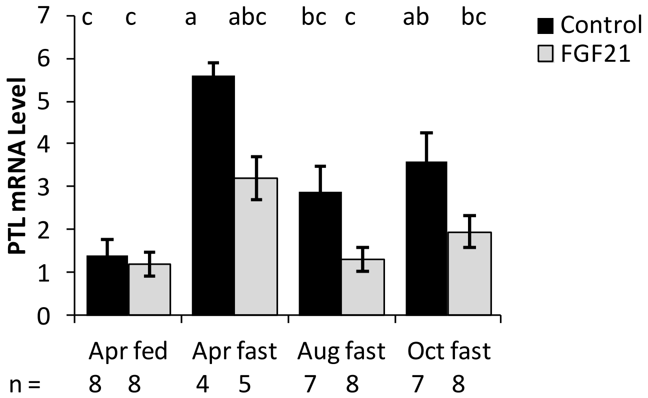

Figure 4.22: Thirteen-lined ground squirrel liver PTL mRNA with increased FGF21. Fasting increased PTL mRNA levels in April. There is a trend toward lower PTL mRNA with increased FGF21, but this trend is not statistically significant as tested by ANOVA followed by Tukey's HSD. Standard error bars are shown.

relative comparison of δδCt values with CycA set as the control gene. An ANOVA followed by Tukey's HSD of the results determined that βKlotho mRNA levels in October control squirrel liver samples were significantly higher than April fed squirrels, April fasted squirrels with increased FGF21, and August fasted squirrels with increased FGF21. The βKlotho mRNA from livers from August fasted squirrels with increased FGF21 was also significantly lower than April fasted control squirrels (Fig 4.21). Dectection of βKlotho all samples indicates that increased FGF21 could result in downstream regulation of target genes in the liver of squirrels.

Ground Squirrel Liver PTL mRNA with Increased FGF21. In pancreatic triglyceride lipase (PTL) is expressed in tissues other than the pancreas and has activity at low temperatures (Bauer, Squire et al. 2001; Squire and Andrews 2003; Squire, Lowe et al. 2003). PTL is important to the utilization of lipids for fuel during hibernation in squirrels. Control squirrels fasted for 7 days in April had significantly higher levels of PTL mRNA compared to all fed squirrels in April, all 7-day fasted squirrels in August, and 7-day fasted squirrels in October with increased FGF21 (Fig

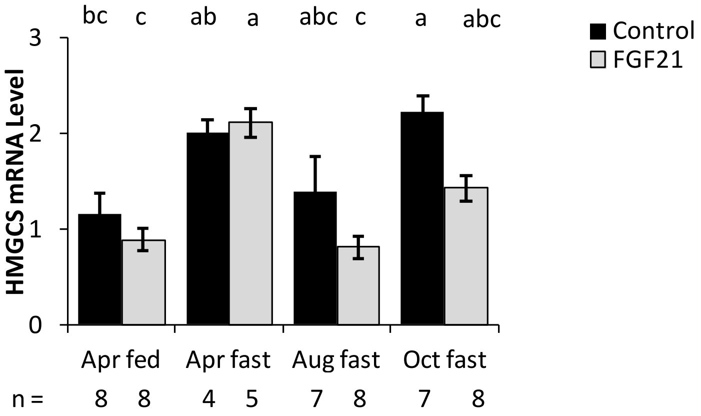

Figure 4.23: Thirteen-lined ground squirrel liver HMGCS mRNA with increased FGF21. Fasting increased liver HMGCS mRNA in April, but this was not significant. Squirrels with increased FGF21 tended to have lower liver HMGCS mRNA but the differences were not significant in any experimental set as tested by ANOVA followed by Tukey's HSD. Error bars shown are standard error.

4.22). October control squirrels fasted for 7 days had increased PTL mRNA compared to all April fed squirrels and August fasted squirrels with increased FGF21. There was a trend for squirrels with increased FGF21 to have lower expression of PTL compared to control squirrels, but the difference was not statistically significant within any experimental time-point. Fasting did increase the expression of PTL in April experiments and this increase is suppressed in squirrels with increased FGF21. In mice FGF21 has been shown to increase liver PTL expression (Inagaki, Dutchak et al. 2007).

Ground Squirrels Liver HMGCS mRNA with Increased FGF21. The mRNA level of hydroxy-methylglutaryl-CoA synthase (HMGCS) in squirrel liver tissue was also evaluated in these experiments. HMGCS is a rate-limiting enzyme in the production of ketone bodies. April fasted squirrels with increased FGF21 and October fasted control squirrels had significantly higher levels of HMGCS mRNA in the liver than fed squirrels in April or fasted squirrels with increased FGF21 in

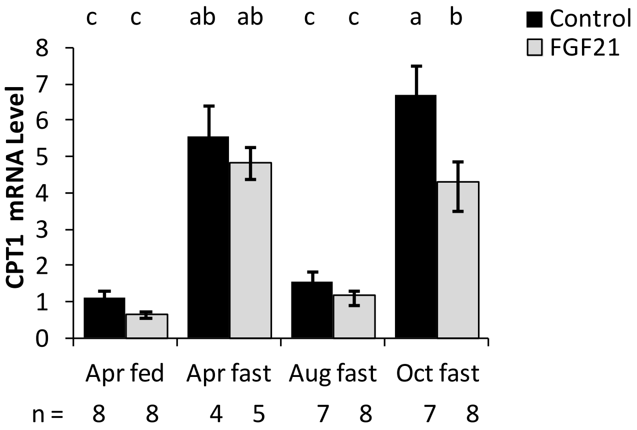

Figure 4.24: Thirteen-lined ground squirrel liver CPT1a mRNA with increased FGF21. Fasting squirrels in April increased liver CPT1a mRNA. There was a trend for squirrels with increased FGF21 to have lower liver CPT1a mRNA that was only significant in October as tested by ANOVA followed by Tukey's HSD. The error bars shown are standard error.

August (Fig 4.23). Squirrels fasted in April had significantly higher levels of liver HMGCS mRNA than April fed squirrels with increased FGF21 and August fasted squirrels with increased FGF21. Squirrels with increased FGF21 did not have significantly different levels of liver HMGCS mRNA than control squirrels within any of the experiments.

Ground Squirrel Liver CPT1a mRNA with Increased FGF21. Carnitine palmitoyl transferase (CPT) transfers fatty acids into the mitochondria for use. The mRNA levels of the 1a isoform of CPT (CPT1a) were evaluated in these experiments. The liver CPT1a mRNA level was higher in squirrels fasted for 7 days in April and in October than in fed April squirrels and fasted August squirrels. Squirrels fasted in October with increased FGF21 had significantly lower liver CPT1a mRNA levels than control squirrels in that experiment (Fig 4.24). Overall, there was a trend for squirrels with increased FGF21 to have lower liver CPT1a mRNA than control squirrels, but this trend was only significant in October. Fasting squirrels in April increased the level of liver CPT1a mRNA.

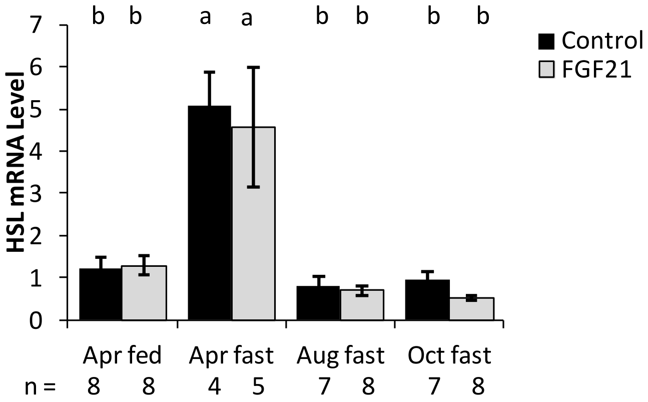

Figure 4.25: Thirteen-lined ground squirrel liver HSL mRNA with increased FGF21. Fasted squirrels in April had increased levels of liver HSL mRNA compared to fed squirrels. Increased FGF21 did not affect liver HSL mRNA levels. Compared using ANOVA followed by Tukey's HSD. Standard error bars are shown.

Ground Squirrel Liver HSL mRNA with Increased FGF21. Hormone sensitive lipase (HSL) breaks down triglycerides to fatty acids and glycerol. Squirrels fasted for 7 days in April had increased liver HSL mRNA levels compared to April fed squirrels and fasted squirrels in August or October (Fig 4.25). Liver HSL mRNA was increased by fasting squirrels and increased FGF21 had no effect on liver HSL mRNA levels.

Ground Squirrel WAT Transcripts with Increased FGF21. The mRNA of βKlotho, PTL, and HSL were also evaluated in WAT in squirrels with increased FGF21. βKlotho mRNA was present for signaling in all samples examined and there was no effect of increased FGF21 or fasting on βKlotho mRNA levels in WAT (Fig 4.26 A). PTL mRNA was not affected by fasting or increased FGF21 in WAT (Fig 4.26 B). The mRNA levels of HSL in WAT were not affected by fasting or by increased levels of FGF21 (Fig 4.26 C). The mRNA levels evaluated in WAT were not affected by fasting or by increased FGF21. In all WAT Q-RT-PCR experiments high C_t values were observed and this may have affected the ability to detect changes

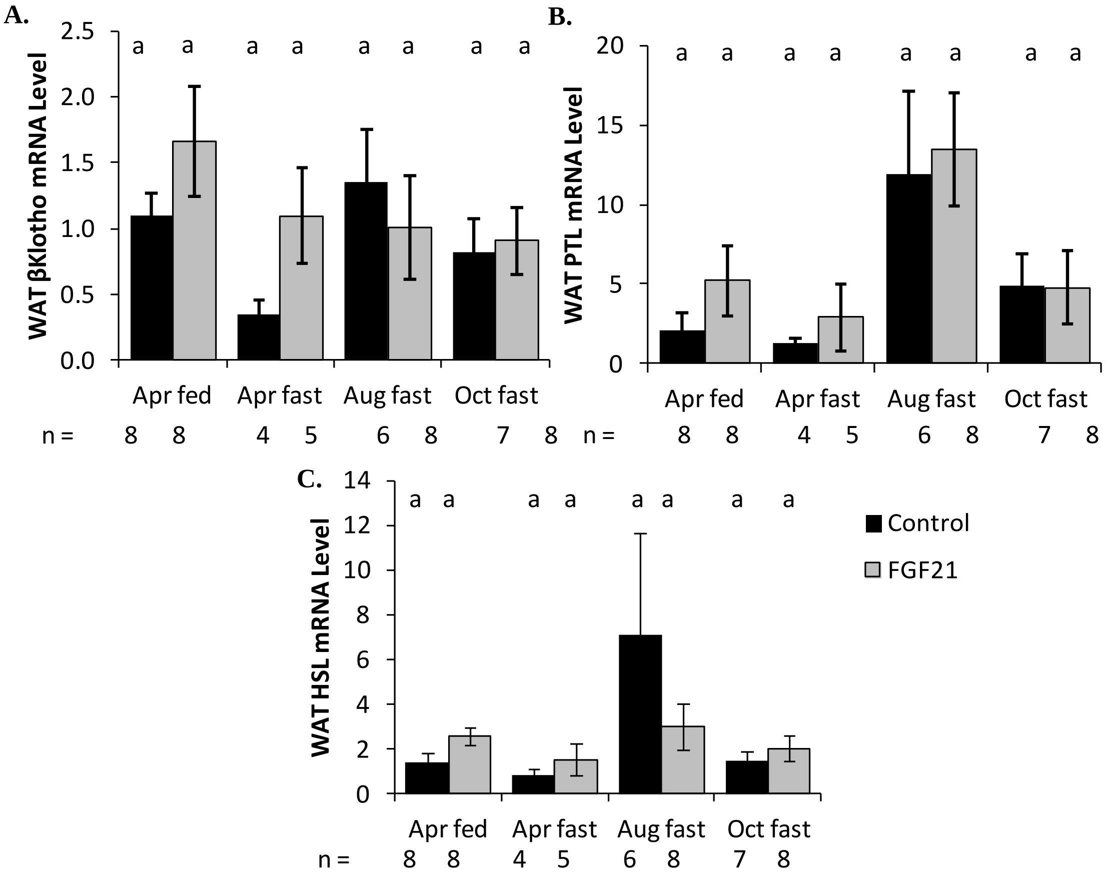

Figure 4.26: Thirteen-lined ground squirrel WAT mRNA with increased FGF21. **(A)** βKlotho was present in all tissues tested, allowing for FGF21 signaling to occur. **(B)** Increasing FGF21 did not affect the WAT PTL mRNA level as tested by ANOVA. **(C)** Increasing FGF21 did not affect WAT HSL mRNA as tested by ANOVA. Standard error bars are shown.

in gene expression in WAT. The high C_t values could be due to low levels of RNA extracted from the tissue.

In summary, increased FGF21 affected liver mRNA levels in squirrels as evaluated by Q-RT-PCR but not WAT mRNA levels. The increase in liver PTL mRNA from fasting in April was suppressed by increased FGF21. Liver CPT1a mRNA tended to be lower with increased FGF21, but this was only significant in the October experiments. Liver HSL mRNA was increased by fasting, but increased FGF21 had no effect on liver HSL mRNA in squirrels.

CHAPTER 5

DISCUSSION

In summary, FGF21 serum protein and liver mRNA levels are increased in squirrels during IBA relative to active squirrels. This increased expression suggests that FGF21 plays an important role during hibernation in this species, but that role is not the induction of torpor. This is in contrast to FGF21 sensitizing mice to enter torpor (Inagaki, Dutchak et al. 2007). This difference in the role of FGF21 in these species is due to mice being daily heterotherms that enter torpor in response to food scarcity when body mass is low and squirrels are seasonal hibernators and enter torpor when body mass is high. This evidence suggests that daily heterotherms have a different signaling mechanism to initiate a torpor response than that in seasonal hibernators.

Physiological Parameters of Torpor in Thirteen-lined Ground Squirrels. Torpor, or physiological activity below typical active levels, was defined using full circadian cycles of physiological activity. The active T_b of squirrels did not have a normal distribution. The distribution of active T_b was skewed more low T_b values than high T_b values. Torpor was defined to begin in squirrels at a T_b less than 32 °C, which is at least 1 °C below the minimum T_b detected in active squirrels. The active HR of squirrels was more variable than the T_b. The HR of squirrels was below the active, normal level at 150 bpm, but this value was occasionally noted in active squirrels. The reduction in HR preceded the decrease in T_b and occurred over a shorter time frame. Movement of squirrels stopped before torpor occurred for most squirrels, but movement was detected in some cases when T_b and HR were below active levels. A T_b less than 9 °C and a HR less than 12 bpm were within the variability noted during maintenance of torpor for squirrels kept at an ambient temperature of 5 °C. The average T_b during maintenance was 6.2 °C and HR averaged 5 bpm. Torpor bouts were shorter early in the hibernation season than during the middle of the season similar to other seasonal hibernators (Geiser and Ruf 1995). During arousal HR began to increase and reach active levels before T_b (Hampton, Nelson et al. 2010). These physiological parameters are typical of a small seasonal hibernator (Lyman, Willis et al. 1982; Geiser and Ruf 1995). Torpor bouts in an animal that experiences daily torpor in response to food scarcity have smaller changes in physiological parameters. For example, the lower T_b reached during torpor in a mouse between 16 and 19 °C is warmer than most seasonal hibernators (Hudson and Scott 1979). This is an example of the differences between species that employ seasonal hibernation and those that use daily torpor in response to food scarcity.

Arrhythmias were noted around torpor bouts and were measured using the coefficient of variation of the inter-beat interval. It was determined that the heart beat was less arrhythmic during arousal from torpor than during maintenance of torpor, and that level of arrhythmias detected were not indicative of an upcoming torpor bout (Hampton, Nelson et al. 2010).

Thirteen-lined Ground Squirrel FGF21 is Increased during Hibernation. The overall expression of genes and proteins is decreased during the extreme reductions in physiological processes during torpor (van Breukelen and Martin 2001; van Breukelen and Martin 2002). The maintenance or increase of gene or protein expression indicates that the protein is likely important during hibernation. Expression of FGF21 mRNA was detected in liver tissue, but not brain, heart, kidney, adrenal glands, skeletal muscle, or WAT of squirrels. Similarly, mouse FGF21 mRNA is largely expressed in liver tissue (Nishimura, Nakatake et al. 2000). The mRNA levels of squirrel FGF21 were significantly increased in the liver during IBA. The 8.7-fold increase in FGF21 serum protein during IBA compared to August active levels suggests that this protein is important for processes that occur during hibernation in squirrels. A smaller increase of 3.4-fold during torpor relative to August activity was not statistically significant, yet indicates that this protein is not rapidly degraded during IBA. The increased levels of FGF21 show that this metabolic hormone has an important role in both the interbout aroused and torpid states of hibernation in squirrels.

FGF21 Signaling Transcripts are Present in Liver and WAT in Thirteen-lined Ground Squirrels. The single-pass transmembrane protein βKlotho is required for FGF21 to activate an FGF receptor (Kurosu, Choi et al. 2007; Ogawa, Kurosu et al. 2007; Kharitonenkov, Dunbar et al. 2008; Suzuki, Uehara et al. 2008). FGFR1 is the preferred receptor for FGF21 signaling activity, although FGF21 is capable of signaling activity in cells expressing FGFR -2 or -3, but not FGFR4 (Kurosu, Choi et al. 2007; Kharitonenkov, Dunbar et al. 2008; Suzuki, Uehara et al. 2008). The combination of tissue-specific βKlotho and FGFR expression regulates tissue specificity of FGF21 action (Kurosu and Kuro 2009). In squirrels βKlotho mRNA was detected in liver, WAT, and adrenal tissue and FGFR1 mRNA was detected in liver, brain, heart, kidney, adrenal, skeletal muscle, and WAT. Both βKlotho and FGFR1 were present in all activity states, including August active, winter torpid, winter IBA, and March active squirrels in both liver and WAT. The presence of these

FGF21 signaling components demonstrates that FGF21 should be capable of signaling in liver and WAT during any activity state including torpor. FGF21 activity is also observed in liver and WAT in mice. A major site of the FGF21 response in mice is adipose tissue where FGFR1 and βKlotho are present (Ogawa, Kurosu et al. 2007; Kharitonenkov, Dunbar et al. 2008). FGF21 also has activity in liver tissue of mice with expression of βKlotho (Fisher, Estall et al. 2011).

Thirteen-lined Ground Squirrel FGF21 is Similar to FGF21 from other Species. TLG squirrel FGF21 was isolated by low-stringency PCR. Comparison of the nucleotide and amino acid sequences to online sequence databases using BLAST resulted in the best matches to FGF21 sequences from humans. FGFs adopt a 12-stranded β-sheet structure in a barrel-like formation (Goetz, Beenken et al. 2007). Homology modeling used to predict the structure of TLG squirrel FGF21 resulted in an acceptable structure similar to other FGFs without major conformational problems. The region of the predicted structure of TLG squirrel FGF21 between β-strands 10 and 12 did not align well and this region in the predicted structure is not accurate (Figure 4.3). This region in canonical FGFs is where binding to heparin occurs. Heparin binding keeps canonical FGFs in the interstitial space and limits them to only paracrine or autocrine signaling (Ornitz and Itoh 2001). The lack of homology of TLG squirrel FGF21 in this region is also noted in the structures of the other endocrine acting FGFs and is predicted to prevent FGF21 from binding heparin and likely allows FGF21 to be capable of endocrine signaling (Goetz, Beenken et al. 2007).

A multiple sequence alignment of TLG squirrel FGF21 to sequences from other species had very few amino acid substitutions that could have affected its binding and signaling capabilities (Figure 4.2). Despite sequence variations in TLG squirrel FGF21, the signaling capability was confirmed in primary mouse adipocytes. The TLG squirrel FGF21 protein was competent of phosphorylating ERK1/2, an important component of the MAPK signaling pathway. Thus, TLG squirrel FGF21 is similar in sequence and structure to other FGF molecules and the resulting expressed protein from this sequence is functional and capable of inducing signaling.

Adenoviral-mediated Expression of FGF21 was Effective in Thirteen-lined Ground Squirrels. In this study an adenoviral vector was produced that lead to significant increases in TLG squirrel FGF21. This is the first time adenoviral vectors have been used in TLG squirrels, and this study shows adenoviral vector-mediated expression is an effective means to increase expression of target proteins in wild-caught squirrels. Although adenoviral-mediated increase in FGF21 expression was effective, the induced level of expression was substantially higher than levels of expression measured naturally. This level of expression that greatly exceeds the normal physiological level may impact the effects observed by increasing FGF21. The use of adenoviral vectors for increasing target gene expression is likely to be effective in other hibernating species. TLG squirrels are annual breeders and the breeding process is more difficult than in species such as mice. By using adenoviral vectors to increase expression the roles of various proteins can be further investigated in a manner similar to examining transgenic animals. This novel approach is likely to provide a greater understanding of hibernation and torpor in annual breeders.

Another possible advantage of using adenoviral vectors in hibernators is the potential to knockdown the expression of genes of interest. Small interfering RNA molecules could be developed in primary tissue cultures and adenoviral vectors could be used to express the small interfering RNAs in squirrels. This ability to knockdown expression will provide crucial information about the necessity of various molecules for hibernation and torpor. In future studies it would be of interest to use this technique to knockdown FGF21 in squirrels to assist in elucidating the role of increased FGF21 expression during IBAs.

Increases of FGF21 did not Induce Torpor in Thirteen-lined Ground Squirrels. Implanted transmitters were used to measure T_b, HR, and activity of squirrels after adenoviral-mediated increases of FGF21. In squirrels that had been active after the hibernation season in the spring, the minimum T_b was 1.2 °C lower in squirrels with increased FGF21 relative to control squirrels. This decrease is similar to the 1 to 2 °C decrease observed in fasted mice with increased FGF21 (Inagaki, Dutchak et al. 2007). This small decrease in T_b to 37.3 °C is not indicative of a typical bout of torpor in a squirrel and is above the T_b of 32 °C required to be considered torpid. In contrast, there were significant increases in mean T_b and mean HR of squirrels fasted in October with increased FGF21, and in mean T_b of squirrels fasted in November with a 12:12 daily light cycle. These increases in mean physiological parameters indicate that squirrels with increased FGF21 spent less time in torpor during the experiments done just before the hibernation season. When comparing the effects of increased FGF21 on torpor bouts to early season torpor bouts in squirrels without interventions there were no notable differences in the lengths of torpor bout phases or the sequence of physiological changes. These results show that increased FGF21 does not induce typical torpor physiology in squirrels nor does increased FGF21 change the characteristics of the torpor bouts observed. This is in contrast to increases in FGF21 sensitizing fasted mice to enter torpor (Inagaki, Dutchak et al. 2007). This evidence demonstrates the differences between torpor induction in a seasonal obligate hibernator and an animal that uses torpor as part of the response during the metabolic stress of reduced food availability.

FGF21 expression was naturally increased in IBAs during the hibernation season. Unfortunately, we were not able to successfully increase FGF21 expression during the middle of the hibernation season and this would have helped elucidate the role of FGF21 in squirrels. The inability to increase FGF21 during hibernation was due to the poor recovery of squirrels from the infusion surgery when they were cycling through bouts of torpor. It may be possible to use a pumping system attached to squirrels before hibernation begins and administer an adenoviral vector through such a pump during hibernation. By developing such a system that does not interfere with the natural progression of hibernation, more information would be available about the role of FGF21 during hibernation.

Increased FGF21 and Serum Metabolites in Thirteen-lined Ground Squirrels. Serum glucose levels are decreased during torpor in squirrels (Figure 4.11) and FGF21 causes decreased serum glucose in mice (Kharitonenkov, Shiyanova et al. 2005; Wente, Efanov et al. 2006; Kharitonenkov, Wroblewski et al. 2007). This led to the expectation that increased FGF21 would decrease serum glucose levels in squirrels. Despite this expectation, increasing FGF21 in squirrels did not affect serum glucose concentrations in any of the experiments. FGF21 is increased during the IBA phase of hibernation when serum glucose levels are similar to active levels. It would be contradictory for increased FGF21 during IBA to lower serum glucose, when glucose metabolism is active.

Serum glucose measurements were not taken at the same times or the circadian cycle for each squirrel. When measuring serum glucose concentrations it is more accurate to measure fasted glucose at the same time of the circadian cycle for each animal. In order to sample at the same time of the circadian cycle for each squirrel, it would have been necessary to enter the environmental chamber where squirrels were hibernating on a daily basis to collect serum. This disruption in the environmental chamber affects the entrance and maintenance of torpor bouts of other squirrels. To decrease disturbances the environmental chamber as much as possible, samples were taken from multiple squirrels at different times on the same day. This allowed us to more accurately measure the torpor bout parameters in squirrels with increased FGF21, but decreased our ability to accurately measure changes in serum metabolites.

During torpor in squirrels there is an increase in the serum concentration of the ketone BHB that coincides with the increased reliance on lipids for fuel. FGF21 also causes increases in serum BHB levels and lipolysis in mice lipolysis (Inagaki, Dutchak et al. 2007; Badman, Koester et al. 2009). This led to the expectation that increased FGF21 would increase serum BHB levels in squirrels. In our experiments, fasting predictably increased serum BHB levels after hibernation in the end of March and early April. Squirrels with increased FGF21 did not consistently show differences in serum BHB concentrations, but in contrast to our expectations there was a trend toward lower serum BHB with increased FGF21. This difference was only statistically significant in samples taken 5 days after adenoviral infusion in October in hibernation conditions.

Serum free FA concentrations are increased during torpor in squirrels when there is an increased reliance on lipolysis (Figure 4.15). In wild-type mice administered FGF21 serum free FA concentrations increase, but in obese mice administered a hyperinsulinemic clamp serum free FA concentrations are decreased with increased FGF21 (Inagaki, Dutchak et al. 2007; Berglund, Li et al. 2009). Squirrels with increased FGF21 exhibited a trend toward decreased serum free FA concentrations. These results were only statistically significant in fed squirrels in April and in squirrels kept in hibernation conditions in October and sampled after 5 days. The lowering of serum free FA concentrations with increased FGF21 in squirrels is similar to the decrease observed in the obese (*ob*/*ob*) mouse model when tested for insulin resistance.

Serum TG concentrations did not vary seasonally in squirrels. Serum TG were expected to be lower in the leaner March active squirrels than squirrels in August that tend to have higher fat reserves. Serum TG concentrations tend to reflect the level of adiposity in hibernators (Dark 2005). In multiple mouse models and in diabetic monkeys, increased FGF21 results in decreased serum TG concentrations (Kharitonenkov, Shiyanova et al. 2005; Wente, Efanov et al. 2006; Inagaki, Dutchak et al. 2007). In squirrels increased FGF21 did not have a consistent effect on serum TG concentrations. Squirrels with increased FGF21 kept in hibernation conditions in October and sampled 5 days after adenoviral infusion have significantly higher serum

TG concentrations. This is in contrast to the effect of FGF21 on TG concentrations observed in mice.

The serum concentrations of glucose, BHB, free FA, and TGs were measured with increased FGF21 to identify if FGF21 causes a shift in metabolic fuel use or production in squirrels. Although the results were not consistent, there was a trend toward lower BHB and FA and higher TG concentrations in serum samples from squirrels with increased FGF21. Taken together this indicates that increased FGF21 in squirrels causes decreased reliance on lipid metabolism. In experiments where squirrels were fasted, increased FGF21 did not cause a metabolic profile that indicated increased reliance on lipolysis as was predicted. Fasting increases FGF21 liver expression and serum protein in mice through PPARα activation, and this increase in FGF21 leads to a metabolic profile that reflects increased lipolysis (Badman, Pissios et al. 2007; Inagaki, Dutchak et al. 2007). Yet in other studies, increased FGF21has been shown to attenuate lipolysis in human adipocytes, which is consistent with the role of FGF21 during feeding (Arner, Pettersson et al. 2008). In squirrels, FGF21 may decrease lipolysis.

Increased FGF21 Decreases Serum Insulin in Thirteen-lined Ground Squirrels. Insulin signaling results in increased cellular uptake of glucose for use and storage. Serum insulin concentrations are typically highest before hibernation occurs, and reflect the level of adiposity in hibernators (Dark 2005). Serum concentrations of insulin and body mass decrease after fasting begins (Lyman, Willis et al. 1982; Florant, Lawrence et al. 1985; Tokuyama, Galantino et al. 1991; Boswell, Woods et al. 1994; Buck, Squire et al. 2002). Increased FGF21 in multiple mouse models and in diabetic monkeys leads to decreased serum insulin concentrations (Kharitonenkov, Shiyanova et al. 2005; Wente, Efanov et al. 2006; Kharitonenkov, Wroblewski et al. 2007). After increasing FGF21 in fed squirrels in April and in squirrels kept in hibernation conditions in October and sampled after 5 days, significantly decreased serum insulin concentrations were observed. In the other experiments, the effect of FGF21 on serum insulin was not significant. The insulin lowering effect of FGF21 in squirrels may be dependent on high serum insulin concentrations, and increasing FGF21 when serum insulin concentrations are low does not decrease serum insulin. The decrease in serum insulin observed in squirrels with increased FGF21 is consistent with observations in other model species. In mice, FGF21 does not directly affect the pancreatic release of insulin (Wente, Efanov et al. 2006; Xu, Stanislaus et al. 2009). Rather the serum insulin lowering effect of FGF21 in mice is related to increasing cellular glucose uptake and reducing serum glucose concentrations. A lowering of serum glucose was not observed with increased FGF21 in squirrels, even in the experimental sets that showed significantly decreased serum insulin concentrations. A lack of effect observed on serum glucose may be a result of our logistical inability to sample overnight fasted serum at the same time of the circadian cycle for each squirrel. Thus, the effect of increased FGF21 in squirrels on metabolic response is not clear.

Increased FGF21 did not Increase Lipolysis-related Transcripts in Thirteen-lined Ground Squirrels. The effect of increased FGF21 on the mRNA levels of lipolysis-related genes was examined. PTL is a lipase important during hibernation. Its expression is increased during hibernation and it is capable of continued lipolysis at low temperatures (Andrews, Squire et al. 1998; Bauer, Squire et al. 2001; Squire and Andrews 2003; Squire, Lowe et al. 2003). Liver PTL expression is increased with increased FGF21 in mice (Inagaki, Dutchak et al. 2007). Fasted squirrels have higher liver PTL levels than fed squirrels in April. This fasting-related increase in liver PTL levels was attenuated in squirrels with increased FGF21. Within any experimental set increased FGF21 did not significantly affect liver PTL mRNA levels (Figure 4.22). HSL is a common lipase and its expression is increased during hibernation (Wilson, Deeb et al. 1992). Fasting also increased liver HSL mRNA levels in squirrels in April. Increasing FGF21 did not affect the level of liver HSL mRNA in squirrels (Figure 4.25). HSL and PTL mRNA levels were also examined in WAT and there was no significant effect of increased FGF21 (Figure 4.26).

CPT1 is involved in the transfer of FA into the mitochondria for metabolism and HMGCS is an enzyme involved in the rate limiting step of ketone production. These two genes, involved in lipolysis, are both upregulated in the liver during hibernation (Epperson and Martin 2002). Increased FGF21 in mice leads to increased CPT1a and HMGCS proteins and decreased FGF21 leads to decreased CPT1a and HMGCS mRNA in the liver (Badman, Pissios et al. 2007; Inagaki, Dutchak et al. 2007). HMGCS mRNA levels in the liver are increased by fasting in squirrels with increased FGF21, and CPT1a mRNA levels are increased by fasting in both control squirrels and those with increased FGF21 in April (Figures 4.23 and 4.24). There was no effect of increased FGF21 on HMGCS mRNA levels within any of the experiments, but in squirrels fasted for 7 days in October, lower levels of CPT1 mRNA were observed in squirrels with increased FGF21.

Predictably, fasting generally increased the mRNA levels of the lipolysis-related genes that were examined in squirrel livers. Increased FGF21 did not generally affect the expression of lipolysis-related genes in the liver, but CPT1a levels were lower in October fasted squirrels with increased FGF21. As with the effect of FGF21 on the metabolite profile, there was not a clear effect of FGF21 but, of the significant changes observed, increased FGF21 in squirrels may indicate reduced lipolysis.

Summary of the Metabolic Effects of FGF21. There were few significant effects of FGF21 on metabolites and mRNA levels of lipolytic genes in squirrels. In some cases increasing FGF21 in squirrels resulted in lower serum BHB and free FA and higher serum TG in addition to attenuated fasting liver PTL and lower CPT1a mRNA levels. Taken together this suggests FGF21 decreases lipolysis in squirrels and this is contrary to our expectations based on the effect of increasing FGF21 in mice (Inagaki, Dutchak et al. 2007). FGF21 also decreased serum insulin concentrations in squirrels in some cases. FGF21 liver mRNA and serum protein levels were significantly increased during the IBA phase of hibernation. FGF21 has more extensively been studied in various mouse models. In mice FGF21 is increased during metabolic challenges including fasting, high fat feeding, and high carbohydrate feeding. The IBA phase of hibernation is an extreme metabolic challenge that is observed in hibernators. During IBA, squirrels may have been fasting for as long as 5 months in the laboratory setting and possibly longer in the wild. Despite being in an extremely long-term fast, squirrels decrease reliance on lipolysis and increase glycolysis during IBAs. The increased levels of FGF21 during IBA may be due to this extreme metabolic challenge. FGF21 may be one signaling component that leads to decreased lipolysis in thirteen-lined ground squirrels during IBA.

During the design of this study, we expected increasing FGF21 in squirrels to increase lipolysis and possibly induce torpor. With that expectation we focused on evaluating the levels of lipolysis-related mRNAs. In light of the results indicating that FGF21 decreases lipolysis in squirrels, it would have been informative to examine the expression of genes related to gluconeogenesis and glycolysis. FGF21 expression is naturally increased during the IBA phase of hibernation, when glycolysis and gluconeogenesis are increased. Considering the dynamic roles of FGF21 in mice, it would be informative to further understand whether FGF21 affects either glycolysis or gluconeogenesis in squirrels.

Torpor Induction in a Seasonal Hibernator is a Different Mechanism than Induction of Daily Torpor. Mice are an example of an animal that use daily torpor in response to a shortage in energy supply. A mouse may become torpid after an overnight fast or during restricted food availability (Overton and Williams 2004). The main energy source for animals that employ daily torpor is ingested food and daily torpor is often entered when body mass is low (Geiser 2004). The daily torpor response observed in fasted mice involves reduced fuel availability and activation of signaling pathways involved in starvation, including increases in PPARα and FGF21. Inagaki, *et al* showed that mice with increased levels of FGF21 and those treated with a PPARα agonist became torpid during a 24 hour fast, while control mice did not (Inagaki, Dutchak et al. 2007). This suggests that increased levels of FGF21 sensitize mice to use torpor in response to a shortage in energy supply. It is possible to conclude that mice with increased levels of FGF21 sense a more extreme starvation state than mice with lower levels of FGF21. This signaling of a more extreme starvation state sensitizes mice to more readily use torpor to conserve energy.

In contrast to mice, squirrels are a seasonal, obligate hibernator. Increasing FGF21 expression in squirrels using an adenoviral vector did not induce a torpor pattern typical to this species. These animals hibernate annually and prepare for a season of multiple torpor bouts by storing excess adipose tissue in the late summer and early fall. During hibernation the main energy source of the squirrel is stored adipose tissue.

Although daily torpor and seasonal hibernation are both entered during fasting, the metabolic situations are different. Short, daily torpor bouts conserve energy when food availability is low and there is little energy stored as fat in the animal. This is a type of emergency response to low energy supply that the animal does not typically prepared for. Seasonal hibernators have a long preparatory period of fattening before the predictable hibernation season. Hibernators employ torpor when there are sufficient reserves of adipose tissue to sustain them over the winter. These differences explain why increased FGF21 sensitizes mice to enter torpor, whereas this effect of FGF21 was not observed in squirrels. Our results suggest the induction of daily torpor during starvation and the induction of seasonal hibernation have different signaling pathways.

Physiological observations have been used to thoroughly characterize the differences between daily torpor and seasonal hibernation (Geiser and Ruf 1995). Here we show that increasing FGF21 in a seasonal hibernator does not induce torpor, in contrast to previous results showing increased FGF21 sensitizes a daily heterotherm to employ torpor (Inagaki, Dutchak et al. 2007). This suggests that daily torpor and seasonal hibernation do not only differ on the physiological level, but also the molecular signals that induce torpor may be different in these different types of heterotherms. This is in addition to evidence that leptin signaling prevents torpor in daily heterotherms while seasonal hibernators have increased levels of leptin just before hibernation begins (Dark 2005; Hampton, Melvin et al. 2011). These molecular differences are important to consider when investigating the induction of torpor and when comparing results between various species.

Possible Roles for FGF21 in Seasonal Hibernation. Although increased FGF21 did not induce a typical torpor pattern squirrels, the results suggest FGF21 signaling has an important role in seasonal hibernation. Squirrels displayed increased liver mRNA and serum protein levels during hibernation with significantly higher levels during IBAs. Overall the expression of biomolecules is significantly decreased during hibernation as a component of the energy saving phenotype, thus increased FGF21 is important for hibernation. Although the purpose of increased FGF21 levels during hibernation is not known, it is tempting to hypothesize possible reasons for this increased expression.

FGF21 KO mice have increased liver weight and accumulate excess lipids in the liver when fed a ketogenic diet and gain weight when control mice lose weight (Badman, Koester et al. 2009; Hotta, Nakamura et al. 2009). This exemplifies that FGF21 is necessary for catabolism of liver lipids, especially during times of metabolic stress. During the metabolic stress of hibernation, squirrels are dependent on the utilization of lipids for fuel. Squirrels have increased total lipid content of the liver during torpor compared to summer active animals (Serkova, Rose et al. 2007). During IBAs the rate of gluconeogenesis increases, liver and muscle glycogen levels increase, and serum glucose levels increase (Burlington and Klain 1967; Galster and Morrison 1975; Green, Brosnan et al. 1984; Yeh, Tam et al. 1995; Staples and Hochachka 1998; Andrews, Russeth et al. 2009). The restoration of glucose metabolism during a fasted state is reliant on glycerol, released from lipid catabolism, and lactate. Thus, it is possible that the role of increased FGF21 during arousal from torpor involves the efficient utilization of liver lipids for gluconeogenesis and restoration of glycogen stores (See Fig 5.1).

Another possible role for FGF21 during arousal from torpor involves its recently evident activity in BAT. Non-shivering thermogenesis is critical for the increase in body temperature during arousal from torpor. During torpor and arousal BAT temperature is warmer than peripheral tissue temperatures (Horwitz, Smith et al. 1968; Smith and Horwitz 1969; Barger, Barnes et al. 2006). Shivering thermogenesis is not efficient and does not occur at the near freezing body temperatures in hibernators (Smith and Horwitz 1969; McArthur, Hanstock et al. 1990; Hashimoto, Gao et al. 2002). The unique expression of UCP1 in BAT results in heat production.

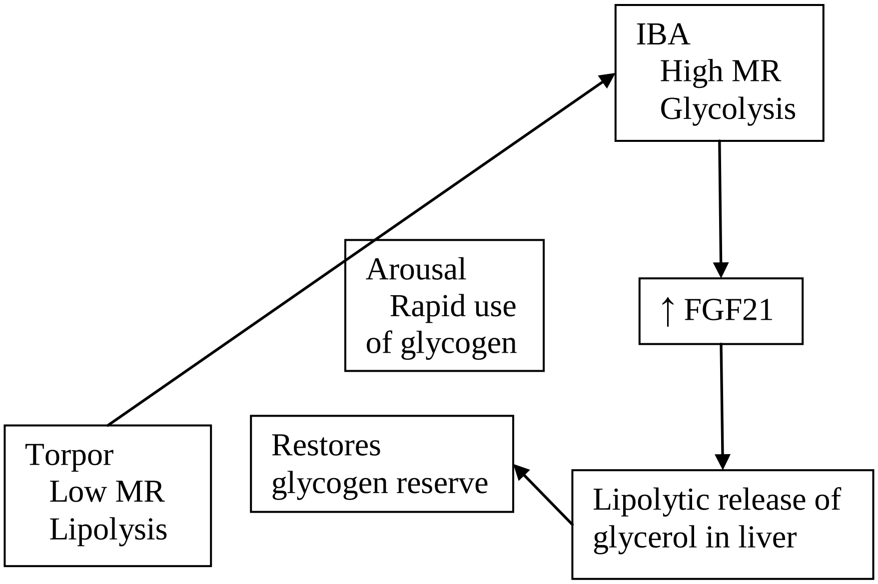

Figure 5.1: FGF21 may restore glycogen reserves during hibernation.

In adaptive thermogenesis, which occurs during cold exposure and excess caloric intake, PPARγ and PGC1α act in concert to increase the expression of UCP1 (Puigserver, Wu et al. 1998). In mouse and cell studies increased FGF21 results in more BAT, increased UCP1 expression in BAT, and increased thermogenic genes in BAT (Kharitonenkov, Shiyanova et al. 2005; Coskun, Bina et al. 2008; Chau, Gao et al. 2010; Hondares, Rosell et al. 2010). Cold exposure induces BAT expression of FGF21 that is released into the blood and also increases PGC1α expression in rats. The increased expression of FGF21 results from β-adrenergic stimulation by norepinephrine mediated by cAMP (Chartoumpekis, Habeos et al. 2011; Hondares, Iglesias et al. 2011). FGF21 treatment is also capable of inducing expression of UCP1 and increasing the protein concentration of PGC1α in some WAT depots, inducing the 'browning' of the WAT stores in mice (Fisher, Kleiner et al. 2012). During hibernation, increased sympathetic nervous system tone initiates arousal from torpor (Milsom, Zimmer et al. 1999; Drew, Buck et al. 2007). The volume of BAT and amount of UCP1 are increased in cold adaptation during hibernation (Boyer, Barnes et al. 1998; Liu, Lin et al. 1998; Barger, Barnes et al. 2006; Kitao and Hashimoto 2012). Thermogenic genes are increased during hibernation in the arctic ground squirrel (Yan, Burman et al. 2006). The BAT of hibernating hamsters has a larger thermogenic capacity than warm-adapted control hamsters at low temperatures (Kitao and Hashimoto 2012). This information taken together with the increases of FGF21 during hibernation, especially IBAs when transcription and translation are able to restore key biomolecules, lead to the hypothesis that FGF21 maintains BAT thermogenic capacity and the ability to subsequently increase body temperature during arousal from torpor. This is a topic that would be useful to investigate in future studies of FGF21 in squirrels.

The increase of FGF21 during IBAs in seasonal hibernators indicates that FGF21 is important for the metabolic adjustments that occur during hibernation. Thirteen-lined ground squirrels are a model hibernating species that is a lean animal after the hibernation season and then accumulates excess adipose tissue and serum insulin is increased, with insulin resistance occurring near the end of the fattening phase (Dark 2005; Martin 2008). This natural annual cycle of fattening and insulin resistance provides an excellent model for understanding metabolic disorders in humans. In nearly all developed countries worldwide there is a rapidly increasing occurrence of obesity and its corresponding metabolic diseases, including insulin resistance and type II diabetes. By researching and understanding the metabolic changes that occur in seasonal hibernators, nature can provide novel solutions to the challenges that obesity is creating in our society.

BIBLIOGRAPHY

Abbotts, B., L. C. Wang, et al. (1979). "Absence of evidence for a hibernation "trigger" in blood dialyzate of Richardson's ground squirrel." Cryobiology **16**(2): 179-183.

Adams, A. C., I. Astapova, et al. (2010). "Thyroid hormone regulates hepatic expression of fibroblast growth factor 21 in a PPARalpha-dependent manner." J Biol Chem **285**(19): 14078-14082.

Altschul, S. F., T. L. Madden, et al. (1997). "Gapped BLAST and PSI-BLAST: a new generation of protein database search programs." Nucleic Acids Res **25**: 3389-3402.

Altschul, S. F., J. C. Wootton, et al. (2005). "Protein database searches using compositionally adjusted substitution matrices." FEBS J. **272**: 5101-5109.

Andrews, M. T. (2007). "Advances in molecular biology of hibernation in mammals." Bioessays **29**(5): 431-440.

Andrews, M. T., K. P. Russeth, et al. (2009). "Adaptive mechanisms regulate preferred utilization of ketones in the heart and brain of a hibernating mammal during arousal from torpor." Am J Physiol Regul Integr Comp Physiol **296**: R383-R393.

Andrews, M. T., T. L. Squire, et al. (1998). "Low-temperature carbon utilization is regulated by novel gene activity in the heart of a hibernating mammal." Proceedings of the National Academy of Sciences **95**(14): 8392-8397.

Armitage, K. B., D. T. Blumstein, et al. (2003). "Energetics of hibernating yellow-bellied marmots (Marmota flaviventris)." Comp Biochem Phys A **134**(1): 101-114.

Arner, P., A. Pettersson, et al. (2008). "FGF21 attenuates lipolysis in human adipocytes - a possible link to improved insulin sensitivity." FEBS Lett **582**(12): 1725-1730.

Arnold, K., L. Bordoli, et al. (2006). "The SWISS-MODEL workspace: a web-based environment for protein structure homology modelling." Bioinformatics **22**(2): 195-201.

Artimo, P., M. Jonnalagedda, et al. (2012) "ExPASy: SIB bioinformatics resource portal." Nucleic Acids Res **Web server issue**.

Aslami, H., M. J. Schultz, et al. (2009). "Potential applications of hydrogen sulfide-induced suspended animation." Curr Med Chem **16**(10): 1295-1303.

Badman, M. K., A. Koester, et al. (2009). "Fibroblast growth factor 21-deficient mice demonstrate impaired adaptation to ketosis." Endocrinology **150**(11): 4931-4940.

Badman, M. K., P. Pissios, et al. (2007). "Hepatic fibroblast growth factor 21 is regulated by PPARalpha and is a key mediator of hepatic lipid metabolism in ketotic states." Cell Metab **5**(6): 426-437.

Barger, J. L., B. M. Barnes, et al. (2006). "Regulation of UCP1 and UCP3 in arctic ground squirrels and relation with mitochondrial proton leak." J Appl Physiol **101**(1): 339-347.

Bauer, V. W., T. L. Squire, et al. (2001). "Expression of a chimeric retroviral-lipase mRNA confers enhanced lipolysis in a hibernating mammal." Am J Physiol Regul Integr Comp Physiol **281**(4): R1186-1192.

Bauman, W. A. (1990). "Seasonal changes in pancreatic insulin and glucagon in the little brown bat (Myotis lucifugus)." Pancreas **5**(3): 342-346.

Bauman, W. A., S. Meryn, et al. (1987). "Pancreatic hormones in the nonhibernating and hibernating golden mantled ground squirrel." Comp Biochem Phys A **86**(2): 241-244.

Baumber, J., F. E. South, et al. (1971). "A possible basis for periodic arousals during hibernation: accumulation of ketone bodies." Life Sci II **10**(8): 463-467.

Berglund, E. D., L. Kang, et al. (2010). "Glucagon and lipid interactions in the regulation of hepatic AMPK signaling and expression of PPARalpha and FGF21 transcripts in vivo." Am J Physiol Endocrinol Metab **299**(4): E607-614.

Berglund, E. D., C. Y. Li, et al. (2009). "Fibroblast growth factor 21 controls glycemia via regulation of hepatic glucose flux and insulin sensitivity." Endocrinology **150**(9): 4084-4093.

Blackstone, E., M. Morrison, et al. (2005). "H2S induces a suspended animation-like state in mice." Science **308**(5721): 518.

Boswell, T., S. C. Woods, et al. (1994). "Seasonal changes in body mass, insulin, and glucocorticoids of free-living golden-mantled ground squirrels." Gen Comp Endocrinol **96**(3): 339-346.

Boyer, B. B., B. M. Barnes, et al. (1998). "Differential regulation of uncoupling protein gene homologues in multiple tissues of hibernating ground squirrels." Am J Physiol **275**(4 Pt 2): R1232-1238.

Brauch, K. M., N. D. Dhruv, et al. (2005). "Digital transcriptome analysis indicates adaptive mechanisms in the heart of a hibernating mammal." Physiol Genomics **23**: 227-234.

Brooks, S. P. J. and K. B. Storey (1992). "Mechanisms of glycolytic control during hibernation in the ground squirrel Spermophilus lateralis." J Comp Physiol B **162**: 23-28.

Buck, M. J., T. L. Squire, et al. (2002). "Coordinate expression of the PDK4 gene: a means of regulating fuel selection in a hibernating mammal." Physiol Genomics **8**(1): 5-13.

Burlington, R. F. and G. J. Klain (1967). "Gluconeogenesis during hibernation and arousal from hibernation." Comp Biochem Physiol **22**: 701-708.

Burlington, R. F., G. A. Meininger, et al. (1976). "Effect of low temperatures on high energy phosphate compounds in isolated hearts from a hibernator and a nonhibernator." Comp Biochem Phys B **55**(3B): 403-407.

Cannon, B. and J. Nedergaard (2011). "Nonshivering thermogenesis and its adequate measurement in metabolic studies." J Exp Biol **214**(Pt 2): 242-253.

Carey, H. V., M. T. Andrews, et al. (2003). "Mammalian hibernation: cellular and molecular responses to depressed metabolism and low temperature." Physiol Rev **83**(4): 1153-1181.

Chartoumpekis, D. V., I. G. Habeos, et al. (2011). "Brown adipose tissue responds to cold and adrenergic stimulation by induction of FGF21." Mol Med **17**(7-8): 736-740.

Chau, M. D., J. Gao, et al. (2010). "Fibroblast growth factor 21 regulates energy metabolism by activating the AMPK-SIRT1-PGC-1alpha pathway." Proc Natl Acad Sci U S A **107**(28): 12553-12558.

Cochet, N., R. Meister, et al. (1999). "Regional variation of white adipocyte lipolysis during the annual cycle of the alpine marmot." Comp Biochem Phys C **123**(3): 225-232.

Coskun, T., H. A. Bina, et al. (2008). "Fibroblast growth factor 21 corrects obesity in mice." Endocrinology **149**(12): 6018-6027.

Dark, J. (2005). "Annual lipid cycles in hibernators: integration of physiology and behavior." Annu Rev Nutr **25**: 469-497.

Dark, J., D. R. Miller, et al. (2003). "Noradrenaline-induced lipolysis in adipose tissue is suppressed at hibernation temperatures in ground squirrels." J Neuroendocrinol **15**(5): 451-458.

Dawe, A. R. and W. A. Spurrier (1969). "Hibernation induced in ground squirrels by blood transfusion." Science **163**(3864): 298-299.

Dawe, A. R., W. A. Spurrier, et al. (1970). "Summer hibernation induced by cryogenically preserved blood "trigger"." Science **168**(3930): 497-498.

Drew, K. L., C. L. Buck, et al. (2007). "Central nervous system regulation of mammalian hibernation: implications for metabolic suppression and ischemia tolerance." J Neurochem **102**(6): 1713-1726.

Dutchak, P. A., T. Katafuchi, et al. (2012). "Fibroblast Growth Factor-21 Regulates PPARgamma Activity and the Antidiabetic Actions of Thiazolidinediones." Cell **148**(3): 556-567.

Eddy, S. F., P. Morin, Jr., et al. (2005). "Cloning and expression of PPARgamma and PGC1-alpha from the hibernating ground squirrel, Spermophilus tridecemlineatus." Mol Cell Biol **269**: 175-182.

Eddy, S. F., P. Morin, Jr., et al. (2005). "Cloning and expression of PPARgamma and PGC-1alpha from the hibernating ground squirrel, Spermophilus tridecemlineatus." Molecular and Cellular Biochemistry **269**: 175-182.

Eddy, S. F. and K. B. Storey (2003). "Differential expression of Akt, PPARgamma, and PGC-1 during hibernation in bats." Biochem Cell Biol **81**(4): 269-274.

El Kebbaj, Z., P. Andreoletti, et al. (2009). "Differential regulation of peroxisome proliferator-activated receptor (PPAR)-alpha1 and truncated PPARalpha2 as an adaptive response to fasting in the control of hepatic peroxisomal fatty acid beta-oxidation in the hibernating mammal." Endocrinology **150**(3): 1192-1201.

Epperson, L. E., T. A. Dahl, et al. (2004). "Quantitative analysis of liver protein expression during hibernation in the golden-mantled ground squirrel." Mol Cell Proteomics **3**(9): 920-933.

Epperson, L. E., A. Karimpour-Fard, et al. (2011). "Metabolic cycles in a circannual hibernator." Physiol Genomics **43**(13): 799-807.

Epperson, L. E. and S. L. Martin (2002). "Quantitative assessment of ground squirrel mRNA levels in multiple stages of hibernation." Physiol Genomics **10**: 93-102.

Epperson, L. E., J. C. Rose, et al. (2010). "Seasonal proteomic changes reveal molecular adaptations to preserve and replenish liver proteins during ground squirrel hibernation." Am J Physiol Reg I **298**(2): R329-340.

Estall, J. L., J. L. Ruas, et al. (2009). "PGC-1alpha negatively regulates hepatic FGF21 expression by modulating the heme/Rev-Erb(alpha) axis." Proc Natl Acad Sci U S A **106**(52): 22510-22515.

Eswarakumar, V. P., I. Lax, et al. (2005). "Cellular signaling by fibroblast growth factor receptors." Cytokine Growth Factor Rev **16**(2): 139-149.

Finck, B. N. and D. P. Kelly (2006). "PGC-1 coactivators: inducible regulators of energy metabolism in health and disease." J Clin Invest **116**(3): 615-622.

Fisher, F. M., P. C. Chui, et al. (2010). "Obesity is a fibroblast growth factor 21 (FGF21)-resistant state." Diabetes **59**(11): 2781-2789.

Fisher, F. M., J. L. Estall, et al. (2011). "Integrated regulation of hepatic metabolism by fibroblast growth factor 21 (FGF21) in vivo." Endocrinology **152**(8): 2996-3004.

Fisher, F. M., S. Kleiner, et al. (2012). "FGF21 regulates PGC-1alpha and browning of white adipose tissues in adaptive thermogenesis." Genes Dev **26**(3): 271-281.

Florant, G. L., A. K. Lawrence, et al. (1985). "Seasonal changes in pancreatic B-cell function in euthermic yellow-bellied marmots." Am J Physiol **249**(2 Pt 2): R159-165.

Forger, N. G., J. Dark, et al. (1986). "Fat ablation and food restriction influence reproductive development and hibernation in ground squirrels." Biol Reprod **34**(5): 831-840.

Frank, C. L., S. P. J. Brooks, et al. (1998). "The influence of hibernation patterns on the critical enzymes of lipogenesis and lipolysis in prairie dogs." Exp Biol Online **3**: 9.

Galster, W. and P. R. Morrison (1975). "Gluconeogenesis in arctic ground squirrels between periods of hibernation." Am J Physiol **228**(1): 325-330.

Galster, W. A. and P. Morrison (1970). "Cyclic changes in carbohydrate concentrations during hibernation in the arctic ground squirrel." Am J Physiol **218**(4): 1228-1232.

Ge, X., C. Chen, et al. (2011). "Fibroblast growth factor 21 induces glucose transporter-1 expression through activation of the serum response factor/Ets-like protein-1 in adipocytes." J Biol Chem **286**(40): 34533-34541.

Geiser, F. (2004). "Metabolic rate and body temperature reduction during hibernation and daily torpor." Annu Rev Physiol **66**: 239-274.

Geiser, F., G. Kortner, et al. (1998). "Leptin increases energy expenditure of a marsupial by inhibition of daily torpor." Am J Physiol **275**(5 Pt 2): R1627-1632.

Geiser, F. and T. Ruf (1995). "Hibernation versus daily torpor in mammals and birds: physiological variables and classification of torpor patterns." Physiol Zool **68**(6): 935-966.

Gerard, R. D. and R. S. Meidell (1995). Adenovirus Vectors. DNA Cloning - A Practical Approach. B. Glover and B. D. Hames. Oxford, Oxford University Press**:** 285-307.

Goetz, R., A. Beenken, et al. (2007). "Molecular insights into the klotho-dependent, endocrine mode of action of fibroblast growth factor 19 subfamily members." Mol Cell Biol **27**(9): 3417-3428.

Green, C. J., J. T. Brosnan, et al. (1984). "Effect of hibernation on liver and kidney metabolism in 13-lined ground squirrels." Comp Biochem Physiol **79B**(2): 167-171.

Gupte, J., L. Yang, et al. (2011). "The FGFR D3 domain determines receptor selectivity for fibroblast growth factor 21." J Mol Biol **408**(3): 491-502.

Hampton, M., R. G. Melvin, et al. (2011). "Deep sequencing the transcriptome reveals seasonal adaptive mechanisms in a hibernating mammal." PLoS One **6**(10): e27021.

Hampton, M., B. T. Nelson, et al. (2010). "Circulation and metabolic rates in a natural hibernator: an integrative physiological model." Am J Physiol Regul Integr Comp Physiol **299**(6): R1478-1488.

Hashimoto, M., B. Gao, et al. (2002). "Arousal from hibernation and BAT thermogenesis against cold: central mechanism and molecular basis." J Therm Biol **27**: 503-515.

Heller, H. C. and G. W. Colliver (1974). "CNS regulation of body temperature during hibernation." Am J Physiol **227**(3): 583-589.

Heller, H. C., G. W. Colliver, et al. (1977). "Thermoregulation during entrance into hibernation." Pflugers Arch **369**(1): 55-59.

Heller, H. C., L. I. Crawshaw, et al. (1978). "The thermostat of vertebrate animals." Sci Am **239**(2): 102-113.

Hindle, A. G., A. Karimpour-Fard, et al. (2011). "Skeletal muscle proteomics: carbohydrate metabolism oscillates with seasonal and torpor-arousal physiology of hibernation." Am J Physiol Reg I **301**(5): R1440-1452.

Hondares, E., R. Iglesias, et al. (2011). "Thermogenic activation induces FGF21 expression and release in brown adipose tissue." J Biol Chem **286**(15): 12983-12990.

Hondares, E., M. Rosell, et al. (2010). "Hepatic FGF21 expression is induced at birth via PPARalpha in response to milk intake and contributes to thermogenic activation of neonatal brown fat." Cell Metab **11**(3): 206-212.

Horton, N. D., D. J. Kaftani, et al. (1998). "Isolation and partial characterization of an opioid-like 88 kDa hibernation-related protein." Comp Biochem Phys B **119**(4): 787-805.

Horwitz, B. A., R. E. Smith, et al. (1968). "Estimated heat contribution of brown fat in arousing ground squirrels (Citellus lateralis)." Am J Physiol **214**(1): 115-121.

Hotta, Y., H. Nakamura, et al. (2009). "Fibroblast growth factor 21 regulates lipolysis in white adipose tissue but is not required for ketogenesis and triglyceride clearance in liver." Endocrinology **150**(10): 4625-4633.

Hsuchou, H., W. Pan, et al. (2007). "The fasting polypeptide FGF21 can enter brain from blood." Peptides **28**(12): 2382-2386.

Huang, X., C. Yu, et al. (2006). "Forced expression of hepatocyte-specific fibroblast growth factor 21 delays initiation of chemically induced hepatocarcinogenesis." Mol Carcinog **45**(12): 934-942.

Hudson, J. W. and I. M. Scott (1979). "Daily Torpor in the Laboratory Mouse, Mus musculus Var. Albino." Physiol Zool **52**(2): 205-218.

Iizuka, K., J. Takeda, et al. (2009). "Glucose induces FGF21 mRNA expression through ChREBP activation in rat hepatocytes." FEBS Lett **583**(17): 2882-2886.

Inagaki, T., P. Dutchak, et al. (2007). "Endocrine regulation of the fasting response by PPARalpha-mediated induction of fibroblast growth factor 21." Cell Metab **5**(6): 415-425.

Itoh, N. (2010). "Hormone-like (endocrine) Fgfs: their evolutionary history and roles in development, metabolism, and disease." Cell Tissue Res **342**(1): 1-11.

Izumiya, Y., H. A. Bina, et al. (2008). "FGF21 is an Akt-regulated myokine." FEBS Lett **582**(27): 3805-3810.

Jinka, T. R., O. Toien, et al. (2011). "Season primes the brain in an arctic hibernator to facilitate entrance into torpor mediated by adenosine A(1) receptors." J Neurosci **31**(30): 10752-10758.

Johnson, C. L., J. Y. Weston, et al. (2009). "Fibroblast growth factor 21 reduces the severity of cerulein-induced pancreatitis in mice." Gastroenterology **137**(5): 1795-1804.

Kabine, M., Z. El Kebbaj, et al. (2004). "Peroxisome proliferator-activated receptors as regulators of lipid metabolism; tissue differential expression in adipose tissues during cold acclimatization and hibernation of jerboa (Jaculus orientalis)." Biochimie **86**(11): 763-770.

Karpovich, S. A., O. Toien, et al. (2009). "Energetics of arousal episodes in hibernating arctic ground squirrels." J Comp Phys B **179**(6): 691-700.

Kersten, S., B. Desvergne, et al. (2000). "Roles of PPARs in health and disease." Nature **405**: 421-424.

Kharitonenkov, A., J. D. Dunbar, et al. (2008). "FGF-21/FGF-21 receptor interaction and activation is determined by betaKlotho." J Cell Physiol **215**(1): 1-7.

Kharitonenkov, A., T. L. Shiyanova, et al. (2005). "FGF-21 as a novel metabolic regulator." J Clin Invest **115**(6): 1627-1635.

Kharitonenkov, A., V. J. Wroblewski, et al. (2007). "The metabolic state of diabetic monkeys is regulated by fibroblast growth factor-21." Endocrinology **148**(2): 774-781.

Kiefer, F., K. Arnold, et al. (2009). "The SWISS-MODEL Repository and associated resources." Nucleic Acids Res **37**: D387-392.

Kitao, N. and M. Hashimoto (2012). "Increased thermogenic capacity of brown adipose tissue under low temperature and its contribution to arousal from hibernation in Syrian hamsters." Am J Physiol Reg I **302**(1): R118-125.

Krilowicz, B. L. (1985). "Ketone body metabolism in a ground squirrel during hibernation and fasting." Am J Physiol **249**(4 Pt 2): R462-470.

Kurosu, H., M. Choi, et al. (2007). "Tissue-specific expression of betaKlotho and fibroblast growth factor (FGF) receptor isoforms determines metabolic activity of FGF19 and FGF21." J Biol Chem **282**(37): 26687-26695.

Kurosu, H. and M. Kuro-o (2008). "The Klotho gene family and the endocrine fibroblast growth factors." Curr Opin Nephrol Hy **17**: 368-372.

Kurosu, H. and O. M. Kuro (2009). "The Klotho gene family as a regulator of endocrine fibroblast growth factors." Mol Cell Endocrinol **299**(1): 72-78.

Lefebvre, P., G. Chinetti, et al. (2006). "Sorting out the roles of PPAR alpha in energy metabolism and vascular homeostasis." J Clin Invest **116**(3): 571-580.

Li, H., Y. Bao, et al. (2009). "Serum fibroblast growth factor 21 is associated with adverse lipid profiles and gamma-glutamyltransferase but not insulin sensitivity in Chinese subjects." J Clin Endocrinol Metab **94**(6): 2151-2156.

Li, K., L. Li, et al. (2012). "The effects of fibroblast growth factor-21 knockdown and over-expression on its signaling pathway and glucose-lipid metabolism in vitro." Mol Cell Endocrinol **348**(1): 21-26.

Li, X., H. Ge, et al. (2009). "Inhibition of lipolysis may contribute to the acute regulation of plasma FFA and glucose by FGF21 in ob/ob mice." FEBS Lett **583**(19): 3230-3234.

Lin, J., C. Handschin, et al. (2005). "Metabolic control through the PGC-1 family of transcription coactivators." Cell Metab **1**(6): 361-370.

Liu, C., S. Li, et al. (2007). "Transcriptional coactivator PGC-1alpha integrates the mammalian clock and energy metabolism." Nature **447**(7143): 477-481.

Liu, X. T., Q. S. Lin, et al. (1998). "Uncoupling protein mRNA, mitochondrial GTP-binding, and T4 5'-deiodinase activity of brown adipose tissue in Daurian ground squirrel during hibernation and arousal." Comp Biochem Phys A **120**(4): 745-752.

Lu, Y., J. H. Liu, et al. (2010). "Fibroblast growth factor 21 as a possible endogenous factor inhibits apoptosis in cardiac endothelial cells." Chin Med J (Engl) **123**(23): 3417-3421.

Lundasen, T., M. C. Hunt, et al. (2007). "PPARalpha is a key regulator of hepatic FGF21." Biochem Biophys Res Commun **360**(2): 437-440.

Lust, W. D., A. B. Wheaton, et al. (1989). "Metabolism in the hamster brain during hibernation and arousal." Brain Res **489**(1): 12-20.

Lyman, C. P. (1958). "Oxygen consumption, body temperature and heart rate of woodchucks entering hibernation." Am J Physiol **194**(1): 83-91.

Lyman, C. P. and P. O. Chatfield (1955). "Physiology of hibernation in mammals." Physiol Rev **35**(2): 403-425.

Lyman, C. P., J. S. Willis, et al. (1982). Hibernation and Torpor in Mammals and Birds. New York, Academic Press.

MacDonald, J. A. and K. B. Storey (2002). "Purification and characterization of fructose bisphosphate aldolase from the ground squirrel, Spermophilus lateralis: enzyme role in mammalian hibernation." Arch Biochem Biophys **408**(2): 279-285.

Mai, K., J. Andres, et al. (2009). "Free fatty acids link metabolism and regulation of the insulin-sensitizing fibroblast growth factor-21." Diabetes **58**(7): 1532-1538.

Mandard, S., M. Muller, et al. (2004). "Peroxisome proliferator-activated receptor alpha target genes." Cell Mol Life Sci **61**(4): 393-416.

Martin, S. L. (2008). "Mammalian hibernation: a naturally reversible model for insulin resistance in man?" Diab Vasc Dis Res **5**(2): 76-81.

Mashili, F. L., R. L. Austin, et al. (2011). "Direct effects of FGF21 on glucose uptake in human skeletal muscle: implications for type 2 diabetes and obesity." Diabetes Metab Res Rev **27**(3): 286-297.

McArthur, M. D., C. C. Hanstock, et al. (1990). "Skeletal muscle pH dynamics during arousal from hibernation measured by 31P NMR spectroscopy." J Comp Physiol B **160**: 339-347.

Micanovic, R., D. W. Raches, et al. (2009). "Different roles of N- and C- termini in the functional activity of FGF21." J Cell Physiol **219**(2): 227-234.

Milsom, W. K., M. B. Zimmer, et al. (1999). "Regulation of cardiac rhythm in hibernating mammals." Comp Biochem Phys A **124**(4): 383-391.

Moreau-Hamsany, C., C. Castex, et al. (1988). "Hormonal control of lipolysis from the white adipose tissue of hibernating jerboa (Jaculus orientalis)." Comp Biochem Phys A **91**(4): 665-669.

Morrison, S. F., K. Nakamura, et al. (2008). "Central control of thermogenesis in mammals." Exp Physiol **93**(7): 773-797.

Moyers, J. S., T. L. Shiyanova, et al. (2007). "Molecular determinants of FGF-21 activity-synergy and cross-talk with PPARgamma signaling." J Cell Physiol **210**(1): 1-6.

Muise, E. S., B. Azzolina, et al. (2008). "Adipose fibroblast growth factor 21 is up-regulated by peroxisome proliferator-activated receptor gamma and altered metabolic states." Mol Pharmacol **74**(2): 403-412.

Nelson, C. J., J. P. Otis, et al. (2010). "Global analysis of circulating metabolites in hibernating ground squirrels." Comp Biochem Phys D **5**(4): 265-273.

Nishimura, T., Y. Nakatake, et al. (2000). "Identification of a novel FGF, FGF-21, preferentially expressed in the liver." Biochim Biophys Acta **1492**(1): 203-206.

Oeltgen, P. R., S. P. Nilekani, et al. (1988). "Further studies on opioids and hibernation: delta opioid receptor ligand selectively induced hibernation in summer-active ground squirrels." Life Sci **43**(19): 1565-1574.

Ogawa, Y., H. Kurosu, et al. (2007). "BetaKlotho is required for metabolic activity of fibroblast growth factor 21." Proc Natl Acad Sci U S A **104**(18): 7432-7437.

Oishi, K., M. Konishi, et al. (2011). "Time-imposed daily restricted feeding induces rhythmic expression of Fgf21 in white adipose tissue of mice." Biochem Biophys Res Commun **412**(2): 396-400.

Ornitz, D. M. and N. Itoh (2001). "Fibroblast growth factors." Genome Biol **2**(3): 3005.3001-3005.3012.

Otis, J. P., L. W. Ackermann, et al. (2010). "Identification of qRT-PCR reference genes for analysis of opioid gene expression in a hibernator." J Comp Physiol B **180**(4): 619-629.

Overton, J. M. and T. D. Williams (2004). "Behavioral and physiologic responses to caloric restriction in mice." Physiol Behav **81**(5): 749-754.

Peitsch, M. C., T. N. Wells, et al. (1995). "The Swiss-3D Image collection and PDB-Browser on the World-Wide Web." Trends Biochem Sci **20**(2): 82-84.

Picard, F., M. Kurtev, et al. (2004). "Sirt1 promotes fat mobilization in white adipocytes by repressing PPAR-gamma." Nature **429**(6993): 771-776.

Plotnikov, A. N., S. R. Hubbard, et al. (2000). "Crystal Structures of Two FGF-FGFR Complexes Reveal the Determinants of Ligand-Receptor Specificity." Cell **101**: 413-424.

Potthoff, M. J., T. Inagaki, et al. (2009). "FGF21 induces PGC-1alpha and regulates carbohydrate and fatty acid metabolism during the adaptive starvation response." Proc Natl Acad Sci U S A **106**(26): 10853-10858.

Potthoff, M. J., S. A. Kliewer, et al. (2012). "Endocrine fibroblast growth factors 15/19 and 21: from feast to famine." Genes Dev.

Puigserver, P., Z. Wu, et al. (1998). "A cold-inducible coactivator of nuclear receptors linked to adaptive thermogenesis." Cell **92**(6): 829-839.

Rauch, J. C. and H. W. Behrisch (1981). "Keton bodies: a source of energy during hibernation." Can J Zoolog **59**: 754-760.

Richard, D., A. C. Carpentier, et al. (2010). "Determinants of brown adipocyte development and thermogenesis." Int J Obes (Lond) **34**: S59-66.

Romanovsky, A. A. (2007). "Thermoregulation: some concepts have changed. Functional architecture of the thermoregulatory system." Am J Physiol Reg I **292**(1): R37-46.

Sanchez, J., A. Palou, et al. (2009). "Response to carbohydrate and fat refeeding in the expression of genes involved in nutrient partitioning and metabolism: striking effects on fibroblast growth factor-21 induction." Endocrinology **150**(12): 5341-5350.

Schoenberg, K. M., S. L. Giesy, et al. (2011). "Plasma FGF21 is elevated by the intense lipid mobilization of lactation." Endocrinology **152**(12): 4652-4661.

Serkova, N. J., J. C. Rose, et al. (2007). "Quantitative analysis of liver metabolites in three stages of the circannual hibernation cycle in 13-lined ground squirrels by NMR." Physiol Genomics **31**(1): 15-24.

Shao, C., Y. Liu, et al. (2010). "Shotgun proteomics analysis of hibernating arctic ground squirrels." Mol Cell Proteomics **9**(2): 313-326.

Smith, R. E. and B. A. Horwitz (1969). "Brown fat and thermogenesis." Physiol Rev **49**(2): 330-425.

Squire, T. L. and M. T. Andrews (2003). "Pancreatic triacylglycerol lipase in a hibernating mammal. I. Novel genomic organization." Physiol Genomics **16**(1): 119-130.

Squire, T. L., M. E. Lowe, et al. (2003). "Pancreatic triacylglycerol lipase in a hibernating mammal. II. Cold-adapted function and differential expression." Physiol Genomics **16**(1): 131-140.

Staples, J. F. and P. W. Hochachka (1998). "The effect of hibernation status and cold-acclimation on hepatocyte gluconeogenesis in the golden-mantled ground squirrel (Spermophilus lateralis)." Can J Zoolog **76**: 1734-1740.

Steinberg, D. and J. C. Khoo (1977). "Hormone-sensitive lipase of adipose tissue." Fed Proc **36**(7): 1986-1990.

Storey, K. B. (1987). "Regulation of liver metabolism by enzyme phosphorylation during mammalian hibernation." J Biol Chem **262**(4): 1670-1673.

Strumwasser, F. (1959). "Thermoregulatory, brain and behavioral mechanisms during entrance into hibernation in the squirrel, Citellus beecheyi." Am J Physiol **196**(1): 15-22.

Suzuki, M., Y. Uehara, et al. (2008). "betaKlotho is required for fibroblast growth factor (FGF) 21 signaling through FGF receptor (FGFR) 1c and FGFR3c." Mol Endocrinol **22**(4): 1006-1014.

Swoap, S. J., M. Rathvon, et al. (2007). "AMP does not induce torpor." Am J Physiol Reg I **293**(1): R468-473.

Tahti, H. (1978). "Seasonal differences in O2 consumption and respiratory quotient in a hibernator (Erinaceus europaeus L.)." Ann Zool Fennici **15**: 69-75.

Tamura, Y., M. Shintani, et al. (2012). "Regulatory mechanism of body temperature in the central nervous system during the maintenance phase of hibernation in Syrian hamsters: Involvement of beta-endorphin." Brain Res **1448**: 63-70.

Tamura, Y., M. Shintani, et al. (2005). "Phase-specific central regulatory systems of hibernation in Syrian hamsters." Brain Res **1045**(1-2): 88-96.

Tashima, L. S., S. J. Adelstein, et al. (1970). "Radioglucose utilization by active, hibernating, and arousing ground squirrels." American Journal of Physiology **218**(1): 303-309.

Tashima, L. S., S. J. Adelstein, et al. (1970). "Radioglucose utilization by active, hibernating, and arousing ground squirrels." Am J Physiol **218**(1): 303-309.

Tokuyama, K., H. L. Galantino, et al. (1991). "Seasonal glucose uptake in marmots (Marmota flaviventris): the role of pancreatic hormones." Comp Biochem Phys A **100**(4): 925-930.

Tomiyama, K., R. Maeda, et al. (2010). "Relevant use of Klotho in FGF19 subfamily signaling system in vivo." Proc Natl Acad Sci U S A **107**(4): 1666-1671.

Tong, X., M. Muchnik, et al. (2010). "Transcriptional repressor E4-binding protein 4 (E4BP4) regulates metabolic hormone fibroblast growth factor 21 (FGF21) during circadian cycles and feeding." J Biol Chem **285**(47): 36401-36409.

Uebanso, T., Y. Taketani, et al. (2009). "Hypocaloric high-protein diet improves fatty liver and hypertriglyceridemia in sucrose-fed obese rats via two pathways." Am J Physiol-Endoc M **297**(1): E76-84.

Uebanso, T., Y. Taketani, et al. (2011). "Paradoxical regulation of human FGF21 by both fasting and feeding signals: is FGF21 a nutritional adaptation factor?" PLoS One **6**(8): e22976.

UniProt, C. (2012). "Reorganizing the protein space at the Universal Protein Resource (UniProt)." Nucleic Acids Res **40**: D71-75.

Uonaga, T., K. Toyoda, et al. (2010). "FGF-21 enhances islet engraftment in mouse syngeneic islet transplantation model." Islets **2**(4): 247-251.

Uyeda, K., H. Yamashita, et al. (2002). "Carbohydrate responsive element-binding protein (ChREBP): a key regulator of glucose metabolism and fat storage." Biochem Pharmacol **63**(12): 2075-2080.

van Breukelen, F. and S. L. Martin (2001). "Translational initiation is uncoupled from elongation at 18 degrees C during mammalian hibernation." Am J Physiol Reg I **281**(5): R1374-1379.

Van Breukelen, F. and S. L. Martin (2002). "Invited review: molecular adaptations in mammalian hibernators: unique adaptations or generalized responses?" J Appl Physiol **92**(6): 2640-2647.

van Breukelen, F. and S. L. Martin (2002). "Reversible depression of transcription during hibernation." J Comp Phys B **172**(5): 355-361.

Volpato, G. P., R. Searles, et al. (2008). "Inhaled hydrogen sulfide: a rapidly reversible inhibitor of cardiac and metabolic function in the mouse." Anesthesiology **108**(4): 659-668.

Wang, H., L. Qiang, et al. (2008). "Identification of a domain within peroxisome proliferator-activated receptor gamma regulating expression of a group of genes containing fibroblast growth factor 21 that are selectively repressed by SIRT1 in adipocytes." Mol Cell Biol **28**(1): 188-200.

Wente, W., A. M. Efanov, et al. (2006). "Fibroblast growth factor-21 improves pancreatic beta-cell function and survival by activation of extracellular signal-regulated kinase 1/2 and Akt signaling pathways." Diabetes **55**(9): 2470-2478.

Wilson, B. E., S. Deeb, et al. (1992). "Seasonal changes in hormone-sensitive and lipoprotein lipase mRNA concentrations in marmot white adipose tissue." Am J Physiol **262**(2 Pt 2): R177-181.

Wu, X., B. Lemon, et al. (2008). "C-terminal tail of FGF19 determines its specificity toward Klotho co-receptors." J Biol Chem **283**(48): 33304-33309.

Xu, J., D. J. Lloyd, et al. (2009). "Fibroblast growth factor 21 reverses hepatic steatosis, increases energy expenditure, and improves insulin sensitivity in diet-induced obese mice." Diabetes **58**(1): 250-259.

Xu, J., S. Stanislaus, et al. (2009). "Acute glucose-lowering and insulin-sensitizing action of FGF21 in insulin-resistant mouse models--association with liver and adipose tissue effects." Am J Physiol-Endo M **297**(5): E1105-1114.

Yamashita, T., M. Yoshioka, et al. (2000). "Identification of a novel fibroblast growth factor, FGF-23, preferentially expressed in the ventrolateral thalamic nucleus of the brain." Biochem Biophys Res Commun **277**(2): 494-498.

Yan, J., B. M. Barnes, et al. (2008). "Modulation of gene expression in hibernating arctic ground squirrels." Physiol Genomics **32**(2): 170-181.

Yan, J., B. M. Barnes, et al. (2008). "Modulation of gene expression in hibernating arctic ground squirrels." Physiol Genomics **32**: 170-181.

Yan, J., A. Burman, et al. (2006). "Detection of differential gene expression in brown adipose tissue of hibernating arctic ground squirrels with mouse microarrays." Physiol Genomics **25**(2): 346-353.

Yeh, I., C. F. Tam, et al. (1995). "Changes in various plasma lipid components, glucose, and insulin in Spermophilus lateralis during hibernation." Comp Biochem Physiol **111B**(4): 651-663.

Yie, J., R. Hecht, et al. (2009). "FGF21 N- and C-termini play different roles in receptor interaction and activation." FEBS Lett **583**(1): 19-24.

Yie, J., W. Wang, et al. (2012). "Understanding the physical interactions in the FGF21/FGFR/beta-Klotho complex: structural requirements and implications in FGF21 signaling." Chem Biol Drug Des **79**(4): 398-410.

Yu, J., B. Yu, et al. (2012). "Conjugated linoleic acid induces hepatic expression of fibroblast growth factor 21 through PPAR-alpha." Br J Nutr **107**(4): 461-465.

Zhang, J., K. Kaasik, et al. (2006). "Constant darkness is a circadian metabolic signal in mammals." Nature **439**(7074): 340-343.

Zhang, X., D. C. Yeung, et al. (2008). "Serum FGF21 levels are increased in obesity and are independently associated with the metabolic syndrome in humans." Diabetes **57**(5): 1246-1253.

Zhang, Z., S. Schwartz, et al. (2000). "A greedy algorithm for aligning DNA sequences." J Comput Biol **7**(1-2): 230-214.